Design, Testing and Validation of a Room Air Conditioner Test Facility

S. M. Rugg and W. E. Dunn

ACRC TR-59 July 1994

For additional information:

Air Conditioning and Refrigeration Center
University of Illinois
Mechanical & Industrial Engineering Dept.
1206 West Green Street
Urbana, IL 61801

(217) 333-3115

Prepared as part of ACRC Project 41
Alternative Refrigerants in Room Air Conditioners
W. E. Dunn and C. W. Bullard, Principal Investigators

The Air Conditioning and Refrigeration Center was founded in 1988 with a grant from the estate of Richard W. Kritzer, the founder of Peerless of America Inc. A State of Illinois Technology Challenge Grant helped build the laboratory facilities. The ACRC receives continuing support from the Richard W. Kritzer Endowment and the National Science Foundation. The following organizations have also become sponsors of the Center.

Acustar Division of Chrysler
Allied-Signal, Inc.
Amana Refrigeration, Inc.
Brazeway, Inc.
Carrier Corporation
Caterpillar, Inc.
E. I. du Pont de Nemours & Co.
Electric Power Research Institute
Ford Motor Company
Frigidaire Company
General Electric Company
Harrison Division of GM
ICI Americas, Inc.
Modine Manufacturing Co.
Peerless of America, Inc.
Environmental Protection Agency
U. S. Army CERL
Whirlpool Corporation

For additional information:

Air Conditioning & Refrigeration Center
Mechanical & Industrial Engineering Dept.
University of Illinois
1206 West Green Street
Urbana IL 61801

217 333 3115

ABSTRACT

DESIGN, TESTING AND VALIDATION
OF A ROOM AIR CONDITIONER TEST FACILITY

Steven Minard Rugg, M.S.
Department of Mechanical and Industrial Engineering
University of Illinois at Urbana-Champaign, 1994
W. E. Dunn, Advisor

This report discusses the design, testing and validation of a room air conditioner test facility. The facility is designed to test the performance of air conditioners rated from 0.5 to 2.5 tons of refrigeration over a wide range of operating conditions. The results from testing are used to validate the accuracy and utility of the facility, as well as to develop a simulation model to predict air conditioner performance at on- and off-design conditions.

The facility is fully constructed and operational. Steady-state and transient facility characterization tests have been run to identify the behavior of the facility. These results are used to calibrate the facility and to determine an optimal test matrix. Air conditioner performance data have been collected for an air-side-instrumented test unit which demonstrate the accuracy of our facility measurements and calorimetry. Test results are also useful for determining performance trends as functions of temperature, humidity, and air conditioner fan speed.

TABLE OF CONTENTS

LIST OF TABLES

LIST OF FIGURES

NOMENCLATURE

English Symbols

A	total surface area of indoor room walls
f	fraction of furnace power transferred directly to indoor room air
f_{fan}	fraction of air conditioner fan power dissipated within indoor room
h_{fg}	enthalpy of vaporization for water
$\dot{m}$	rate of moisture loss from indoor room air
$\dot{m}c_p$	mass flow rate-specific heat product for fan/coil unit
mc_{pa}	mass times specific heat product for indoor room air
mc_{ph}	mass times specific heat product for humidifier
mc_{pm}	mass times specific heat product for indoor room metal
mc_{pp}	mass times specific heat product for partition wall nodes
mc_{pw}	mass times specific heat product for wall nodes
$\dot{q}$	fan/coil unit heat transfer
$\dot{Q}_{12}, \dot{Q}_{23}, \dot{Q}_{34}, \dot{Q}_{45}$	heat transfers between wall nodes
$\dot{Q}_{1p2p}$, $\dot{Q}_{2p3p}$, $\dot{Q}_{3p4p}$, $\dot{Q}_{4p5p}$	heat transfers between partition wall nodes
$\dot{Q}_{5amb}$	heat transfer between wall node 5 and ambient air
$\dot{Q}_{5po}$	heat transfer between partition wall node 5 and outdoor room air
$\dot{Q}_{a/c}$	parasitic sensible heat loss through air conditioner
$\dot{Q}_{ah}$	heat transfer between indoor room air and humidifier
$\dot{Q}_{am}$	heat transfer between indoor room air and metal
$\dot{Q}_{evap}$	heat transfer from humidifier to indoor room air due to evaporation

$\dot{Q}_{fan}$	power used by both air conditioner fans
$\dot{Q}_{hm}$	heat transfer between humidifier and metal
$\dot{Q}_{m1}$	heat transfer between metal and wall node 1
$\dot{Q}_{m1p}$	heat transfer between metal and partition wall node 1
$\dot{Q}_{moist}$	parasitic latent heat loss through air conditioner
$\dot{Q}_{room}$	thermal energy added to indoor room by all sources other than the air conditioner fans
$\dot{Q}_{R}$	thermal energy added to indoor room
$\dot{Q}_{Rfan}$	thermal energy added to indoor room by evaporator fan of air conditioner
$\dot{Q}_{T}$	thermal energy removed from indoor room by refrigerant loop of test unit
$\overline{\overline{T}}$	area-weighted average temperature of air spaces surrounding indoor room
T_1, T_2, T_3, T_4, T_5	average wall node temperatures
T_{1p}, T_{2p}, T_{3p}, T_{4p}, T_{5p}	average partition wall node temperatures
T_a	average indoor room air temperature
T_{amb}	average guard space air temperature
$T_{cold,in}$	inlet temperature of ethylene glycol mixture in fan/coil unit
$T_{hot,in}$	inlet temperature of air in fan/coil unit
T_h	average humidifier temperature
T_m	average metal temperature
T_o	average outdoor room air temperature
$UA_{a/c}$	effective thermal conductance through air conditioner cabinet
$UA_{a/c\text{-}off}$	effective thermal conductance through air conditioner cabinet with a/c fans off

$UA_{a/c\text{-}on}$	effective thermal conductance through air conditioner cabinet with a/c fans on
UA_{amb}	effective thermal conductance between wall node 5 and the ambient air
UA_{ha}	effective thermal conductance between humidifier and indoor room air
$UA_{m\text{-}off}$	effective moisture conductance through air conditioner cabinet with a/c fans off
$UA_{m\text{-}on}$	effective moisture conductance through air conditioner cabinet with a/c fans on
UA_{ma}	effective thermal conductance between metal and indoor room air
UA_{mh}	effective thermal conductance between metal and humidifier
UA_{moist}	effective moisture conductance through air conditioner cabinet
UA_{mp}	effective thermal conductance between metal and partition wall node 1
UA_{mw}	effective thermal conductance between metal and wall node 1
UA_{o}	effective thermal conductance of walls surrounding the outdoor room
UA_{p}	effective thermal conductance between partition wall nodes
UA_{po}	effective thermal conductance between partition wall node 5 and outdoor room air
UA_{w}	effective thermal conductance between wall nodes
UA_{walls}	effective thermal conductance of walls surrounding the indoor room

Greek Symbols

ε	coil heat exchanger effectiveness
ρ_g	density of indoor room air
ω_a	humidity ratio of indoor room air
ω_o	humidity ratio of outdoor room air

Acronyms

ASHRAE	American Society of Heating, Refrigerating and Air-Conditioning Engineers
EER	energy efficiency ratio = ratio of the heat removal rate of an air conditioner in Btu/hr to its power requirement in W
COP	coefficient of performance
DC	direct current
PVC	polyvinyl chloride
RH	relative humidity
RTD	resistance temperature detector

1. INTRODUCTION

The future design of room air conditioners is being driven primarily by (a) increased energy efficiency standards and (b) the need to eliminate ozone-depleting working fluids. Various national and international agencies continue to impose more stringent requirements for energy efficiency. In addition, consumer pressure to select units with lower operating costs further drives the need for improved performance. This creates the need to develop heat exchangers with fewer irreversibilities and more efficient compressors, to name a few possibilities. Because most commonly-used refrigerants have been found to destroy the ozone layer when exposed to the atmosphere, there is also tremendous pressure to develop more environmentally-safe fluids. For these reasons, air conditioner manufacturers will need more powerful design tools and a better understanding of the performance of the latest-technology components and refrigerants to remain competitive in the world market.

These needs provide the motivation for the work described within this document. This work is part of an ongoing project to (a) design and validate a room air conditioner test facility, (b) develop a simulation model to predict air conditioner performance, (c) perform transient and cycling testing on various air conditioners, and (d) perform testing with various components and alternative refrigerants. The design and validation of the facility involves equipment selection, construction, and performing both facility characterization and air conditioner performance tests. The results from performance testing indicate the accuracy and usefulness of the facility for future work. Once the facility is validated, the performance data obtained from testing is compared to the performance predicted by a simulation model. This comparison determines the model's ability to be used as a design tool over a wide range of conditions. Since running simulations of air conditioner tests is much cheaper, simpler and faster than experimental testing, an accurate model is of great value to researchers and manufacturers. The facility will also be used to measure air conditioner performance during transient and cycling operation. This will be of great importance since most units are exposed to this type of operating in the market. The fourth focus of the project is to test air conditioners with various types of heat exchangers, compressors, capillary tubes, and refrigerants to determine possible improvements for the future units. The focus of this paper is to describe the design, testing, and validation of the test facility.

Although many air conditioner test facilities are currently in use, we identified the need to design a facility with somewhat different capabilities. Because one of our

goals is to develop a simulation model that can be utilized at off-design conditions, we need to have a facility that can provide a variety of indoor and outdoor room environments. This differs substantially from typical test facilities, which are used to determine performance at a single rating condition. This flexibility also provides more information about individual air conditioner components and various relevant phenomena. For example, testing the evaporator over a wide range of conditions produces flooded cases (where the refrigerant is two-phase throughout the heat exchanger), superheated cases, and varying degrees of wetted evaporator surfaces (where water condensation is present). Each of these situations provides useful data for better understanding issues relating to component design, heat transfer and pressure losses within the system.

Our test facility also will allow for refrigerant-side measurements of pressure and temperature. These values will provide greater accuracy in determining refrigerant properties, as well as valuable information about the effects of adding instrumentation to the refrigerant loop on performance. Because our facility will be used as a design tool, the data we collect are not subject to the legal implications that are of concern when applying the standard. This also enables us to reduce the cost and complexity of the facility without compromising the goals of the project. Thus, there are many significant reasons that necessitate the design and construction of our test facility.

2. DESIGN OF THE TEST FACILITY

When designing our test facility, we chose to use ASHRAE Standard 16-1983 as a starting point. However, it is important to note that the Standard was used only as a guide throughout our design process and not as a strict set of rules. It is necessary for our facility to deviate from standard test facilities for many of the reasons presented in Chapter 1. Nevertheless, the Standard does serve as a useful guide when addressing many design issues. The Standard describes two different types of test chambers. The first is called a calibrated room calorimeter and is shown in Figure 2.1. It consists of an indoor and outdoor compartment to simulate the inside and outside of a house, each of which can be maintained at a given temperature and relative humidity. The air conditioner is placed in the wall separating the two compartments. The indoor room contains reconditioning equipment (a heater and humidifier) to add enough thermal energy to balance the sensible and latent heat being removed by the test unit. The room also contains a fan to circulate air throughout the compartment and mixing devices to ensure that the air conditioner sees a well-mixed flow of air. Similarly, the outdoor room contains a cooler and a dehumidifier to remove the sensible and latent heat added by the test unit. Again, a fan and mixers are present to circulate air throughout the compartment that is uniform in temperature and humidity (ASHRAE 1984).

A pressure equalizing device is mounted in the wall between the compartments to alleviate any pressure difference between the rooms. The air flow that passes through the equalizing device must be measured to determine the amount of heat and moisture leakage between the compartments. While the walls surrounding the indoor compartment are sealed to prevent moisture leakage to the surrounding air spaces, there is still sensible heat transfer through the walls to the surrounding air. Thus, the amount of energy that is removed from the indoor room by the test unit is determined by measuring the amount of energy added by the heater and humidifer and subtracting the sensible heat lost through the walls. By calibrating the room to know how much thermal energy is lost as a function of the temperature difference across the walls, the capacity of the test unit can be accurately determined (ASHRAE 1984).

The second type of facility is the balanced ambient calorimeter, shown in Figure 2.2. This facility is similar to the first one, except that there is a controlled-temperature air space that surrounds the facility on all sides. The temperature of this air space is adjusted such that it matches the temperature in the indoor compartment. This eliminates any heat transfer from the indoor room to the ambient, and thus means that

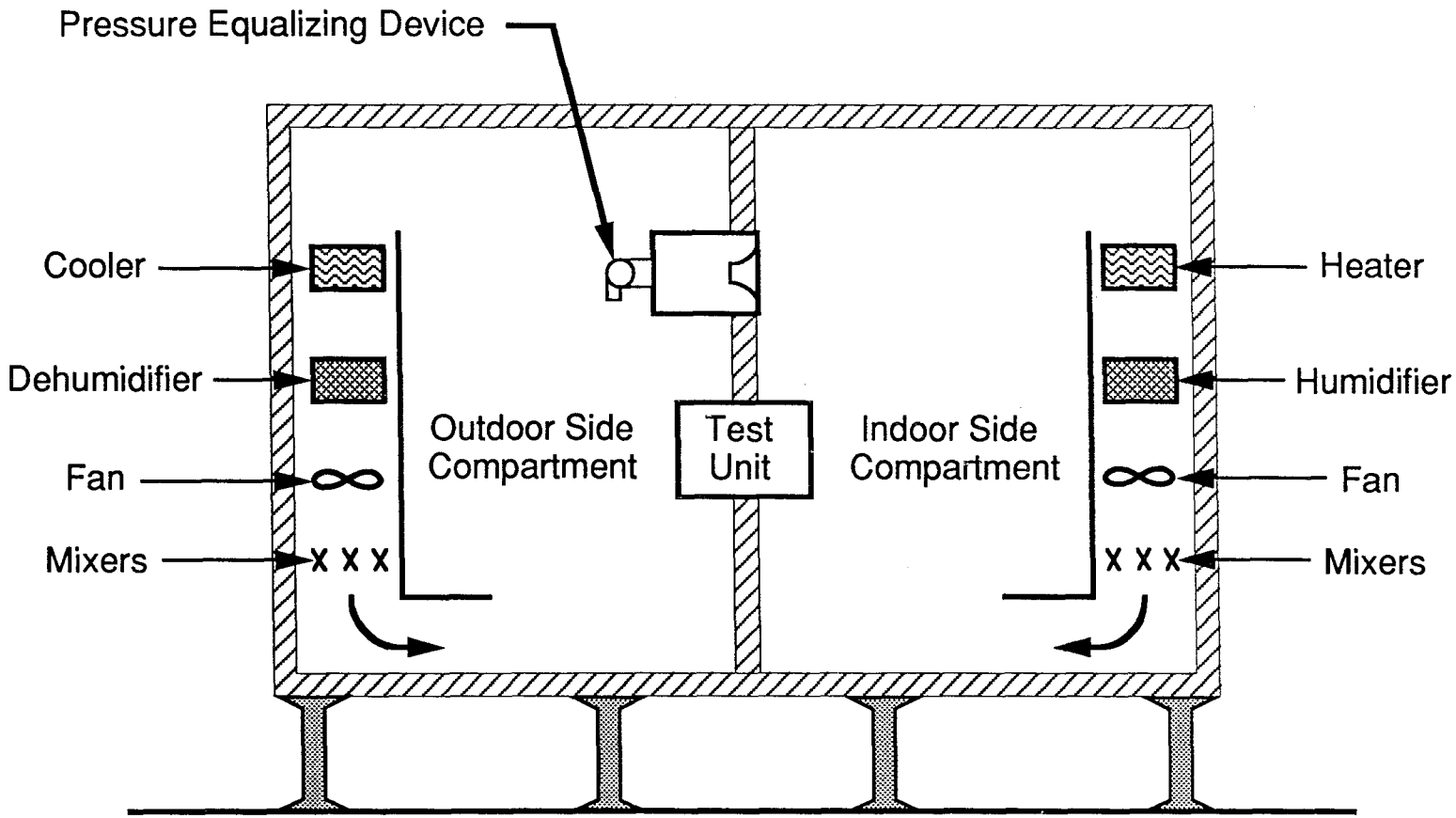

Figure 2.1 Calibrated Room Calorimeter (reprinted with permission from Fleming)

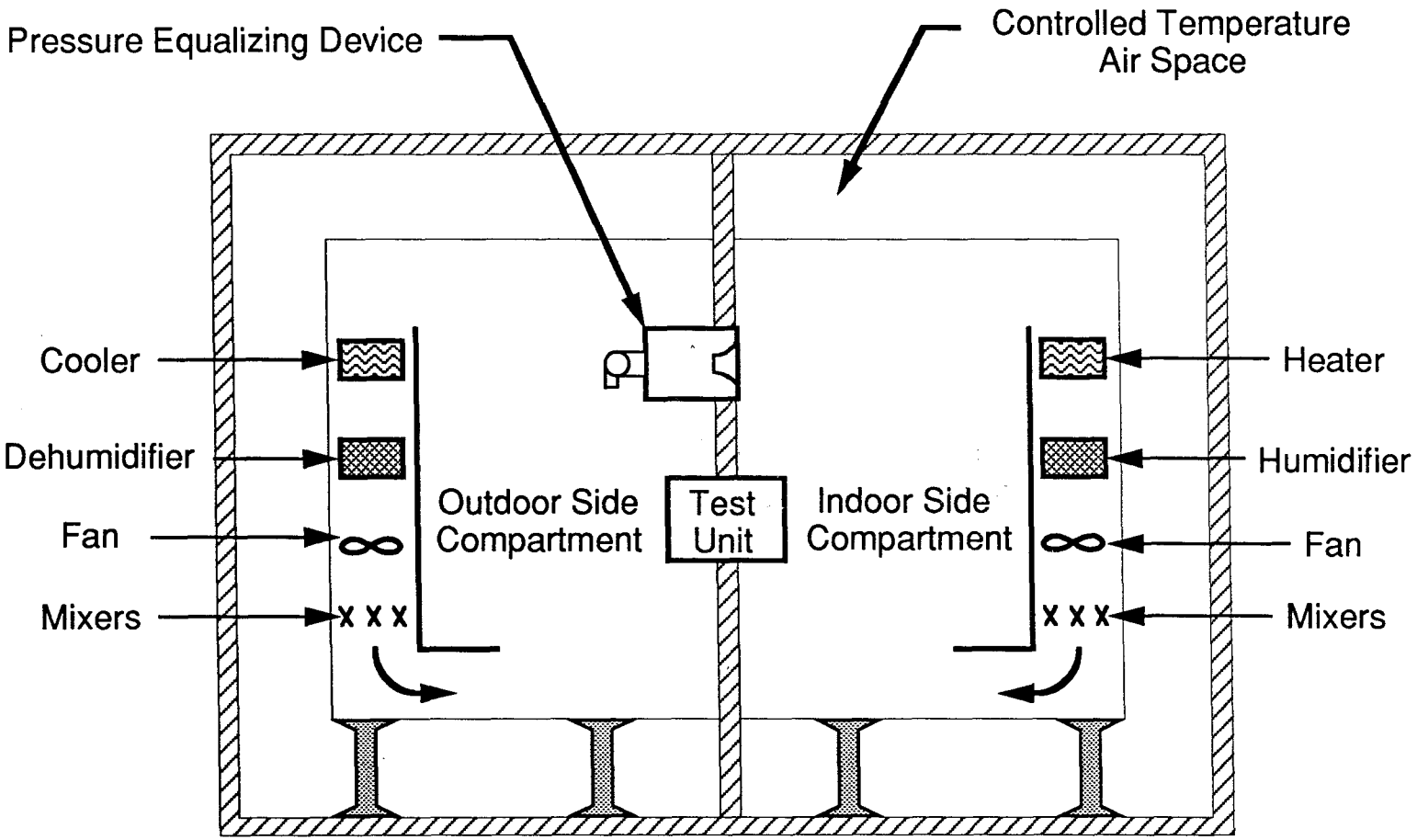

Figure 2.2 Balanced Ambient Room Calorimeter (reprinted with permission from Fleming)

the amount of energy that is added by the indoor room reconditioning equipment equals the energy removed by the test unit. This type of facility is more accurate since only the heat transfer between the two compartments needs to be calibrated (ASHRAE 1984).

We decided to construct a calibrated room calorimeter because it was most compatible with our existing facilities. The operating envelope for the facility was chosen so that each air conditioner can be tested at a full range of temperatures and humidities. For a typical unit, this requires indoor room temperatures from 50 to 120 °F and outdoor room temperatures from 70 to 120 °F. We also selected a range of relative humidities from 5 to 95% for each chamber. The temperature and humidity can be independently controlled in the indoor chamber, but are somewhat interrelated on the outdoor side. This will be addressed later in the discussion of the outdoor room characteristics. The overall facility is designed to test room air conditioners and split systems with capacities ranging from 0.5 to 2.5 tons of refrigeration (1.8 to 8.8 kW).

The construction of the test facility utilized an existing room (14.75 x 20 x 8.5 ft internal dimensions) that included a 3-ft guard space on five sides and a plaster and cork wall on the sixth. Because of the placement of the facility and the layout of the building, there isn't enough room to construct a sixth guard space. We then divided the room into an indoor chamber (to simulate conditions inside a room or building) and an outdoor chamber (to simulate outdoor conditions). The air conditioner is located in the wall separating the two chambers.

2.1 Design of the Indoor Room

As was previously mentioned, the room air conditioner test facility is a calibrated-room calorimeter. In the steady-state operation of this type of facility, the amount of energy removed by the air conditioner is determined by measuring the energy (both sensible and latent) added to the indoor room and subtracting the amount of energy lost due to heat or moisture transfer. Thus, it is crucial that all energies gained and lost be accurately known in order to calculate the air conditioner capacity. Another factor that must be accounted for is the transient response of the facility. The energy balance must include an additional correction if the indoor room has not reached a steady-state condition.

2.1.1 Physical Attributes

The indoor and outdoor chambers were constructed by separating the facility into two equal parts (each with dimensions 14.75 x 10 x 8.5 ft) and installing a 12-in. layer of foam between the halves. A 12-in. layer of foam was also added to all of the remaining five surfaces of the indoor chamber. The foam walls are composed of 4 layers of polyisocyanurate insulation with aluminum foil on the face of each layer. The innermost layer has an aluminum-embossed laminate face to provide a protective layer for the indoor room. The R-value of the foam is 7.2 hr-ft^2-°F/Btu-in., which corresponds to a total R-value of 86.4 hr-ft^2-°F/Btu for each wall. The foam layers are installed in a bank-vault style, with each layer overlapping the adjacent ones. All joints are sealed with silicone caulk and covered with aluminum foil tape. This sealing technique, along with the embossed laminate facing, eliminates any air exchange or moisture transfer through the walls of the indoor room.

The walls are supported by an aluminum unistrut framework which is completely enclosed within the indoor room. Using an internally contained frame reduces the number of penetrations through the walls, and thus the associated conduction heat transfer losses. However, some penetrations are necessary for the facility. PVC pipe was chosen instead of higher thermal conductivity metal conduit to carry the electrical power to the indoor room. All instrumentation lines are also housed within PVC pipe. Two additional PVC tubes are mounted in and through the partition wall so that two pressure relief valves could be installed (one allowing air to pass from the indoor chamber to the outdoor room, and the other providing an air path in the opposite direction). These valves have a cracking pressure of 0.4 in. of water and are designed to equilibrate pressures between the indoor and outdoor chambers during transients (periods of changing conditions). Once barometric equilibrium is achieved between the two chambers, the relief valves remain closed and do not contribute to any air exchange (and thus energy transfer) between the rooms. In fact, during most transients air exchange through the air conditioner provides pressure equalization between the rooms and prevents the relief valves from opening.

The partition wall between the indoor and outdoor chambers contains two removable sections: a door used for access purposes and a foam collar in which the air conditioner is mounted. These sections are constructed in a bank-vault style and are secured in place with a steel framework located in the outdoor room. This framework also serves to support the partition wall from the outside, since the foam possesses little structural strength. All joints are sealed with silicone caulk and

covered with aluminum foil tape to prevent air and moisture transfer. Several layers of closed-cell neoprene foam are used as gasket material and are applied to all mating surfaces between the partition wall and the removable sections. Because the neoprene has a very low water absorptivity and only a small amount of it is exposed to the indoor room, the air and moisture transfer through the gaskets is negligible.

An opening is cut in the foam collar and the air conditioner is mounted inside this space, as shown in Figure 2.3. These joints are also sealed with silicone caulk and aluminum foil tape. Because the foam does not provide much structural stability, the air conditioner is secured to a heavy-duty cart located in the outdoor room. The test unit is strapped to a sheet of plywood and is positioned in a cantilever fashion in the partition wall. The plywood sheet is attached to the cart with three adjustable leveling mounts, which can be raised or lowered as needed to properly align the air conditioner. The cart is balanced with several bars of steel stock to offset the weight of the test unit.

2.1.2 Sensible Heat Addition System

In order to maintain a steady-state temperature in the indoor chamber, a thermal energy source must be present to balance the sensible heat removed by the air conditioner. The heat source must be able to provide enough energy to test the units at 100% sensible load conditions, where none of the energy transfer is due to condensation on the evaporator. The maximum energy input required was determined to be 10 kW based on the cooling capacities of the largest units (8.8 kW), the parasitic heat losses from the indoor room (150 W maximum), and the fact that the test units have higher capacities at many non-rating conditions (up to 50% higher than the rated performance).

After investigating many options, a commercial furnace was chosen as the sensible heat source. The furnace is relatively inexpensive, comes in a prepackaged unit, and is easy to implement and control. The furnace adds energy through two 5-kW resistive heating elements and a fan that can operate at various air flow rates. Although the power dissipated by the fan remains essentially constant, the power supplied to the heating elements can be continuously varied from 0 to 10 kW using a time-proportioning microprocessor controller.

The furnace fan speed chosen for testing depends on the size of the air conditioner being evaluated. As was previously mentioned, the ASHRAE Standard for testing room air conditioners specifies the circulation fan for the indoor room (in our

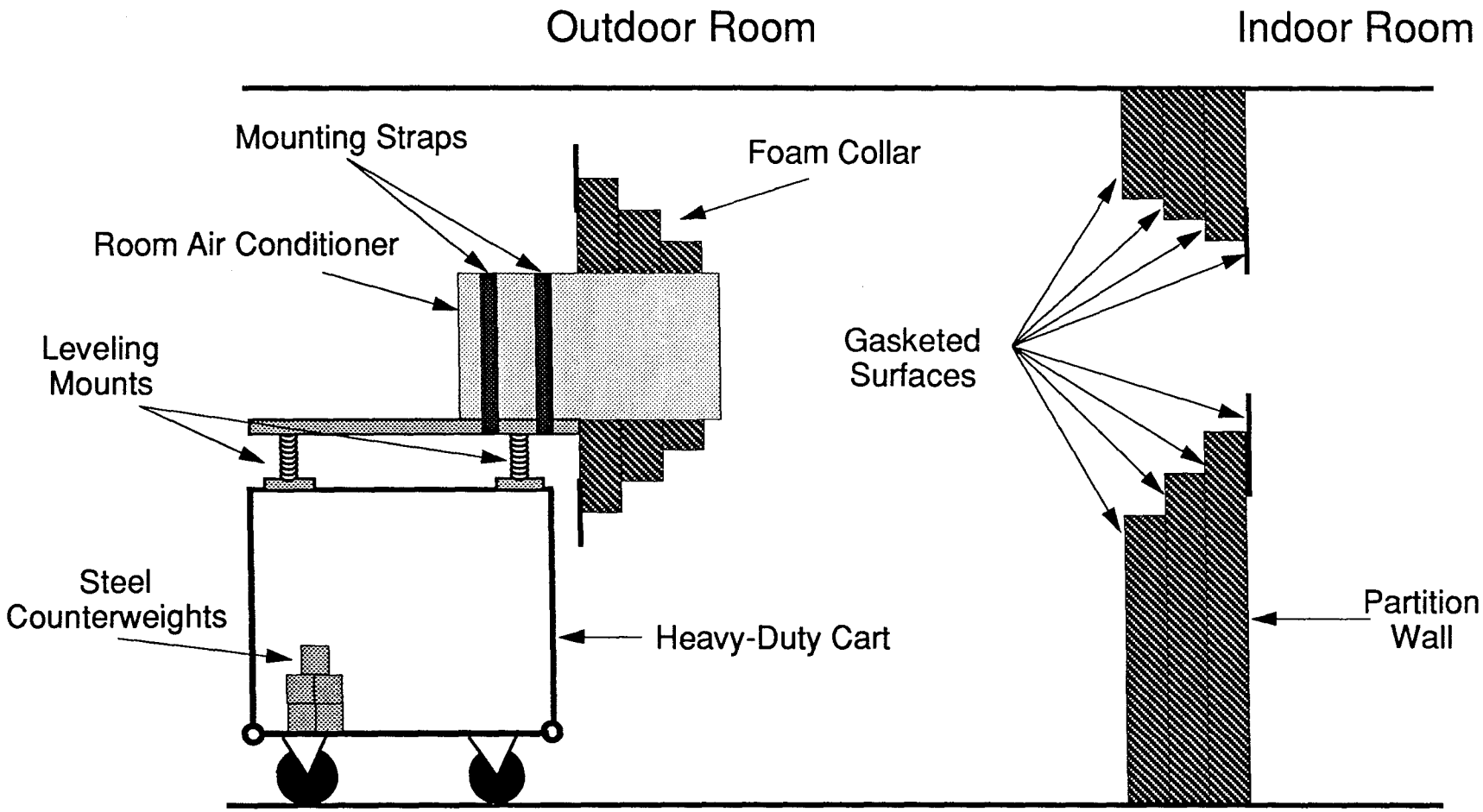

Figure 2.3 Room Air Conditioner Support and Mounting Diagram

case, the furnace fan) have a volume flow rate at least twice as large as that of the evaporator fan, and provide for at least one room air change per minute (ASHRAE 1984). Because the volume of the indoor room is 663 ft^3, this sets the minimum furnace fan flow rate at 663 cfm. However, the largest air conditioners have evaporator air flow rates up to 700 cfm and thus require a higher furnace fan capacity.

For different reasons, the furnace fan capacity is limited on the high side as well. Since the fan runs continuously even when the heating elements are receiving no power, the air conditioner always has to remove the energy it dissipates. In most cases the unit is also removing some amount of latent heat as well. Thus, some of the smaller air conditioners can be overwhelmed by the energy added in both sensible and latent forms, and certain steady-state conditions cannot be achieved. Therefore, it is important to operate the furnace fan at a capacity that doesn't greatly exceed the ASHRAE (1984) specifications for circulation. The manufacturer data specifies that the fan can operate at several capacities ranging from 1150 to 1860 cfm, and is adjusted as necessary for testing.

The controller allows the operator to add energy to the heating elements in two ways. The easiest control scheme is to set the furnace to supply a certain constant percentage of its full output power. This method is referred to as manual control and requires no tuning of the controller. However, since most test conditions are specified by temperatures and not power levels, it is a trial-and-error process to determine what power level corresponds to each temperature. This would cause testing to be very time consuming and impractical. In addition, manual control does not provide the quickest response for the indoor room, which is discussed in Chapter 3. The preferred method of control is to set the controller to a certain temperature and to vary the furnace power to maintain that temperature. This method is known as automatic control and requires several tuning parameters (that are automatically determined by the controller) to provide optimal control.

The controller uses a time-proportional on/off duty cycle to provide power to the furnace. This means that if the controller is set to run the furnace at 30% power, the furnace will be on at full power for 30% of the duty cycle and off (except for the fan) for the remaining portion of the cycle. The length of the cycle can be chosen by the operator and is currently set at 1 s to reduce the transient effects of on/off operation. The furnace control system schematic is shown in Figure 2.4. The controller sends an on/off signal to a solid-state relay, which in turn opens or closes the furnace power circuit. Power to the furnace is cut off if the temperature in either the indoor or outdoor chamber exceeds 125 °F. The furnace also contains a high-temperature safety switch

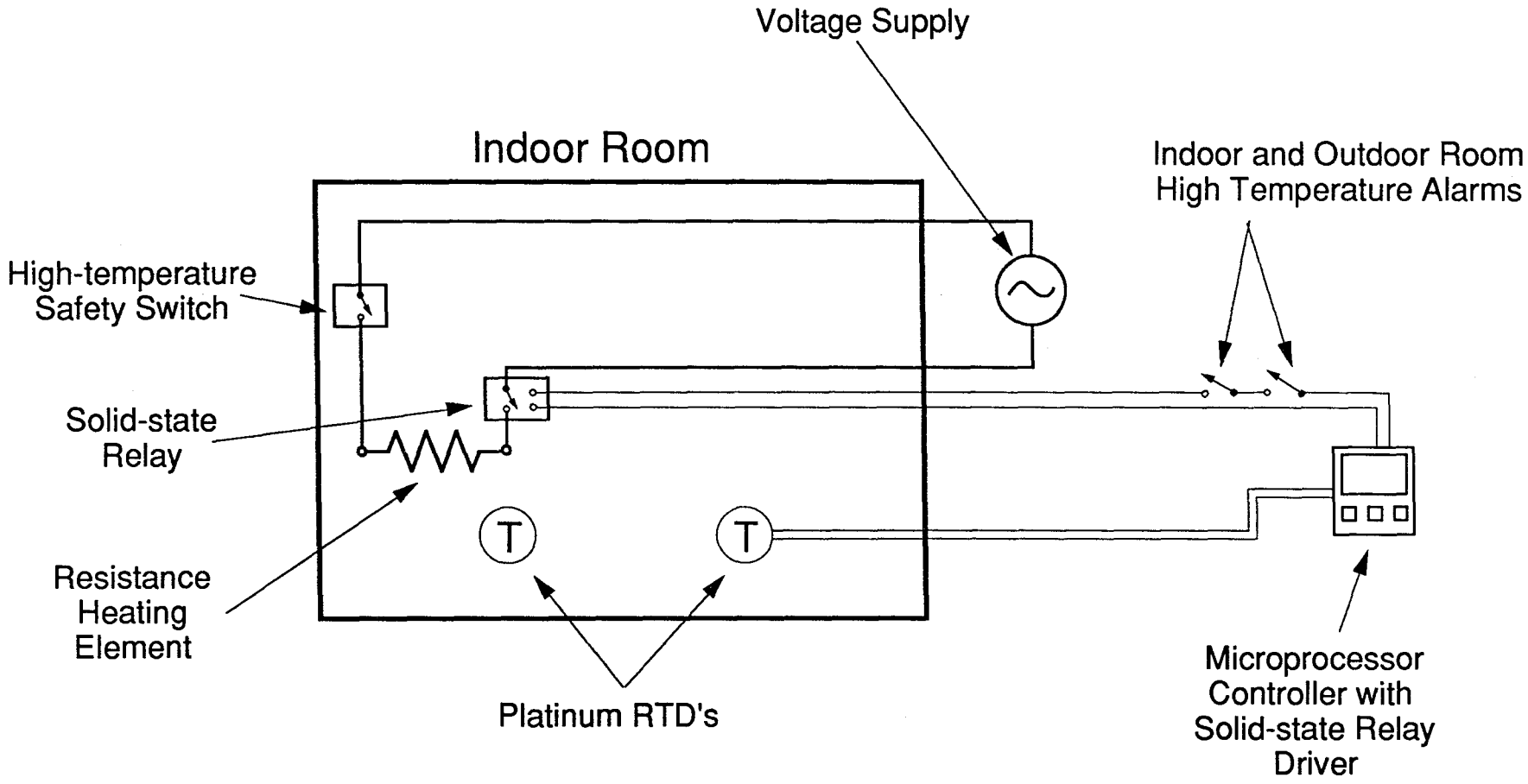

Figure 2.4 Furnace Control System Schematic

that opens the power circuit when the heating elements exceed a manufacturer-specified temperature. Although the energy used by the furnace is not independently measured, the total power added to the indoor room is accurately determined by a power measurement device to be described in a later section. We have verified the control and capacity of the furnace and have found its operation satisfactory for our requirements.

In order to meet the ASHRAE specifications presented earlier, the air distribution within the indoor room needs to be controlled. We designed and implemented the air-handling system shown in Figure 2.5. This system is located against the wall opposite the room air conditioner and takes advantage of buoyancy-driven circulation to control air movement. Air is drawn in through fine-mesh screens located on either side of the furnace and then over the heating elements by the furnace fan. The hotter air is then released through the lower screens and into the rest of the indoor room, where it rises due to its natural buoyancy. The screens are used to diffuse the air flow to increase mixing and to ensure that the air velocity within 3 ft of the test unit is less than 100 fpm. The selection of the screens is discussed by Fleming (1993).

2.1.3 Moisture Addition System

In the same way that our energy balance is used to determine the amount of heat being removed by the air conditioner, a moisture balance defines the latent capacity of the test unit. The amount of moisture entering the indoor room is measured and any latent heat losses are determined from moisture loss tests. The moisture addition system has to be able to produce a steam flow that is continuously variable between 0 and 27 lb_m/hr (the latent load of the largest test units). The steam should enter the indoor room air flow in front of the furnace exit screens for a few reasons. First, the air is hottest at this location and is able to hold more moisture than the rest of the indoor room air. Second, the moisture enters the air stream before it has mixed with the majority of the room air. This yields the greatest amount of mixing, and thus helps to reduce moisture concentration gradients within the indoor room. Another important requirement for the moisture addition system is that it not disturb the room bulk air flow. It is also crucial that the amount of moisture being added to the room be easily and accurately quantified.

Many types of humidifying systems were investigated for our application. We ultimately chose the barrel humidifier, shown in Figure 2.6, for reasons discussed by Fleming (1993). The system consists of a 24-gal stainless-steel drum with four

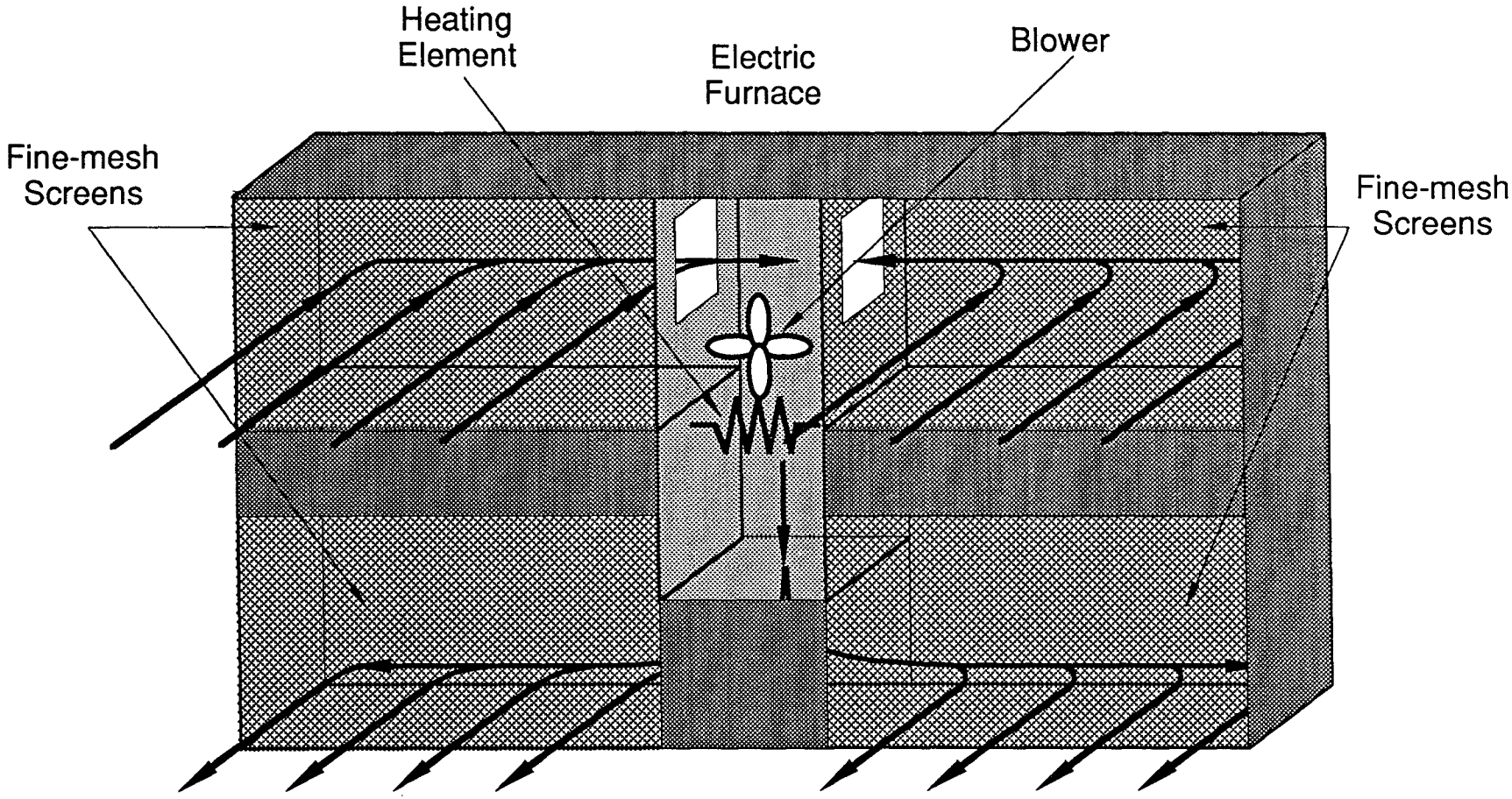

Figure 2.5 Indoor Room Air Distribution System

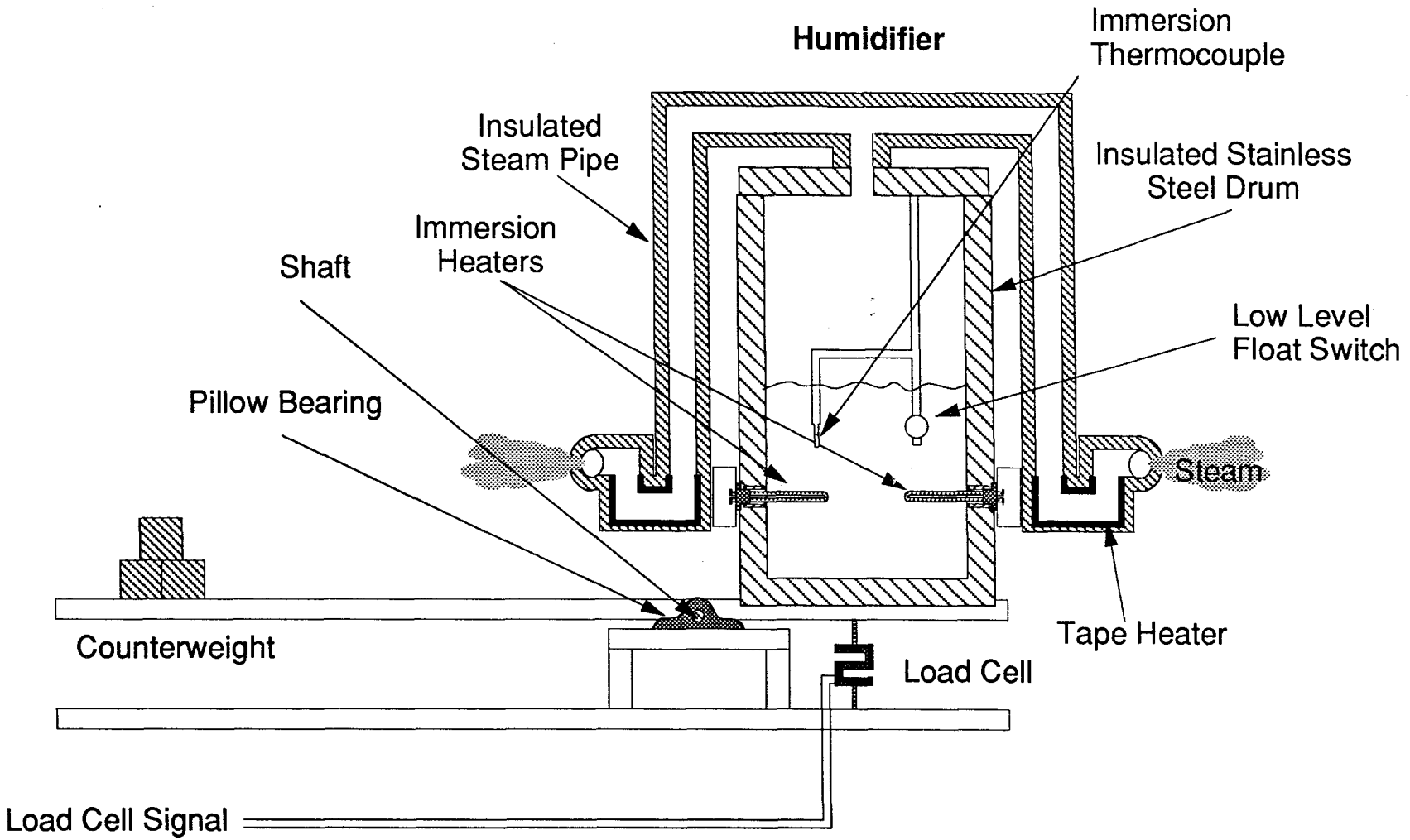

Figure 2.6 Barrel Humidifier and Moisture Addition Measurement System

immersion heaters welded to and extending through the barrel wall. Each heater delivers 2 kW of power to the system, and the 8 kW total can produce more than 27 lb_m of steam every hour. An insulated pipe network is attached to the barrel lid and allows the steam to be released into the air exiting the furnace screens. Because some steam is likely to condense within the copper pipes, a tape heater is wrapped around each U-bend to evaporate any condensate collected there. These heaters are operated by temperature controllers which maintain a temperature of 250 °F in the pipe bends. This ensures that all of the steam leaving the barrel enters the room. The drum was coated with several inches of polyurethane insulation and was then placed within a larger polyethylene barrel to protect the foam from damage. A thermocouple within the drum measures the water temperature and a float switch shuts off power to the heaters if the water level drops below a predetermined level. This ensures that the heaters are always immersed in water and do not exceed their temperature rating.

To measure the amount of moisture entering the atmosphere, we decided to measure the change in weight of the humidifier over time because this is a simple and direct measurement that is easily and accurately performed with a load cell. Because the resolution of the load cell depends on the maximum weight it can measure, we designed a counterweight system to reduce the size of the load cell needed. The entire humidifier is mounted on a platform which rests on a shaft that acts as a fulcrum. The counterweights are placed on the opposite end of the platform to balance the weight of the barrel and associated pipe network. A 50-lb_m load cell is located directly underneath the drum and measures the change in weight due to water evaporation. The position of the humidifier is fixed by two mounting brackets so that it is always centered over the load cell. Because the load cell can be used in tension or compression, we have a device that can effectively measure 100 lb_m in mass change. For our largest water removal rate (27 lb_m/hr), we can operate for almost four hours without refilling, which is adequate to achieve steady state moisture conditions.

The humidifier control is similar to that of the furnace and is shown in Figure 2.7. A microprocessor controller sends an on/off signal to a solid-state relay, which in turn opens and closes the circuit to the humidifier. Like the furnace, the power to the boiler shuts off when either the indoor or outdoor room exceeds 125 °F. In addition, the low-level float switch opens the heater circuit if the water drops within 4 in. of the heaters. The controller can be used in manual (controlling power) or automatic (controlling room humidity) mode, and its on/off duty cycle is set for 1 s to reduce transient effects. The energy used by the humidifier is metered with the previously mentioned indoor room power measurement system.

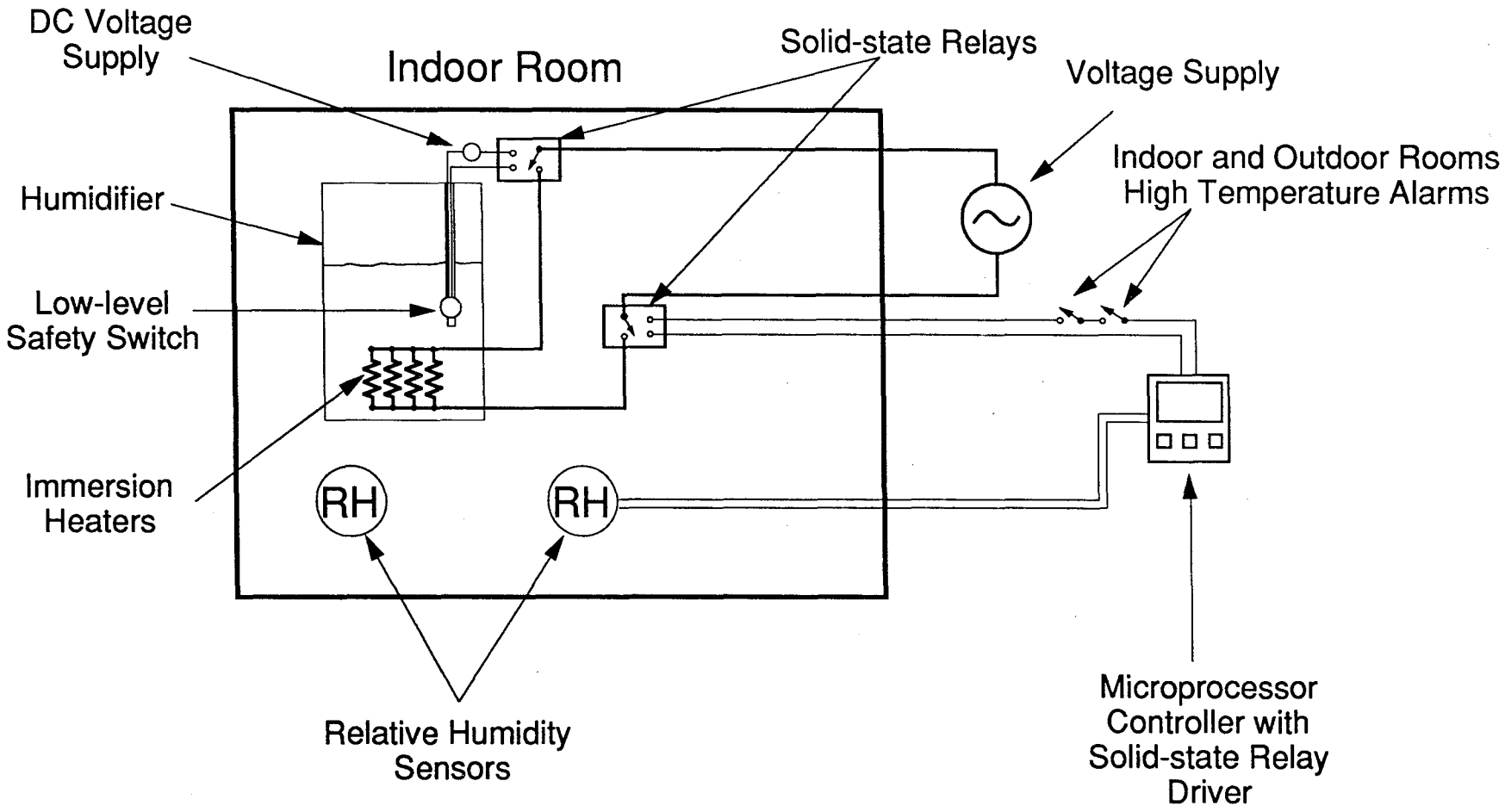

Figure 2.7 Humidifier Control System Schematic

We verified the accuracy and capabilities of the humidifier system prior to testing. The load cell has a rated accuracy of 0.1% of full scale, or 0.05 lb_m, and we verified this accuracy using a scale accurate to ±2.2e-5 lb_m. Our calibration tests indicated that we can achieve stable boiling and water removal rates, and that there is a proportional relationship between the power added and the moisture evaporated. We also detected a significant amount of fluctuation in the signal from the load cell due to vibrations caused by boiling within the humidifier. Because the signal ranges from 0 to 30 mV, it is greatly affected by this type of signal variation. This problem was overcome by continuously scanning the load cell reading and then averaging the signal once every 5 min when the other facility signals are logged. This restores the uncertainty in the load cell reading to ±0.05 lb_m. Although the actual load cell reading is somewhat temperature sensitive, its differential accuracy at each temperature is identical. This means that the load cell measures a change of one pound of water identically at 60 °F and at 120 °F. This provides for more than adequate measurement capability at any steady-state condition. The change in the load cell reading as a function of temperature has been determined and can be corrected for during transient testing.

A remote water-addition system enables the operator to add more water to the humidifier without removing the door to the indoor room. A section of PVC and brass pipe carries water from a fitting located in the outdoor room to the humidifier. The exit of the pipe is located directly over a small hole in the lid of the drum and allows water to drop into the barrel. Because the pipe is not attached to the humidifier, it does not affect the load cell reading. The operator simply attaches a hose to the outdoor room fitting and monitors the amount of water being added by watching the load cell reading on the datalogging equipment. Although water can be added at any time, the energy stored within the added water will introduce error into the indoor room energy balance. For this reason, we shall add water only between data points.

2.1.4 Indoor Room Instrumentation and Data Acquisition

2.1.4.1 Temperature and Humidity Measurements

The properties of the indoor room air are measured with two combined temperature and relative humidity probes. These probes are typically centered around the air conditioner and measure the temperature and relative humidity of the room air. Because the air within the indoor room is well mixed, the two sensors measure

properties that well represent those of the bulk air stream. Because the air conditioner itself introduces temperature and humidity stratification within the room, it is not necessary to eliminate that effect.

We chose this type of probe because it provides excellent accuracy for both temperature and relative humidity and is packaged in a small and unobtrusive unit. The temperature is measured with a platinum RTD, which has an accuracy of ±0.5 °F. The capacitive-type humidity sensor has an accuracy of 2% in the range of 0 to 90% relative humidity and 3% in the 90 to 100% RH range. We calibrated the humidity probes and verified that the rated accuracies were matched or exceeded in all cases (Fleming 1993). The temperature/humidity probes are housed within aspirated radiation shields to reflect incident radiation and to provide more accurate temperature measurement. Air is drawn over each probe with the use of an aspirating fan, which allows the probe to measure properties that are more representative of the bulk indoor room air. As shown in Figures 2.4 and 2.7, the probes are used to control the temperature and relative humidity within the indoor room.

The indoor room also contains twelve 30-gauge, type-T (copper-Constantan) thermocouples, which are attached to the floor, ceiling, and three of the room walls. These instruments monitor the temperature distribution within the room and help provide information to reduce unnecessary thermal stratification. As was previously mentioned, the humidifier contains a thermocouple to monitor the water temperature. Both types of thermocouples have an absolute accuracy of ±0.9 °F based on manufacturer data and are utilized to predict the thermal response of the indoor room, which is discussed in Chapter 3. We determined that the thermocouples have an accuracy of ±0.45 °F when used to measure temperature differences between two locations if the thermocouples are from the same batch of wire. Using thermocouples from the same spool reduces the uncertainty in the composition of the wires, and thus increases the chances that the thermocouples will produce similar results. It is still possible that there is some variation in the composition of the wire along the length of the thermocouple, but this effect cannot be eliminated.

2.1.4.2 Electrical Power Requirements and Measurement

The issues related to electrical power usage within the test facility are of extreme importance for the following reasons. The power used by the devices within the indoor room needs to be precisely measured to obtain a reasonable energy balance on the room, and thus determine the capacity of the air conditioner being tested. For the

same reason, all energy losses from electrical cables and wires, transformers, and junction boxes need to be accounted for. To achieve steady-state conditions, certain system components require regulated power sources. In addition, the distribution of the electrical panels must allow for easy access during testing. The panel distribution must also incorporate power measurement devices for the necessary facility components.

Power Distribution

The power panel distribution for the test facility is shown in Figure 2.8. The facility is supplied with 200 A, 240 V, three-phase power, which can be disconnected from the facility with the safety shut-off breaker. The power is then run through a secondary surge arrester (to protect the equipment from electrical transients) and to the main distribution panel. This panel distributes the necessary electricity to the system components, including the indoor room, air conditioner, chiller, and miscellaneous devices. The power to the indoor room is recorded by a power measurement device so that all energy added to that chamber is monitored and the indoor room energy balance remains accurate. The components that utilize this energy are the furnace, humidifier, tape heaters, mixing fan, aspirator fans, and the 240/120 V transformer. This transformer is placed within the indoor room so that the heat it dissipates (which is recorded by the power measurement device) is added to the indoor room. All indoor room devices other than the furnace and humidifier operate with 120 V power.

A voltage regulator is used to condition the power used by the air conditioner. We determined this was necessary because we observed fluctuations of ±5% in the voltage of the electricity supplied to the test facility. This fluctuation causes the power supplied to the indoor room and air conditioner to vary, and thus prohibits the facility from reaching a steady-state condition. When the furnace and humidifier are temperature and humidity controlled respectively (in automatic modes), the power supplied to these devices is automatically adjusted to overcome these fluctuations. However, because the air conditioner operates continuously at full power, its performance is directly affected by the supply voltage. This same problem affects the indoor room power if the controllers are used in manual mode. The regulator controls the voltage to within ±0.5% and has a response time of five cycles (0.0833 s). The power used by the air conditioner is measured downstream of the regulator so that the energy used by the regulator is not included. A watt transducer measures the power

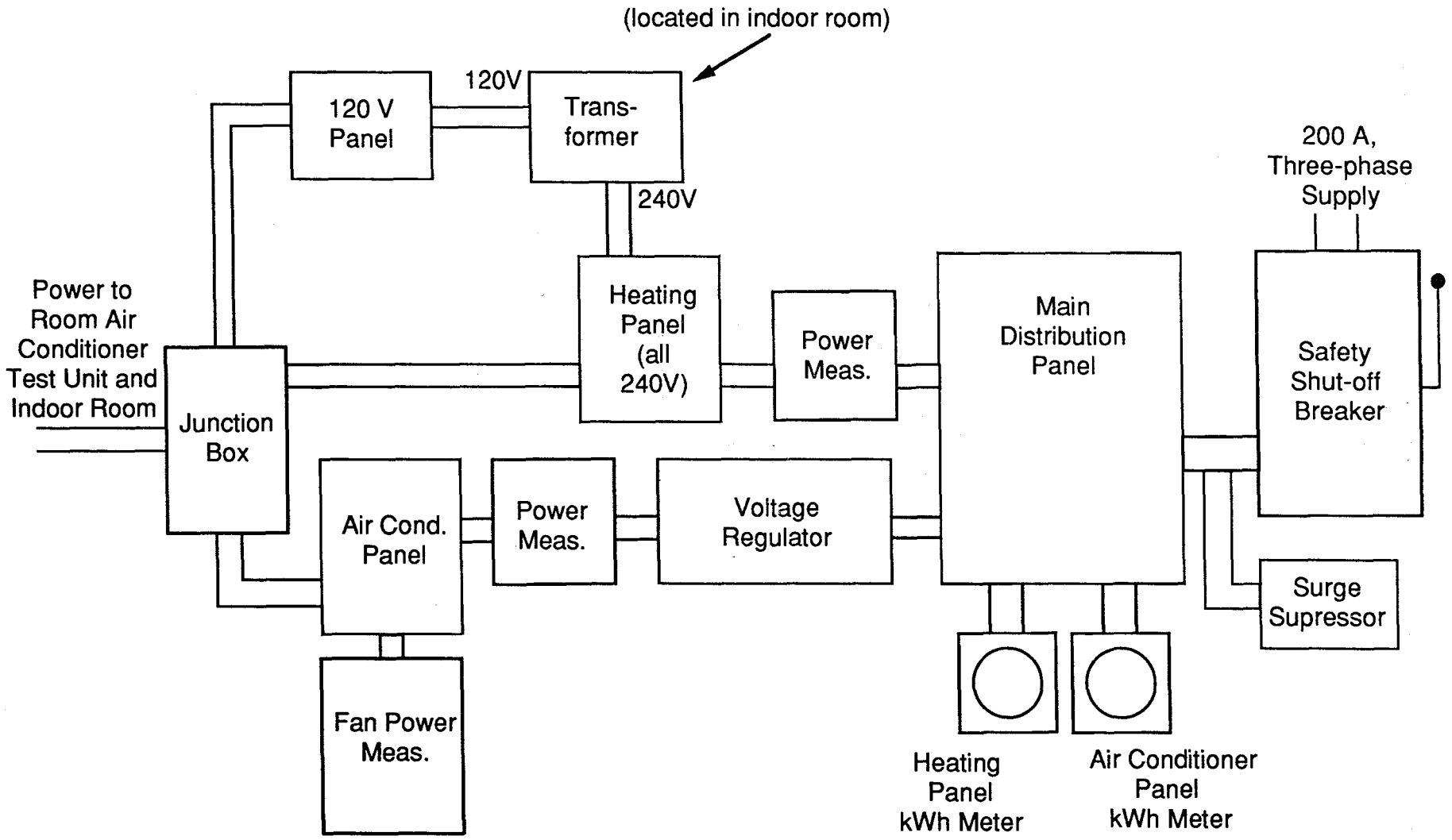

Figure 2.8 Room Air Conditioner Test Facility Power Distribution System

used by the air conditioner fans. For energy balance reasons, we calculated the energy lost through resistive heating of the electrical lines within the facility to be less than 2 W, and have thus neglected this loss.

All of the panels in Figure 2.8 (except for the transformer) are located in the outdoor room. This chamber has easy access during and between tests and allows the operator to turn electricity on and off to various system components quite easily. All indoor room subsystems, including the air conditioner, can be turned on from the outdoor room. This greatly reduces the need for the operator to remove the indoor room door, which provides significant time and effort savings.

Power Measurement

As has been previously mentioned, the measurement of the power used by the indoor room devices and the air conditioner is crucial in determining the performance of the test unit. In our current setup, the power used is displayed by the kWh meters shown in Figure 2.8 and is recorded by hand. The operator counts the number of turns on the dial and uses a stopwatch to determine the time elapsed. Based on comparisons with other power measurement devices, this method is accurate within ±1%. However, the major drawback is that continuous data is difficult to obtain. In addition, we wish to achieve greater accuracy in our power measurement. For these reasons, we have developed and designed a more advanced system to record the power used by the facility. All components of the final power measurement devices are in place and calibrated, with the exception of the digital signal processor. The following description discusses the final configuration of the power measurement system once the processor is received, installed and calibrated.

One of the power measurement devices records the energy added to the indoor room, which is used to determine the capacity of the air conditioner. The other device measures the power used by the air conditioner compressor and fans. The two measurements together determine the COP (coefficient of performance) and EER (energy efficiency ratio) of the test unit. The measurement devices are located in the guard space on the north side of the facility. We chose this location instead of the outdoor chamber because the guard space temperature is relatively cool and does not vary significantly with time. This assists in keeping the power measurement devices cool and helps maintain their rated accuracies. In addition, the measurement systems are located within five feet of the indoor room to minimize the electrical losses between themselves and the intended loads.

A schematic of one of the hybrid analog and digital power measurement assemblies is shown in Figure 2.9. A low-resistance, low-temperature-dependence current shunt is placed in series with one of the 240 V power lines. This precision resistor causes a small drop in voltage, which is read by the measurement system. Since the resistance of the shunt is accurately known, the voltage drop is directly proportional to the current passing through that conductor according to Ohm's Law. Thus, this measurement provides us with the current used by a particular circuit. A second voltage measurement is taken between the shunt and one of the other power lines. For the indoor room measurement device the other 240 V line is used, while for the air conditioner device either the neutral or 240 V line will connected depending on the type of air conditioner being tested. This second measurement simply measures the voltage of the power being supplied. By knowing the current and voltage, the real-time power use of a circuit can be determined.

The two voltage signals, one measuring load voltage and the other proportional to the load current, are fed to an isolation amplifier circuit. This device sets the gain and offset of each incoming signal and then scales it to a range that can be used by the components downstream within the measurement circuit. The amplifier circuit also helps to eliminate ground loops and provides intrinsic safety for high-current applications. The scaled voltage and current signals are then sent to a digital signal processor, which calculates the real-time power used by each circuit. The processor can also integrate the power signal over a user-specified time interval, so that a time-averaged power level can be determined. This capability is important since the indoor room controllers use on/off duty cycles to maintain constant conditions, and thus produce waveforms which are discontinuous and complex. Each digital signal processor provides four user-selectable analog outputs (such as voltage, current, and power integrated over different time intervals) that can be read by the data acquisition equipment. Each processor also consists of an RS-232 interface, which allows the operator to collect data digitally and to select options for the analog outputs through a personal computer. The complete power measurement system is designed to have an overall accuracy of 0.1%.

2.1.4.3 Data Acquisition and Reduction

The data acquisition for our facility is handled by a Fluke 2280 datalogger. This device reads all RTD, thermocouple, and voltage signals from the facility and converts all but the thermocouple signals to their proper units. For reasons that will be

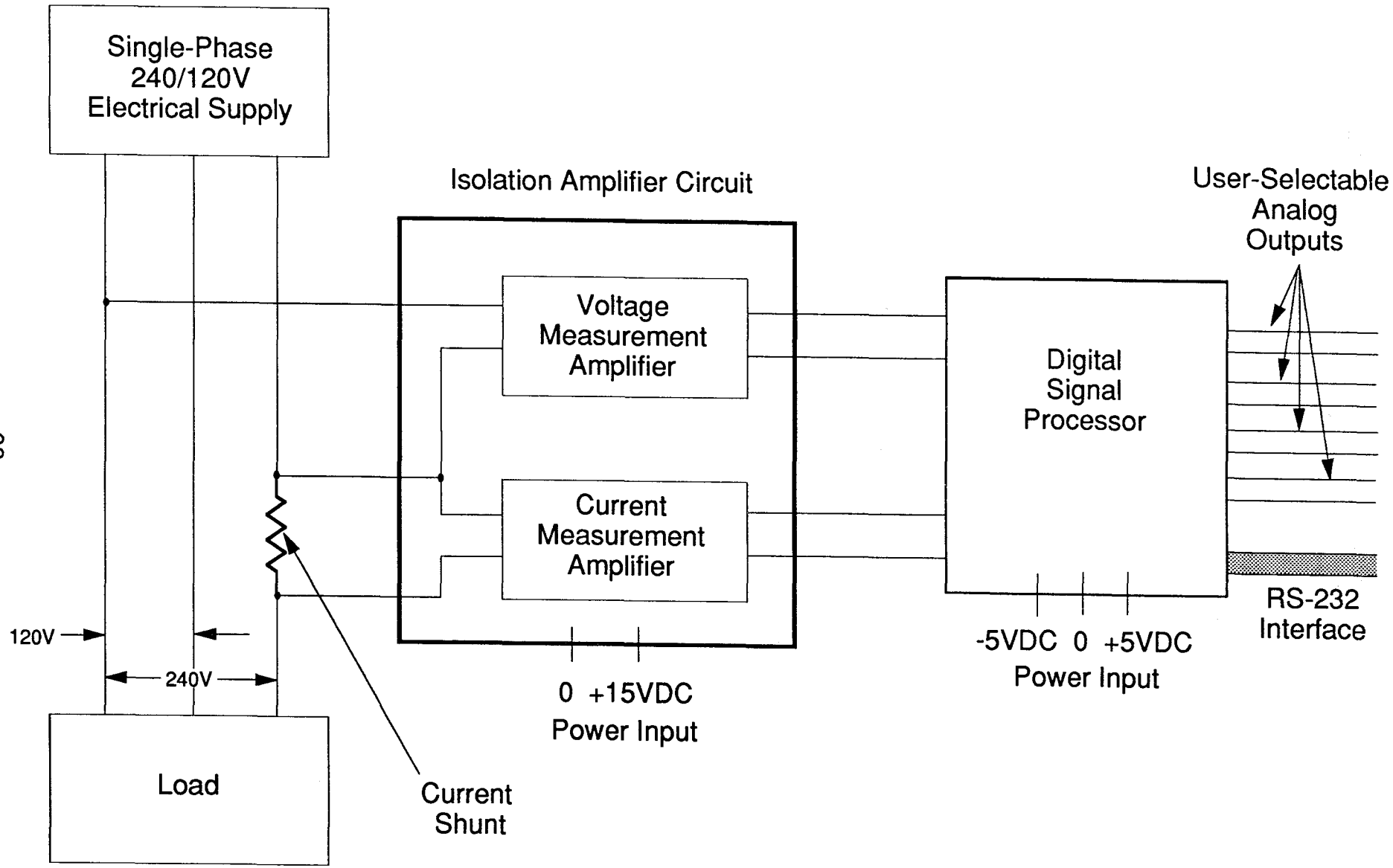

Figure 2.9 Power Measurement Schematic

discussed later, the thermocouple signals are converted within a separate data reduction program. After completing the initial data conversion, the datalogger sends the data to a laptop personal computer, which provides the user interface for the datalogger. Here the data is displayed on a screen and also saved on a floppy disk for further analysis by the data reduction program. This program completes the data reduction, calculates many additional values, and writes the output to a text spreadsheet, which can be accessed by various data-handling applications.

Although the datalogger can read up to 100 channels at a time, 20 of these channels are occupied by a RTD conversion board. This leaves 80 operational channels and over 100 possible measurements. However, since many of the measurements are not crucial in determining room or air conditioner performance and are used primarily for diagnostic purposes, these signals can be left unmonitored. The datalogger can read incoming signals at a maximum scan rate of 15 channels per second, although this speed is reduced somewhat if internal calculations are necessary to obtain the correct units. This limitation should not be a factor during steady-state testing, since scans are only necessary every few minutes.

The accuracy of the datalogger varies depending on what type of input signal is read. The RTD's for the indoor and outdoor rooms can be read to ±0.36 °F, whereas DC voltages can be read to ±0.03% of the input signal. These types of signals constitute most of the crucial measurements, including room temperatures and humidities, power used, and the humidifier load cell. For these signals, the capability of the datalogger is not the limiting factor in the overall accuracy of the measurements. Since some of the monitored signals contain significant amounts of electrical noise or signal variation (like the load cell reading that was discussed earlier), we employ averaging schemes which are selected within the datalogger software. Each noisy signal is scanned continuously and is averaged during each normal scan time. This method effectively eliminates most of the signal distortion from our measurements.

During the calibration of the thermocouples for the room air conditioners, we noticed significant temperature variation (up to 1 °F) among the beads, even when located within an isothermal bath. Further diagnostics indicated that errors in the assumed reference temperatures for the thermocouples were the source of this problem. In order to obtain an accurate thermocouple measurement, it is necessary to know both the temperature at the reference junction and the voltage induced between the junction and the bead of the thermocouple (at the item being measured). For each datalogger board there is only one reference temperature for twenty thermocouple measurements. Although the boards were designed to be isothermal, we found that

the temperature of the thermocouple junctions varied about one degree across the length of the board. This means that the reference temperature is not an accurate representation of all the junctions on the board, and leads to error in thermocouple measurements.

We eliminated this problem by bypassing the datalogger's reference temperature and using our own. We fabricated an isothermal junction box where all of our instrumentation signals are terminated before being sent to the datalogger. The box is well insulated and uses a thermistor to accurately determine the temperature within the box. The box was tested to demonstrate its isothermal nature and we found that the temperature was uniform throughout the box within 0.2 °F. The box temperature and thermocouple voltages are read by the datalogger as DC voltages (not thermocouples) and are converted to temperatures within the data reduction program mentioned earlier. We incorporated a similar isothermal box within the indoor room to house the thermocouple junctions for the room air conditioner being tested.

2.2 Design of the Outdoor Room

As was previously mentioned, we specified the range of temperatures and relative humidities for the outdoor chamber to be 70 to 120 °F and 5 to 95% RH. This necessitates that the outdoor room reconditioning equipment be capable of removing all sensible and latent heat rejected by the air conditioner. Since an air conditioner rejects more energy to the outdoor room than it removes from the indoor side, the outdoor reconditioning equipment must have a significantly higher capacity than the test unit. Also, the outdoor room bulk air flow should meet the requirements dictated by the ASHRAE Standard (ASHRAE 1984). This chamber houses several previously mentioned subsystems, including the power distribution panels, the air conditioner cart, and the unistrut support frame for the partition wall.

2.2.1 Physical Attributes

The outdoor chamber of the test facility is 14.75 x 10 x 8.5 ft and is intended to simulate the ambient conditions outside of a house or room. No additional insulation was added to this room since minimizing the heat loss from this chamber is not of great importance. The existing walls already contain a 3-in. sheet of fiberglass insulation on all sides, and a 6-in. layer in the ceiling guard space. These walls are covered with two coats of a latex vapor barrier paint and all joints and cracks are

sealed with silicone caulk. Most cracks and seams are also covered with the same aluminum foil tape that is utilized in the indoor room. All PVC conduit used for housing instrumentation lines are sealed with waterproof clay to eliminate air exchange to the indoor room or guard spaces. Several gaskets were added to the outdoor chamber door to minimize air and moisture leakage in that area. A 3-in.-thick polyisocyanurate foam door was built to reduce heat losses through the doorway, but is not permanently attached to the facility. This allows for visual inspection of the outdoor room during testing.

2.2.2 Reconditioning Equipment

We investigated many options for the cooling and dehumidification requirements of the outdoor chamber of our test facility before choosing the chiller and fan/coil unit shown in Figure 2.10. A complete discussion of the issues in this selection process is presented by Feller (1993). A large water chiller supplies cold fluid to a heat exchanger coil located in the outdoor room. A fan circulates the outdoor room air over the coil, thus cooling down the air and heating the chiller fluid. The warmer fluid then returns to the chiller and the added energy is removed by another water-to-air heat exchanger. A control valve is placed in parallel with the coil to vary the amount of chiller fluid being circulated through the coil itself, thus controlling the coil heat transfer and, in turn, the outdoor room temperature. The temperature of the cooling fluid determines the outdoor room dew point, and thus relative humidity. Our goal for the design of the outdoor chamber specifies that the temperature and humidity be independently controllable. This goal was somewhat achieved, although not to the extent that was desired, and is discussed later.

2.2.2.1 Reconditioning System Components

We purchased a 7-ton (24.6-kW) air-cooled recirculating chiller to provide the sensible and latent cooling for the test facility. We chose an oversized unit for several reasons. First, the capacity of the chiller decreases with either increasing ambient air temperature, or decreasing circulating fluid temperature. Second, there can be significant heat transfer in the lines between the chiller and the coil, as well as within the chiller itself, that reduces its effective capacity. Third, the extra capacity of the chiller allows for more rapid changes in the outdoor room conditions. The chiller is located in a workspace adjoining the test facility, and the fluid is circulated to the coil

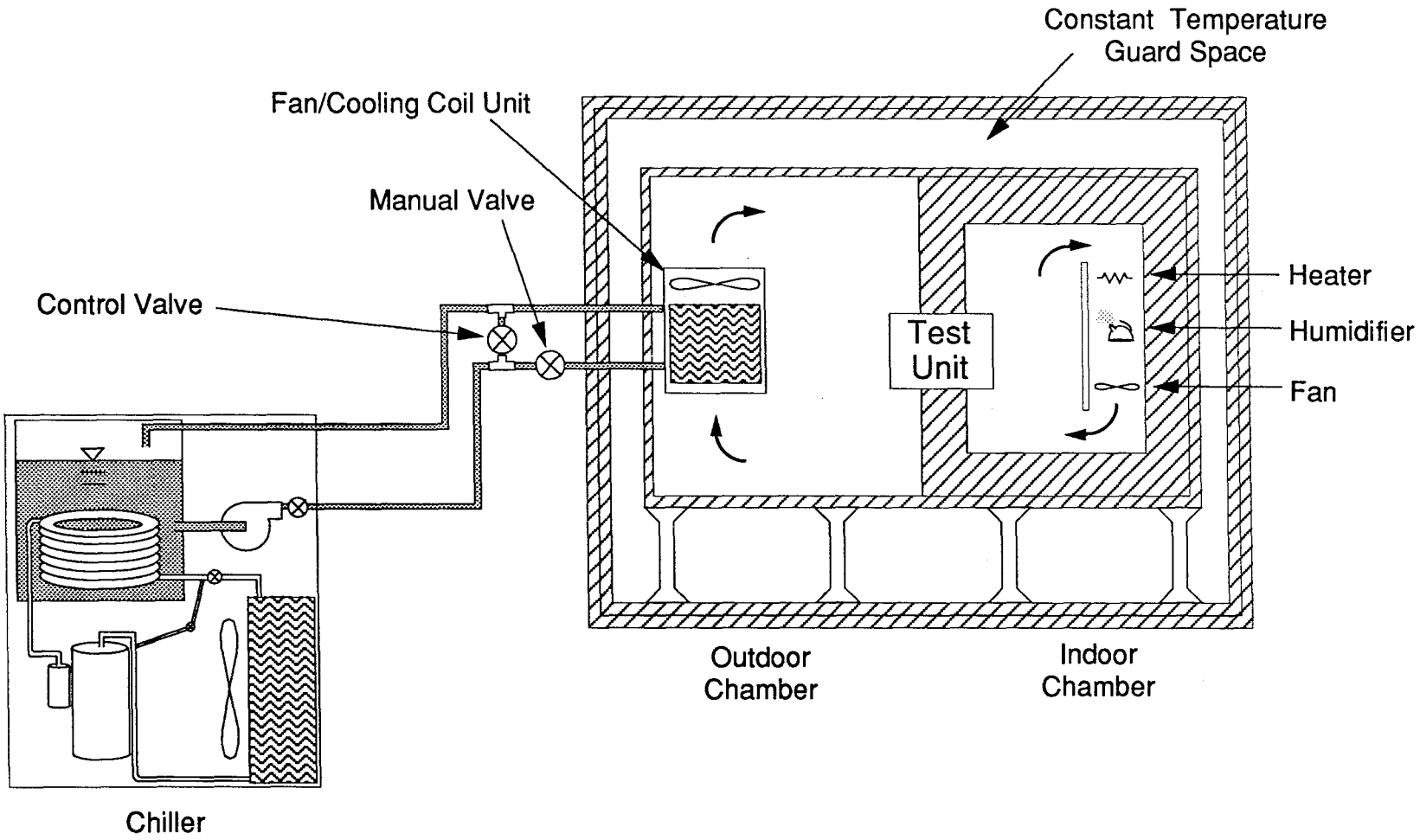

Figure 2.10 Chiller and Fan/Coil System

through 1-in.-diameter flexible hoses. The chiller contains a 2.5-hp centrifugal pump to circulate the working fluid around the loop.

The chiller can supply water in the temperature range of 8 to 35 °C, or a water and ethylene glycol mixture in the -15 to 35 °C range. The ethylene glycol mixture allows the unit to operate at below-freezing temperatures. The temperature of the fluid within the outdoor room coil determines the dew point of the room air. A microprocessor controller is used to maintain a steady chiller reservoir tank temperature, which also provides a stable outdoor room relative humidity. Unlike the furnace and humidifier controllers, this controller outputs a continuous signal proportional to the desired chiller tank temperature. The chiller is rated to provide a ±0.1 °C temperature stability, and achieves this control with the use of an internal hot-gas bypass system.

A packaged fan/coil unit transfers energy from the outdoor room air to the chiller working fluid. The coil is rated to remove up to 4.5 tons (15.8 kW) of combined sensible and latent heat and utilizes a 1500-cfm blower to draw the outdoor room air over the heat exchanger tubes. After the air passes over the coil, it is released into the outdoor room through a rigid foam manifold. This exhaust system ensures that the air velocity within three feet of the air conditioner is less than 100 fpm, in compliance with the ASHRAE Standard (ASHRAE 1984). Although the Standard specifies that the reconditioning equipment circulate at least twice as much air as the condenser fan, our present testing apparatus will not be adequate for the larger air conditioners (2 tons and larger). We decided to deviate from the Standard on this point because we are using it only as a guide for the construction of our test facility, and not as a set of fixed requirements. This deviation also allowed us to realize a significant time and money savings, because this particular unit was a stock item. Because the fan/coil package removes significant amounts of latent heat in addition to sensible heat, a drain was installed in the base pan of the unit to remove the condensed moisture.

In order to obtain automatic control for the glycol flow rate through the coil, a pneumatic-actuated control valve was placed in parallel with the coil. The valve requires a 35-psig air supply to physically move the valve stem, which is delivered by a continuous operation air compressor. We also inserted a manual valve in the coil line to add further control to the coil flow rate. This manual valve is adjusted to an optimal position and then left alone for all tests with a particular air conditioner. As was stated before, the amount of flow circulated through the coil is used to determine the temperature of the outdoor room. A microprocessor controller reads the outdoor room temperature and uses a milliamp signal to indicate the desired valve position.

Then the pneumatic positioner adjusts the valve stem accordingly to maintain a steady outdoor room temperature.

We decided not to place the control valve in series with the coil for two main reasons. First of all, if the pressurized air source is lost, the valve closes and cuts off flow to the coil. This in turn causes the chiller to shut off and thus eliminates the heat removal source from the outdoor room. Because a large amount of energy is being added to the outdoor chamber by the air conditioner, a loss of coolant would cause the room temperature to rise substantially and might threaten the structural integrity of many outdoor room components. Secondly, placing the valve in series introduces more pressure drop into the chiller loop than putting it in parallel. Since the chiller uses a centrifugal pump to circulate the ethylene glycol mixture through the coil, an increased pressure drop would decrease the flow through the coil, and would thus reduce its maximum capacity. This would make it difficult, if not impossible, to test the largest air conditioner units. For these two reasons, we decided to place the control valve in parallel with the coil.

2.2.2.2 Reconditioning System Performance

During preliminary testing, we verified that the outdoor room reconditioning equipment operated to our satisfaction with one exception. We observed that we were not able to independently control the outdoor room temperature and relative humidity over the full desired ranges. We determined that this is due to low air-side heat transfer in the fan/coil unit. Heat transfer through a heat exchanger is often expressed with the equation

$$\dot{q} = \varepsilon \left(\dot{m} c_p \right)_{min} \left(T_{hot,in} - T_{cold,in} \right) \qquad (2.1)$$

where

$\dot{q}$ = coil heat transfer

ε = coil heat exchanger effectiveness

$\left(\dot{m} c_p \right)_{min}$ = the smaller mass flow rate-specific heat product between the air and ethylene glycol mixture

$T_{hot,in}$ = inlet temperature of the hotter fluid (air in this case)

$T_{cold,in}$ = inlet temperature of the colder fluid (ethylene glycol mixture).

When the control valve is fully closed (so that all chiller flow goes through the coil), the $\dot{m}c_p$ product for the glycol is more than twice that of the air. For example, if the glycol mass flow rate is reduced by 30%, the heat transfer through the coil is almost unchanged since the air still has the minimum $\dot{m}c_p$ product, and since the other values in Equation 2.1 remain essentially the same.

Because of this relationship, using the glycol mass flow rate to control the energy removed from the outdoor room is only effective if the $\dot{m}c_p$ for the glycol is smaller than that of the air. This method of control can be utilized by significantly reducing the glycol mass flow rate, but this also causes the heat transfer rate through the coil to be too small to remove all of the energy entering the outdoor room. The glycol control scheme can be effective if the air mass flow rate was increased such that the $\dot{m}c_p$ of the air was larger than that of the glycol. This option would require a higher-capacity fan and possibly a larger coil. Another way to independently control the outdoor room temperature is to vary the air mass flow rate with a variable-speed blower. We have considered both of these options for achieving the independent humidity and temperature control we originally desired. However, we will first decide if the current effectiveness of the control valve is acceptable for the tests we anticipate to run.

2.2.3 Outdoor Chamber Instrumentation

Like the indoor chamber, the outdoor room also contains two combined temperature and relative humidity probes to measure the air properties. These probes are also centered around the air conditioner and are located in a well-mixed air stream. The accuracies of the probes is the same as those found in the indoor room. We attached fourteen type-T thermocouples to the ceiling and walls of the outdoor room for diagnostic purposes. In addition, we use four thermocouples to measure the temperature of the guard spaces on four sides of the facility. These measurements are important to calculate the heat loss through the walls of the indoor room. We have also installed thermocouples on the pipe surfaces of the inlets and outlets of both the chiller and the coil, as well as in the inlet and outlet air streams of the coil. These are used to estimate the magnitude of heat transfer occurring in these heat exchangers

and to verify their cooling capacities. All outdoor chamber thermocouples have the same accuracies as those found in the indoor room. The chiller loop also contains pressure gauges at the inlets and outlets of the chiller and coil to monitor pressure drops throughout the glycol loop.

2.3 Room Air Conditioner Instrumentation

The instrumentation of the air conditioners themselves provides us with the following major challenges. Since most units are tightly-arranged packages, there is often a space limitation which must be overcome. Thus, the added measurement devices must be small enough to be placed within the existing air conditioner package. The interfacing of instrumentation with the test unit introduces a second concern. Certainly, we wish to obtain measurements that are as accurate as possible to calculate capacities, pressure drops, and heat losses in the various system components. However, it is difficult to achieve great accuracy in most measurements without introducing some disturbances to the original system. For example, using an immersion thermocouple to measure the refrigerant temperature within a tube provides more accuracy than does a surface thermocouple. However, the flow disturbances introduced by the immersion probe affects the temperature of the fluid at that point. Thus, there is a trade-off between the accuracy and the intrusiveness of most measurements.

For this reason, future work will attempt to quantify the effects of adding various levels of instrumentation to the air conditioners we test. For the first step, we will add thermocouples to the surfaces of the refrigerant tubes, and to the air-side inlets and outlets of the evaporator and condenser. The surface thermocouple measurements are fairly unobtrusive, yet they may not accurately monitor the fluid temperature within the refrigerant tubes. After a full set of tests are run on the unit in this condition, we will add immersion thermocouples and pressure gauges to measure refrigerant properties. These devices will most likely introduce more disturbances to the refrigerant flow than the surface thermocouples, yet they should also provide more accurate properties. By comparing the change in performance of the air conditioner, we can determine the effect of the increased instrumentation on the operation of the unit. This will hopefully lead to an increased understanding of the optimal amounts and locations of air conditioner instrumentation.

We currently take several additional steps to increase the certainty of our measurements. First, we measure the volume flow rate of the air circulated through

each air conditioner fan. We also run all air conditioner thermocouples through an isothermal box located within the indoor room. The junctions in this box enable the air conditioner and its instrumentation lines to be removed from the facility, while leaving the lines from the isothermal box to the data acquisition unit intact. This allows for easy switching between test units during facility operation. Keeping the box at a uniform temperature helps reduce errors than can be introduced by temperature gradients at thermocouple junctions. In future work, we will drain and refill the refrigerant in all units that we test. This will ensure that we know precisely how much refrigerant is present within each air conditioner, and will help us to gain experience with recharging systems.

2.3.1 Air-side Instrumentation

2.3.1.1 Air-side Thermocouples

As of this time, we have fully instrumented a one-ton air conditioner with 33 type-T thermocouples to measure air temperatures at various locations. We placed a grid of eight thermocouples immediately upstream of the evaporator coil and another grid downstream to measure the thermal gradients found in these areas, and to check the accuracy of using the air-side data to perform energy balances on the evaporator. We also added three more thermocouples at the outlet of the evaporator fan to determine the amount of energy added to the air stream by the fan itself. The condenser is instrumented with a grid of six thermocouples on both the upstream and downstream sides of the heat exchanger. Like the evaporator measurements, these thermocouples can be used to monitor thermal gradients and to calculate energy balances. We also placed two thermocouples at the condenser air intake grill. The number and spacing of the thermocouples in the air-side grids was chosen somewhat arbitrarily to obtain the most representative measurements of the air flow temperature at each location.

2.3.1.2 Surface Thermocouples

Our current test unit is instrumented with more than 30 additional thermocouples that are attached to various tube surfaces of the refrigerant loop. These are used to measure refrigerant temperatures, which can provide information about transition zones, heat losses, and component capacities. They are attached to the tube surfaces with thermally conductive but electrically resistive epoxy. This adhesive aids

heat transfer from the tube to the thermocouple bead so that it essentially reads the tube surface temperature. However, the electrical resistance of the epoxy helps to eliminate erroneous readings due to stray currents within the test unit. Each thermocouple is covered with a section of polyurethane insulation to help read a more accurate tube surface temperature. For this reason, the thermocouples are typically attached in areas where heat transfer is not intended to occur, such as the return bends of each heat exchanger and the compressor inlet and outlet. Thus, the insulation does not affect the performance of the test unit in any significant way.

Although installing thermocouples on tube surfaces is a fairly easy way to determine the refrigerant temperature, it is not the most accurate. An immersion thermocouple introduces the least amount of error when determining the fluid temperature, because the only thermal resistance between the bead and the refrigerant involves the heat transfer coefficient of the fluid. Since refrigerant typically moves at a relatively high velocity through the loop, the heat transfer coefficients in most areas are large, thus meaning that the immersion thermocouple reads very close to the fluid temperature. On the other hand, the heat transfer between a surface thermocouple and the refrigerant depends on the fluid heat transfer coefficient, the thermal conductivity of the tube, and the quality of the insulation covering the bead. The last two factors increase the thermal resistance between the bead and the refrigerant, and thus introduce more error into the surface thermocouple measurement. However, confidence in the surface measurement is increased because the thermal conductivity of copper tubes is very high, and the insulation eliminates most of the air-side heat transfer from the thermocouple. The precise effectiveness of the thermocouples depends on the air and refrigerant velocities at each location, as well as the quality of the epoxy bond and the size of the polyurethane insulation. A more complete discussion of the accuracy of surface thermocouple measurements is presented by Porter (1994), where he suggests that the majority of our measurements should be accurate within ±5%.

2.3.1.3 Air Flow Measurements

To obtain accurate energy balances from the air-side data, it is necessary to know the air volumetric flow rate circulated through both the evaporator and condenser fans on each test unit. A partial data set is usually provided by the manufacturer, but more extensive data is typically necessary to determine these values at all conditions. Also, it is reasonable to check the numbers supplied by the

manufacturers to validate their accuracy. In addition, it is important to note if the airflow rates are sensitive to any of the parameters involved with the operation of the air conditioners, such as temperature, power supplied, etc. For these reasons we designed and constructed a volume air flow measurement system. A complete description of the measurement apparatus and results is found in Appendix A.

2.3.2 Refrigerant-side Instrumentation

None of the units we currently possess contain any refrigerant-side instrumentation. As mentioned earlier, we plan to implement this level of instrumentation after completing air-side data collection. At that point, we shall add approximately eight immersion thermocouples at certain locations throughout the air conditioners. We will certainly place one thermocouple at the inlet and outlet of both the evaporator and condenser to obtain accurate heat exchanger capacity information. Some likely locations for the remaining instruments are in the lines near the compressor and accumulator.

We also plan to add five or six pressure gauges to the refrigerant loop. Each heat exchanger will have two gauges; one to measure the absolute pressure at the inlet, and one to measure the pressure drop across the heat exchanger. These measurements will be important to obtain high-accuracy energy balances from refrigerant-side data. We will also use a differential pressure gauge to measure the pressure difference between the top and bottom of the accumulator. This difference will indicate the liquid level within the accumulator, and will thus provide information about the distribution of charge throughout the system. Another differential gauge may be placed in the suction line to monitor the pressure drop there.

3. TEST RESULTS FROM FACILITY OPERATION

There are several purposes for gathering data with our room air conditioner test facility. The first and most important reason is to verify that the facility can produce useful results regarding air conditioner performance. Without confirming the validity of the data collected, all information obtained for future purposes is of dubious value. The validation of the facility is primarily determined by comparing the data we collect to those obtained by manufacturers for similar test units. The validation also depends on the accuracy of the calibration of each facility subsystem, which is discussed in Chapter 2.

Once we validate our test facility, we can use it to meet the second primary objective of testing: to validate and improve a simulation model that predicts room air conditioner performance. This model is currently being modified to more accurately represent the operation of each test unit. A complete description of the simulation program is presented by Mullen (1994). Once the model is validated, it will be used as a design tool to predict air conditioner performance with various components, geometries and refrigerants. Another purpose behind testing is to observe trends in performance when temperatures, humidities and fan speeds are varied. In addition, we wish to accurately determine the heat transfer into and out of each of the system components. This information helps identify possible improvements on both the component and system levels.

Testing within our facility falls into two general categories: facility characterization tests and air conditioner performance tests. We perform characterization tests to better understand the accuracy and response characteristics of the test facility. Some characterization tests involve quantifying the amount of energy transfer (in the form of both sensible and latent heat) that occurs when the air conditioner is not operating, so that the amount distributed by the air conditioner during performance testing can be separated out. Other tests identify the time response of the facility to changes in sensible or latent heat added. After the operation of the facility is understood, we can run air conditioner performance tests to gain an understanding of each test unit. These tests are described in further detail in Section 3.2.

3.1 Facility Characterization Tests

3.1.1 Indoor Room

As mentioned previously, the energy balance on the indoor chamber of the facility needs to be highly accurate in order to determine the capacity of the test unit. Thus, we need to perform characterization tests to measure the energy that is not removed by the air conditioner, which we refer to as parasitic losses. When the furnace adds sensible heat to the room, some of the energy is lost through the chamber walls and other openings while additional energy is stored within the walls themselves. By running steady-state and transient sensible heat tests, we can quantify these parasitic losses. Because the indoor room also contains a moisture source, we run similar tests to quantify the moisture losses from the indoor room. Table 3.1 summarizes the primary results from the facility characterization tests performed on the indoor room. The following sections discuss the tests and results in detail.

3.1.1.1 Sensible Heat Loss Tests

Steady-state Results

In order to quantify the sensible heat loss from the indoor room, we ran several tests in which we added a known amount of power and recorded the final steady-state temperatures of the indoor room air and of the surrounding air spaces. These tests are used to calculate the effective thermal resistance of the indoor room in various configurations. Once the facility reaches a steady-state condition, we calculate the power removed by the air conditioner to be the power entering the indoor room (which is measured) minus the power lost through the walls and other openings (which is quantified by the steady-state heat loss tests). For the first tests we removed the air conditioner from the partition wall and sealed this opening with a 12-in.-thick foam plug. We then added a 100-W light bulb to the indoor room and used a variac to control the power supplied to the light. We operated the light at four different power levels and recorded the air temperatures throughout the facility once a steady-state condition was achieved. The results from these tests are shown in Figure 3.1. Since the only mode of heat transfer from the indoor chamber is conduction through the walls, the heat loss can be expressed as

Table 3.1 Summary of Indoor Room Facility Characterization Tests

TEST	RESULTS
SENSIBLE HEAT LOSS	
STEADY STATE	
Indoor Room Sealed	UA_{walls} = 7.8 Btu/hr–°F
Air Conditioner in Wall but Not Operating	$UA_{a/c\text{-}off}$ = 2.7 Btu/hr–°F
Air Conditioner Fans Operating	f_{fan} = 0.33, $UA_{a/c\text{-}on}$ = 11.8 Btu/hr–°F
TRANSIENT	
Air Conditioner in Wall but Not Operating	Forcing function sets time to steady state at approximately 200-250 hr
Air Conditioner Fans Operating	Forcing function sets time to steady state at approximately 40-100 hr
LATENT HEAT LOSS	
Air Conditioner in Wall but Not Operating	$UA_{m\text{-}off}\rho_g$ = 0.72 lb_m air/hr, forcing function sets time to steady state at 160 hr, 6% of heat transfer through test unit due to quasi-diffusional effects
Air Conditioner Fans Operating	$UA_{m\text{-}on}\rho_g$ = 14.5 lb_m air/hr, forcing function sets time to steady state at 12 hr, 29% of heat transfer through test unit due to quasi-diffusional effects

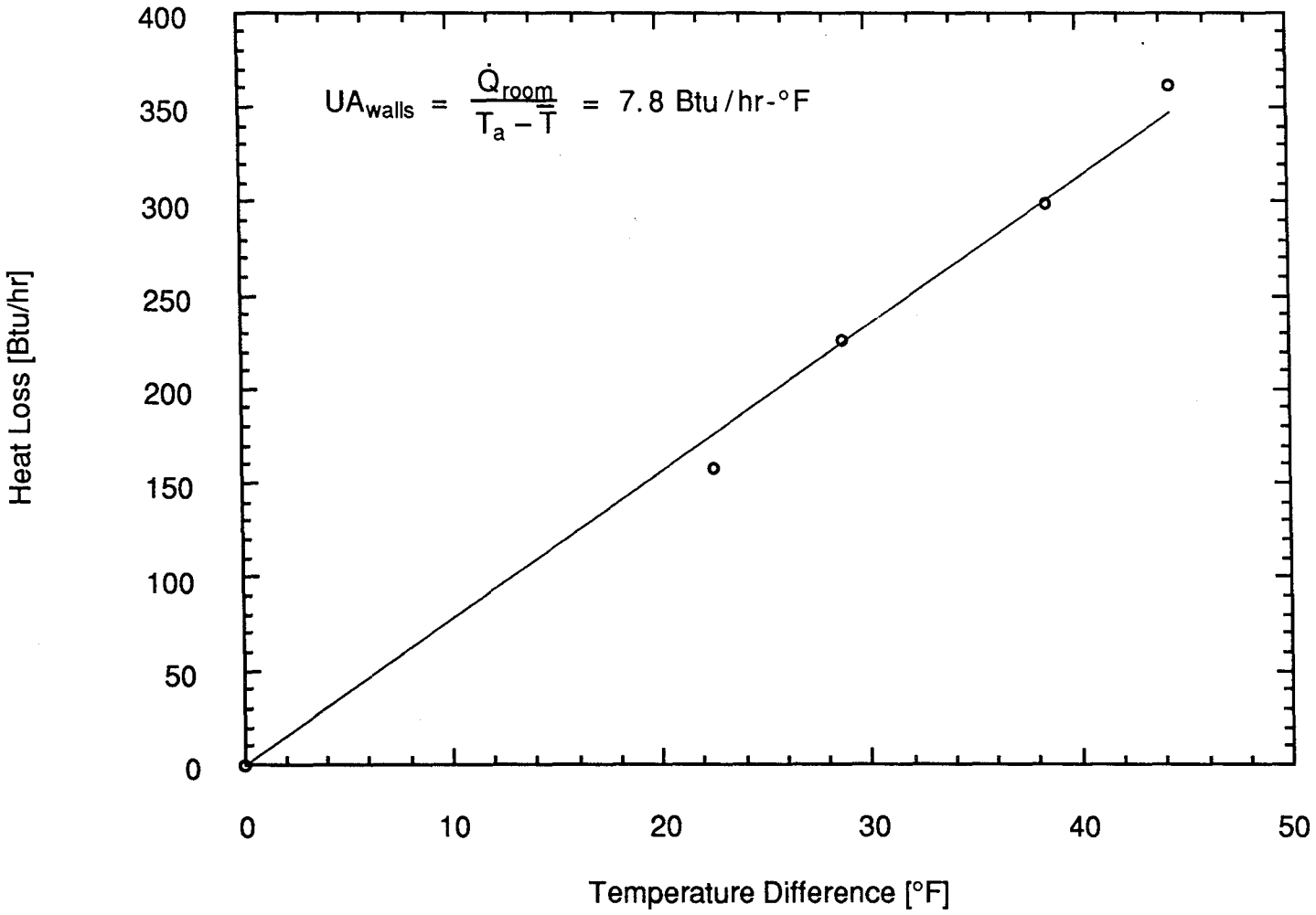

Figure 3.1 Steady-state Heat Loss with Plugged Wall

$$\dot{Q}_{room} = UA_{walls} (T_a - \overline{T}) \quad (3.1)$$

or

$$UA_{walls} = \frac{\dot{Q}_{room}}{T_a - \overline{T}} , \quad (3.2)$$

where $\dot{Q}_{room}$ is the power added to the room, UA_{walls} is the effective thermal conductance of the walls, T_a is the steady-state indoor room air temperature, and $\overline{T}$ is the steady-state area-weighted average temperature of the air spaces surrounding the indoor room. The use of Equations 3.1 and 3.2 assumes that all of the indoor chamber walls act as a lumped resistance, which is a good approximation for most heat loss tests since all of the surrounding air temperatures are relatively similar. $\overline{T}$ is given by

$$\overline{T} = \frac{1}{A} \sum_{i=1}^{6} A_i T_i \quad (3.3)$$

where A_i is the area of one of the six walls of the indoor room, T_i is the corresponding temperature of the air surrounding the indoor room on that side, and A is the total surface area of the indoor chamber walls. Figure 3.1 indicates that UA_{walls} = 7.8 Btu/hr–°F. This value is used to determine the parasitic losses due to other heat transfer mechanisms once the air conditioner is mounted in the partition wall.

The second set of heat loss tests was run with a 1-ton Amana air conditioner installed in the test facility but not operating. We operated the indoor room at two different power levels with the air conditioner turned off to quantify the parasitic heat loss through the test unit itself. The heat loss from the indoor room in this configuration is

$$\dot{Q}_{room} = UA_{walls} (T_a - \overline{T}) + UA_{a/c\text{-}off} (T_a - T_o) , \quad (3.4)$$

where $UA_{a/c\text{-}off}$ is the effective thermal conductance of the air conditioner when not operating, and T_o is the steady-state temperature of the air in the outdoor room. This equation can be rearranged to solve for $UA_{a/c\text{-}off}$:

$$UA_{a/c\text{-}off} = \frac{\dot{Q}_{room} - UA_{walls}\,(T_a - \overline{T})}{T_a - T_o} \quad . \tag{3.5}$$

By measuring the power entering the room and the steady-state air temperatures in the facility for the two tests, we calculate $UA_{a/c\text{-}off}$ to be 2.7 Btu/hr–°F. This heat loss is due to (a) air exchange between the indoor and outdoor chambers through cracks in the test unit and (b) conduction through the test unit. Although these tests don't provide any information about how much of the loss is due to each heat transfer mode, a latent heat loss test to be described later is able to shed more light on this issue. It should be noted that since different test units have different designs, it is necessary to repeat all steady-state and transient heat loss tests for each new unit to be performance tested.

A third set of heat loss tests was run with the same configuration as the last, except that the air conditioner fans (but not the compressor) were operating at high speed. These tests were run to see if the increased circulation had any effect on the heat loss through the air conditioner. The calculation of the heat loss for these cases is slightly more complex than before. Not only do the fans increase the circulation, but they also dissipate power into the air. Since both the evaporator and condenser fans are attached to the same shaft and motor, it is difficult to know how much of the power used by the fans is dissipated in the indoor and outdoor rooms, respectively.

To address this uncertainty we ran two tests with the air conditioner fans on: one with no power source other than the air conditioner fans, and one with a second power source in the indoor room. We measured the power used by the indoor room source and the air conditioner, as well as the temperatures around the facility. By performing an energy balance on the indoor chamber we obtain the equation

$$\dot{Q}_{room} + f_{fan}\,\dot{Q}_{fan} = UA_{walls}\,(T_a - \overline{T}) + UA_{a/c\text{-}on}\,(T_a - T_o) \quad , \tag{3.6}$$

where f_{fan} is the fraction of the fan power that goes directly to the indoor chamber, $\dot{Q}_{fan}$ is the power used by both fans, and $UA_{a/c\text{-}on}$ is the effective thermal conductance of the air conditioner with the fans on. Since both f_{fan} and $UA_{a/c\text{-}on}$ are unknowns, we must use the data from both tests to solve for these values. When the necessary measured quantities are inserted into Equation 3.6, we calculate that $f_{fan} = 0.33$ and $UA_{a/c\text{-}on} = 11.8$ Btu/hr–°F. Thus, about one-third of the power used by the air conditioner fans is dissipated directly into the indoor room air. Also, the heat lost

through the air conditioner alone increases by more than 300% when the fans are operating. The increased UA for the air conditioner indicates that the steady-state heat loss through the test unit is roughly as significant as that lost through the walls. This UA value is too large to ignore relative to the capacity of the test units. For example, a test run with a 1-ton test unit and a 20 °F temperature difference between the indoor and outdoor rooms would expect to show 236 Btu/hr heat transfer through the unit. If the capacity is roughly 12,000 Btu/hr at that condition, then the heat loss is approximately 2% of this capacity, and certainly needs to be accounted for. Again, energy is transferred through the air conditioner by a combination of air exchange and conduction. The magnitudes of the losses due to each heat transfer mode are determined from a moisture loss test to be described later.

Transient Results

From the results of the steady-state heat loss tests, we noticed that there is another issue that is important to the indoor room energy balance. The transient response of the indoor room depends on two primary factors: the thermal mass of the room and the forcing function used to introduce a change in conditions. For all tests the thermal mass of the room remains essentially constant. However, the forcing functions that are used to change conditions can vary significantly between test configurations. For example, operating the facility with the air conditioner off generates a much different response time than operating it with the test unit on. Thus, it is important to quantify the effects of using different forcing functions to move between indoor room conditions.

We observed that using a light bulb or a small fan to add power utilizes a forcing function that causes the facility to take several days for the temperatures to reach a steady level. This presents a significant challenge when attempting to test air conditioners in an expedient manner at a variety of indoor room conditions. We decided to take the following steps to speed up the testing process when slow-response forcing functions are used. First, we select the order of air conditioner tests such that the indoor room temperature is changed as infrequently as possible. This concept is further discussed in a later section. Secondly, we utilize a simulation model to predict the response of the indoor room so that we can anticipate what the final facility temperatures will be. This allows us to speed up the testing process whenever the indoor room temperature is changed. The details regarding the simulation model

are presented in Section 3.1.1.3. This section will focus on the results from the transient sensible heat loss tests.

We first recorded transient data for the heat loss tests with the air conditioner in the partition wall but not operating. We logged the temperatures throughout the facility and the power used by the indoor room power source at 10 min intervals. Figure 3.2 shows the response of the indoor room T_a, outdoor room T_o, and weighted ambient $\overline{T}$ temperatures when 125 W of power is added to the indoor room. After one week, the indoor room temperature is still rising to its final equilibrium state. Figure 3.3 indicates a similar response when the 125-W power source is turned off and the indoor room temperature is allowed to coast down to the ambient temperature. Because we do not possess control on the ambient temperature, and because we didn't utilize any control in the outdoor room, both the outdoor room and guard space temperatures fluctuated slightly during the heat loss tests. However, the variations are quite small relative to the temperature difference between the indoor room and the other air spaces, and thus do not introduce significant uncertainty into the heat loss tests.

After analyzing the data, we determined that the slow response during these tests is primarily due to (a) the thermal mass of the walls, metal, and humidifier within the indoor room, (b) the thermal resistance of the walls and humidifier, and (c) the type of forcing function utilized for these tests. Because any type of insulating wall possesses the ability to store energy, this will also affect the thermal response of the room. The humidifier and metal framework located in the indoor chamber also store significant quantities of thermal energy. We calculated the mass of the walls, metal and humidifier and determined the combined mc_p product to be approximately 490 Btu/°F. Thus, if we change the temperature of the indoor room by 10 °F, the amount of energy stored by the indoor chamber components changes by about 4900 Btu. Since the smallest air conditioners we test remove around 6000 Btu/hr of energy from the indoor room, the amount of thermal storage is certainly significant relative to the capacity of the test unit.

As we mentioned above, the thermal resistance of the walls and humidifier also affects the response of the indoor room. This is not surprising since the purpose of using foam for insulation is to reduce heat transfer. For example, the Fourier number for the walls is 0.0264*(time in hours), indicating that the heat conduction through the walls is small relative to the energy storage within the walls. In addition, the humidifier is covered with 3 in. of insulation on all sides, which increases its response time substantially. Thus, we should expect that some time will be necessary to change temperatures in the indoor room.

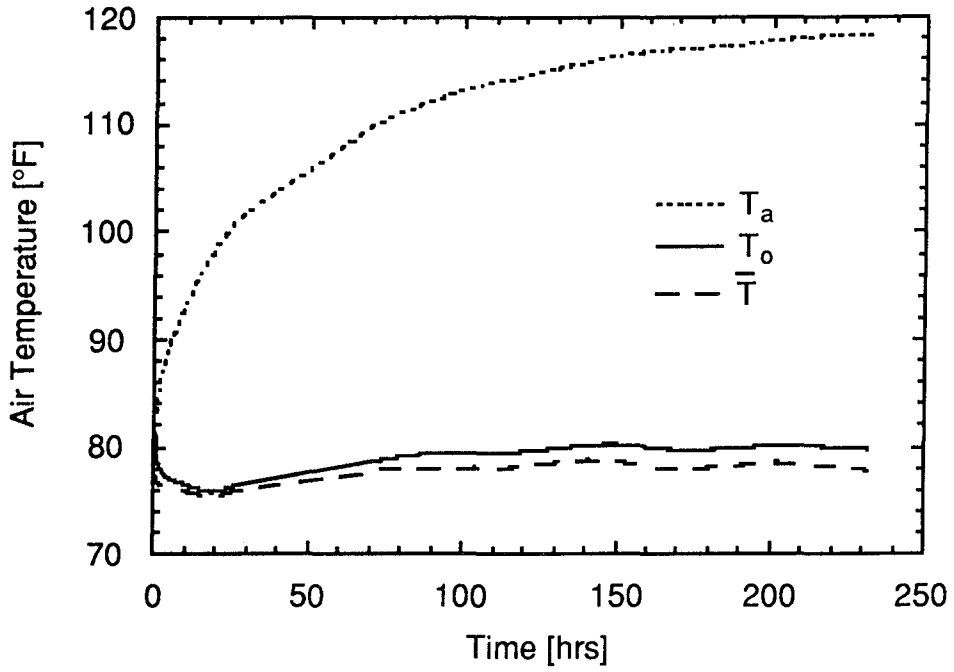

Figure 3.2 Facility Transient Response for 125-W Heat Loss Test

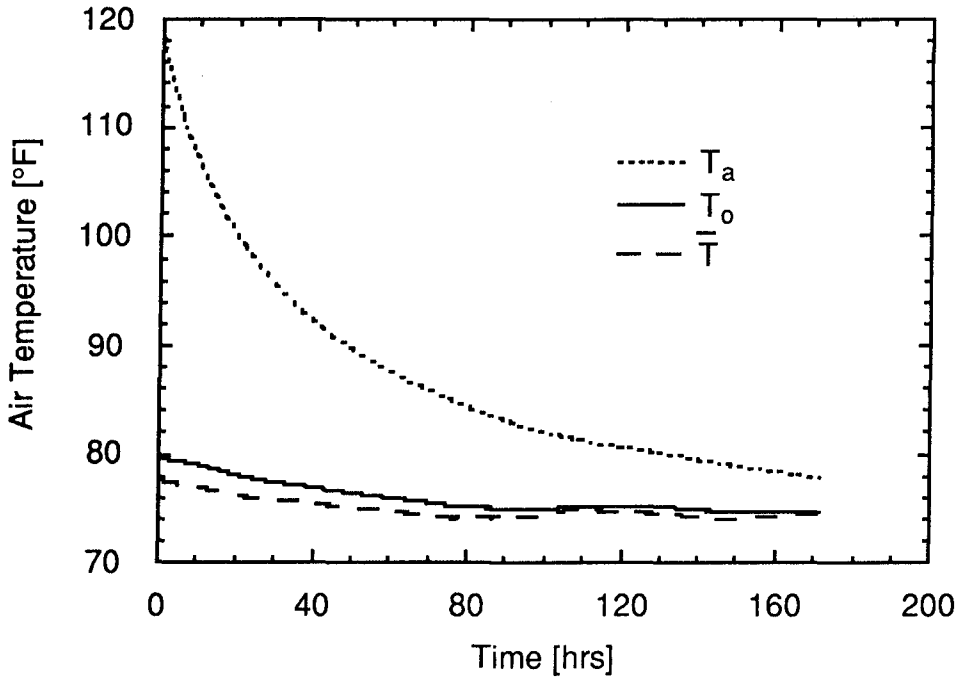

Figure 3.3 Facility Transient Response for 125-W Coast-down Test

The third factor that affects the response time of the room is the type of forcing function used to introduce a change in conditions. For example, if 100 W of power is added to the indoor room, the chamber will achieve the new steady-state condition slower if the energy is added with a light bulb instead of a small fan. The fan forces a more rapid response because it introduces increased heat transfer coefficients between the air and the walls of the chamber. Similarly, using the furnace fan to dissipate energy will further speed up the response of the room due to increased circulation. As we will later see, running a test with the air conditioner fans on also introduces a forcing function that increases the response of the room. The forcing function is also affected by the method of control on the energy source. For example, using a microprocessor controller on the energy source to achieve a certain indoor room temperature will cause the facility to reach a new equilibrium state faster than if no control is used.

Next we recorded the transient response of the indoor room with the air conditioner fans operating at high speed. Figure 3.4 shows the response with the fans being the only power source for the indoor chamber, whereas Figure 3.5 displays the response with an additional 143 W added to the indoor room. Figure 3.5 shows the indoor and outdoor chamber temperatures, the humidifier temperature T_h, and T_{amb}, which is the area-weighted temperature of the guard spaces that surround the indoor room on five sides. The variable T_{amb} is more useful than $\overline{T}$ for future testing because the outdoor room and ambient temperatures can differ by up to 50 °F for some conditions. In those cases, it is not accurate to represent the walls on all six sides as one lumped wall mass. Thus, the partition wall is considered separately.

The most significant result of these two transient tests is that the facility reaches steady state more quickly if the air conditioner fans are operating. In the first test, the indoor air required only about 40 hr to stabilize, which is a significant improvement over the transient tests with no fans on. In Figure 3.5, the indoor room temperature shows signs of stabilizing after 120 hr, while the 125-W heat loss test from Figure 3.2 indicates that the indoor chamber requires well over 200 hr to reach a steady condition. Clearly, operating with the air conditioner fans on introduces a forcing function that greatly improves the response of the room. The primary cause of the increased response speed is the increased heat transfer through the test unit. When the air conditioner fans are on, more energy is transferred to the outdoor chamber, which responds to changes in power much more quickly. Because the air conditioner fans are on during the normal operation of the test unit, this decreased response time is more representative of the actual facility response that is seen during air conditioner

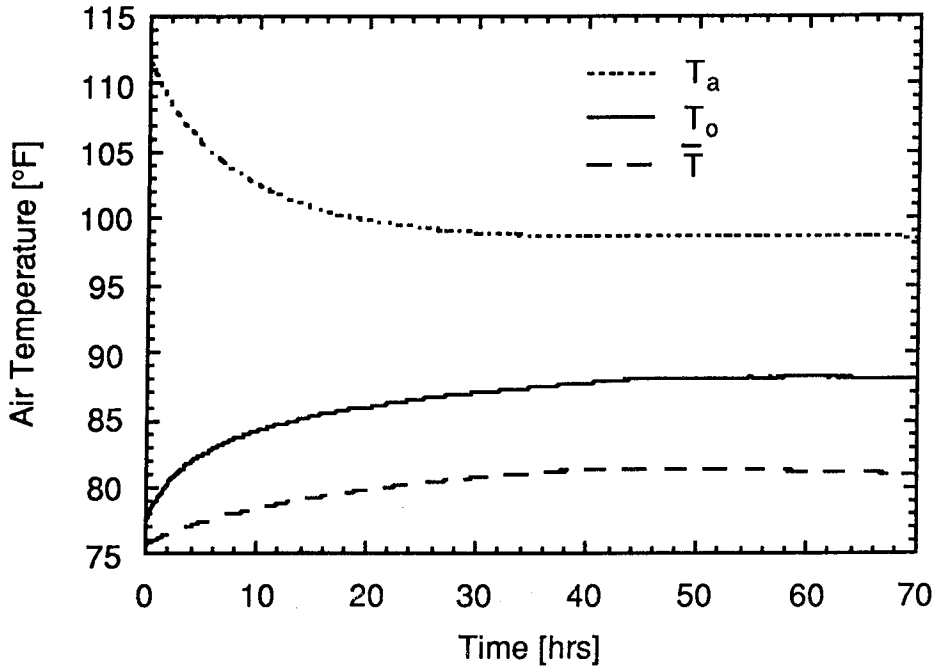

Figure 3.4 Facility Transient Response with Air Conditioner Fans Operating

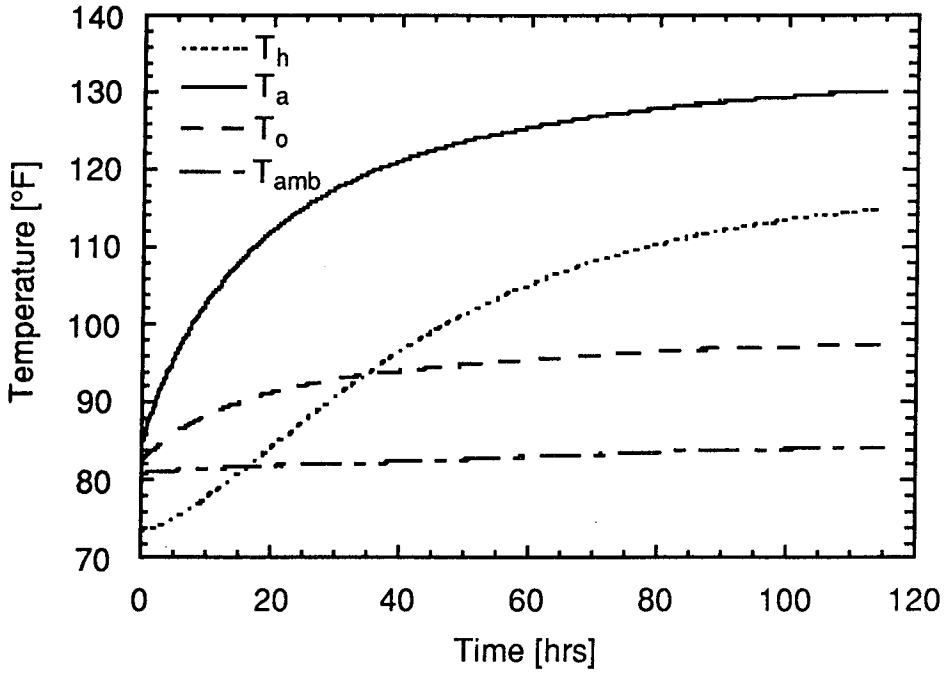

Figure 3.5 Facility Transient Response with Air Conditioner Fans Operating and Additional Indoor Room Power Source

performance testing. For this reason, we do not plan to use the heat loss tests with the fans off to validate the room simulation model to be discussed later.

Another observation we made is that the indoor room air changes temperature more slowly when it is being heated than when it is cooling off. This phenomenon is caused by evaporation within the humidifier. Since some of the water within the barrel is always evaporating, this naturally cools the humidifier water. Thus, when the indoor room is decreasing in temperature, evaporation assists the cooling of the humidifier and increases the response rate of the indoor chamber. However, during tests in which the indoor room is heating up, the evaporation process slows down the heating of the barrel, thus providing a slower forcing function with which to change the indoor room temperature. Therefore, we account for this effect within the simulation model. Several brief tests were run to determine the evaporation rate as a function of indoor room temperature, and this correction is applied to the energy balance on the humidifier.

3.1.1.2 Latent Heat Loss Tests

Just as it is important to quantify the sensible heat losses from the indoor room, it is also necessary to determine the rate of moisture loss from this chamber. Since the indoor room walls are sealed from moisture transmission with aluminum facing on all foam pieces and aluminum foil tape over all cracks, the only way moisture can be transferred from this chamber is through the openings in the air conditioner. Although there are also two pressure relief valves installed in and penetrating through the partition wall, they have never been observed to open because any pressure difference between the chambers is relieved by the air conditioner itself. Thus, it is not necessary to perform a steady-state moisture loss test with no air conditioner in the wall. Because all objects within the indoor room are sealed to prevent moisture absorption, we also do not need to quantify the amount of moisture storage within the facility. As with the sensible heat loss tests, it is necessary to repeat all moisture loss tests for every air conditioner that is tested within the facility.

We first attempted to run a steady-state moisture loss test with the air conditioner fans off on the 1-ton Amana unit. However, we were not able to operate our humidifier at a power level that was low enough to match the steady-state moisture transmission through the test unit. Therefore, we ran the humidifier for a short time so that we achieved a high relative humidity in the indoor room. Then we turned off the humidifier and recorded the temperature and relative humidity of the indoor and outdoor air

spaces over time. The humidity ratios of the indoor and outdoor room air are shown in Figure 3.6. The rate of moisture loss from the indoor room, $\dot{m}$, can be expressed as

$$\dot{m} = UA_{m\text{-}off}\, \rho_g\, (\omega_a - \omega_o) \ , \qquad (3.7)$$

where $UA_{m\text{-}off}$ is the effective UA for moisture transfer through the test unit with the air conditioner fans off, ρ_g is the indoor room air density, and ω_a and ω_o are the humidity ratios of the air in the indoor and outdoor rooms, respectively. Using this equation and Figure 3.6, we calculated that $UA_{m\text{-}off}\, \rho_g$ = 0.72 lb_m air/hr for this air conditioner.

This UA value accounts for moisture transfer due to both air exchange and moisture diffusion between the indoor and outdoor chambers. We will refer to the combination of these two effects as quasi-diffusional effects. This information can be used to determine what fraction of the sensible heat transfer through the unit is due to these effects. We perform this calculation on the steady-state heat loss test performed with the air conditioner in the wall but not operating, which is discussed in Section 3.1.1.1. The parasitic loss through the air conditioner for that test was 105 Btu/hr. Since we already calculated that 0.72 lb_m air/hr is transferred between the indoor and outdoor room, then there is also 6.7 Btu/hr of energy exchanged in the air mixing. Therefore, about 6% of the parasitic heat loss through the test unit is due to quasi-diffusional effects. The remainder of the heat transfer is due to conduction through the walls and components of the air conditioner.

We also performed a moisture loss test with the air conditioner fans operating. The results of this test are presented in Figure 3.7. By again using Equation 3.7, we calculate $UA_{m-on}\rho_g$ to be 14.5 lb_m air/hr, which is roughly 20 times greater than the moisture UA with the fans off. This result is not surprising since the increased circulation within the test unit moves substantially more air through the cracks in the unit. Using this information and the data from the corresponding steady-state sensible heat loss test, we determine that approximately 29% of the heat transfer through the unit with the fans on is due to quasi-diffusional effects. Like the sensible heat UA value, $UA_{m\text{-}on}$ is too large to be ignored relative to typical moisture removal rates of the air conditioners we test.

The other significant result we obtain from the latent heat loss tests is the difference in response times of the indoor room humidity ratio for the two tests. While the indoor and outdoor air humidity ratios had yet to reach equilibrium after 160 hr with the air conditioner fans off, moisture equilibrium was achieved after only 12 hr when

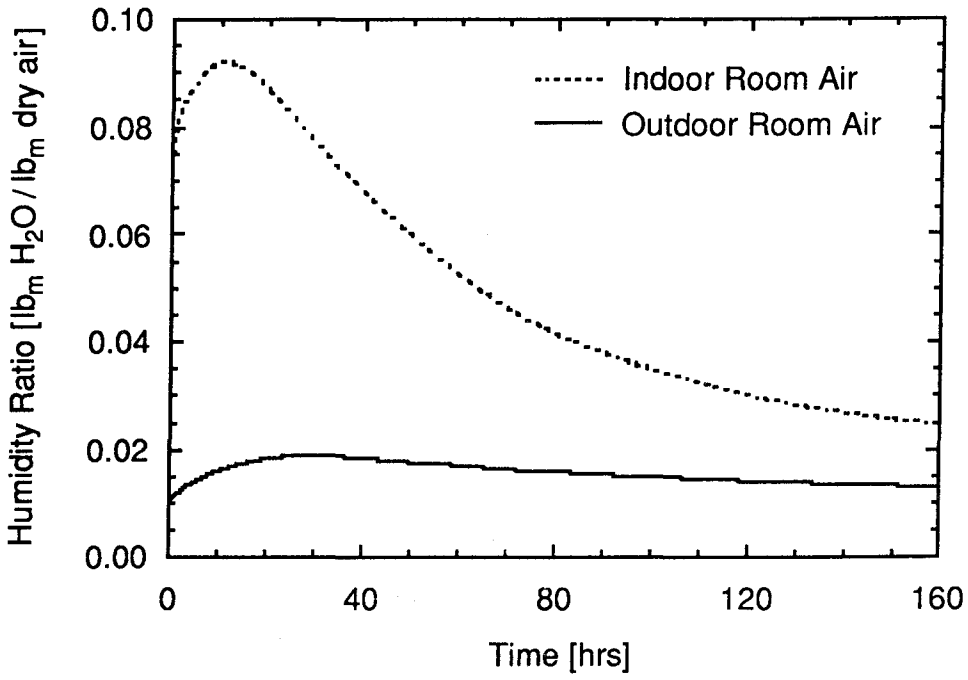

Figure 3.6 Moisture Loss Test with Air Conditioner Fans Off

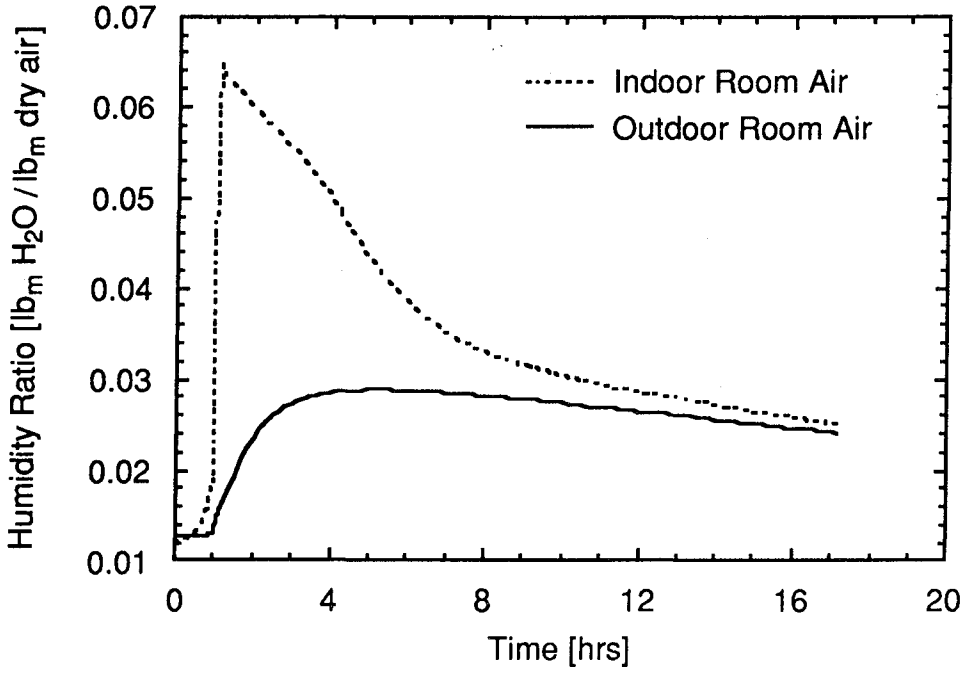

Figure 3.7 Moisture Loss Test with Air Conditioner Fans Operating

the fans were on. As with the sensible heat loss tests, operating with the air conditioner fans on introduces a forcing function that increases the response of the indoor room. Again, this result is not surprising because of the increased circulation within the test unit with the fans on. Since the air conditioner fans are almost always on during performance testing, the moisture UA for this configuration is most commonly used to quantify the losses through the test unit.

3.1.1.3 Room Performance Simulation Model

There are several motivations behind developing an indoor room simulation model. First of all, the model enables us to predict the steady-state temperatures and heat exchanges for the facility without waiting until steady-state is actually achieved. This capability is most useful when running tests in which the indoor room temperature is changed. Secondly, the model helps us to gain understanding about the operating characteristics of the facility. We can observe which components of the indoor room store the most energy, which ones respond the quickest, and which ones have response characteristics that are well simulated and understood. A third benefit of the model is that it enables us to observe the interaction between the indoor room components. This can assist us in finding the optimum locations and configurations for each device to reduce the time needed to reach a steady-state condition.

A FORTRAN code has been developed to simulate the indoor room performance. The governing equations for the room are solved recursively for each desired time step using a general ODE (ordinary differential equation) solving algorithm. A recursive solution means that the new solution of the governing equations is based on the solution from the previous time step. While some simulations use other solution methods by utilizing real-time data to determine the heat transfer between components, we must employ a recursive solution since we do not have any temperature measurements of the indoor room walls. The user supplies the initial conditions and parameter values to the model, and the code outputs the temperatures throughout the facility as a function of time.

The model does not include the moisture response of the facility because (a) there is no moisture storage in the indoor room and (b) the moisture response is quite rapid relative to the thermal response. The model does not currently simulate tests where the humidifier is operating because we don't have a separate measurement of how much power is used by the humidifier alone. However, the model has been validated for various configurations of dry tests. Figure 3.8 shows a schematic of all

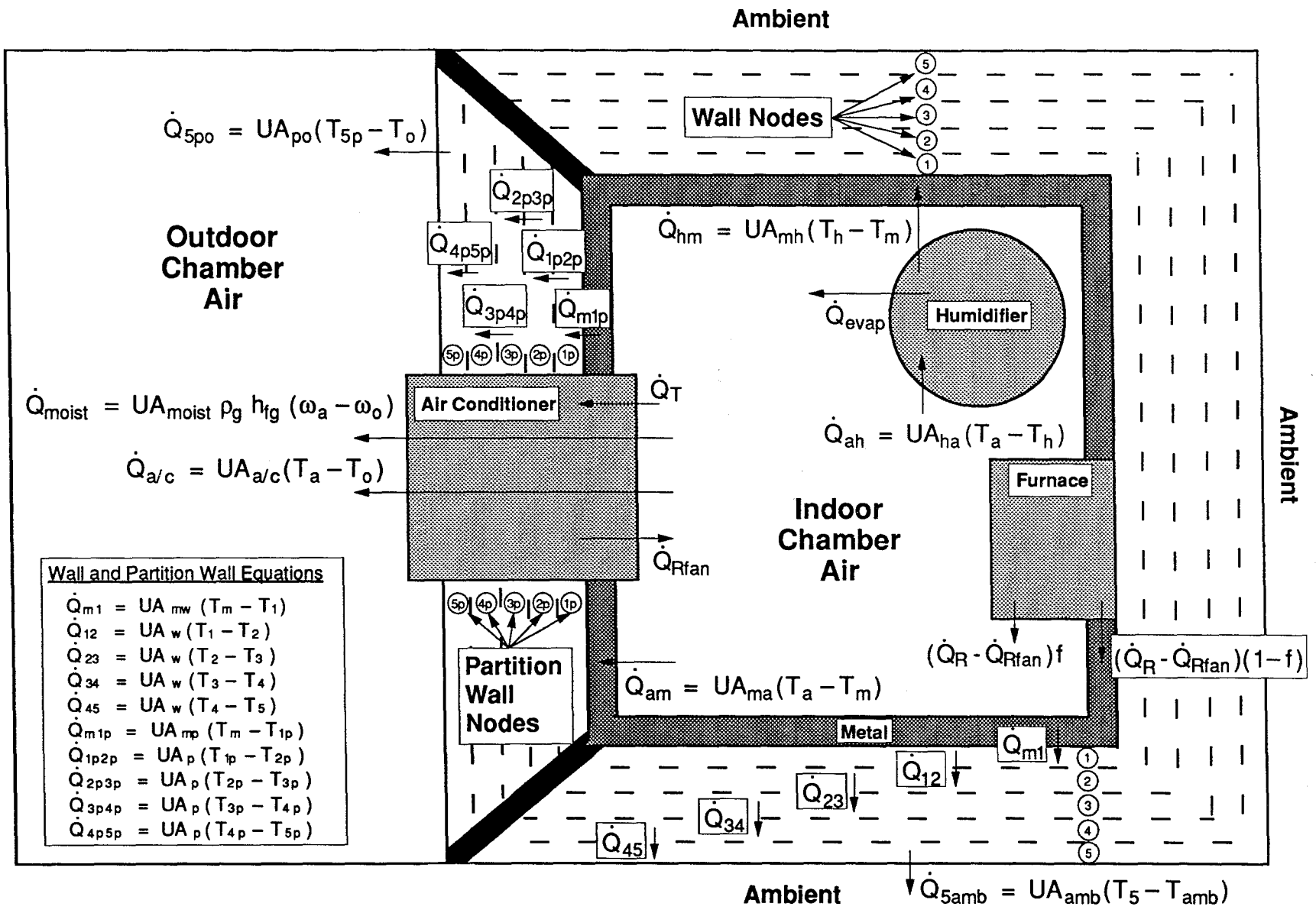

Figure 3.8 Schematic of Heat Transfers Simulated by Indoor Room Model

the heat transfers simulated by the indoor room model. Table 3.2 describes the assumptions made for the model, the governing equations, and the operation of the model. Table 3.3 presents the parameters used within the model, along with their optimum values, uncertainties, and importance to the performance of the model. A high importance indicates that varying that parameter has a large effect on the model's ability to accurately predict the temperatures within the facility. The parameters that have no listing for their importance are parameters that have an uncertainty of less than ±5%.

In order to validate the performance of the room model, we used it to predict the temperature response of the facility for two different tests during which the air conditioner was not operating. We did this so that we could eliminate one unknown value (the energy removed by the test unit) from the set of governing equations. The values for the parameters presented in Table 3.3 are the optimal numbers for our validation tests. The performance of the model is shown in Figures 3.9 and 3.10. Figure 3.9 shows the measured and predicted temperatures of the indoor room air and the humidifier for a test with the furnace fan and the air conditioner fans operating. Figure 3.10 compares the model prediction with experimental data for a heat loss test with the air conditioner fans operating.

The performance of the simulation model for the furnace test is quite good. Both the indoor room air and humidifier temperatures are well predicted by the model, as is the temperature of the indoor room metal (not shown for clarity). There is a slight discrepancy between the measured and predicted air temperatures at the beginning of the test, which we attribute to the fact that there is a small lag time between adding power with the furnace fan and observing a temperature increase in the indoor room air. However, the temperature predictions for the remainder of the test are excellent. The model prediction for the heat loss test is slightly less accurate over the full length of the test. However, this particular test was run for 115 hr, which is much longer than typically seen for an air conditioner performance test. For the short time scale (less than 10 hr) the model prediction is similar to that observed for the furnace test. It is possible to vary some of the model parameters with high uncertainties in order to achieve better prediction for the heat loss test. However, this corresponds to less accurate model performance for the furnace test. We feel it is more important to closely match the data from the furnace test since the furnace fan is always operating during air conditioner performance testing.

Table 3.2 Summary of Indoor Room Simulation Model

Basic Assumptions

1. The air in the indoor room can be represented by a single average temperature T_a and humidty ratio ω_a. The product of the mass times the specific heat is mc_{pa}.

2. The humidifier can be represented by a single average temperature T_h and mass times specific heat product mc_{ph}. The humidifier includes the water, barrel, heaters, steam distribution tubes, and insulation.

3. The metal within the indoor room can be represented by a single average temperature T_m and mass times specific heat product mc_{pm}. The metal includes the aluminum foil facing on the surface of the walls, the structural members, electrical conuit and boxes, the furnace, and the air distribution screens.

4. The walls surrounding the indoor room are divided into ten nodes. The wall between the indoor and outdoor chambers is called the partition wall and is divided into five nodes of equal thickness. Each node is represented by a single average temperature (T_{1p} for the node closest to the indoor room and T_{5p} for the furthest node) and mass times specific heat product mc_{pp}. The remainder of the walls are also divided into five nodes of equal thickness. Each node is represented by a single average temperature (T_1 for the node nearest to the indoor room and T_5 for the furthest node) and mass times specific heat product mc_{pw}.

5. The air in the outdoor room can be represented by a single average temperature T_o and humidity ratio ω_o.

6. The air in the guard spaces surrounding the indoor room can be represented by a single average temperature T_{amb}.

7. Several modes of heat transfer are present within the test unit. The refrigerant loop of the air conditioner removes thermal energy from the indoor room air, which is denoted by $\dot{Q}_T$. The indoor room air exchanges sensible heat with the outdoor room air due to (a) conduction through the air conditioner cabinet and (b) air exchange through the cracks in the test unit. This rate of heat exchange $\dot{Q}_{a/c}$ is given by $UA_{a/c}(T_a - T_o)$, where $UA_{a/c}$ is the effective thermal conductance between the rooms. The two chambers also exchange latent heat through the openings within the test unit. This rate of heat exchange $\dot{Q}_{moist}$ is given by $UA_{moist}\,\rho_g\,h_{fg}\,(\omega_a - \omega_o)$ where $UA_{moist}\,\rho_g$ is the effective moisture conductance between the chambers and h_{fg} is the enthalpy of vaporization of water.

8. The total amount of thermal energy added to the indoor room by the reconditioning equipment is $\dot{Q}_R$. For dry tests this energy is added by the furnace and the evaporator fan of the air conditioner. The portion of this energy that is added by the evaporator fan is $\dot{Q}_{Rfan}$. A fraction (1 – f) of the thermal energy output of the furnace ($\dot{Q}_R - \dot{Q}_{Rfan}$) is transferred directly to the walls by conduction through the structural members. The remaining fraction (f) is transferred to the air.

Table 3.2 Summary of Indoor Room Simulation Model (continued)

9. The humidifier exchanges thermal energy with the indoor room air. The rate of this exchange $\dot{Q}_{ah}$ is given by $UA_{ha}(T_a - T_h)$ where UA_{ha} is the effective thermal conductance bewteen the air and humidifier. The humidifier also adds latent heat $\dot{Q}_{evap}$ to the air, and the magnitude of this exchange is determined experimentally. The humidifier exchanges thermal energy with the supporting metal framework. The rate of heat exchange $\dot{Q}_{hm}$ is given by $UA_{mh}(T_h - T_m)$ where UA_{mh} is the effective thermal conductance bewteen the metal and humidifier.

10. The indoor room air exchanges thermal energy with the metal. The rate of heat exchange $\dot{Q}_{am}$ is given by $UA_{ma}(T_a - T_m)$ where UA_{ma} is the effective thermal conductance between the air and metal. The air does not exchange thermal energy directly with the walls surrounding the indoor room.

11. The metal exchanges energy with the innermost wall node. This rate of heat exchange $\dot{Q}_{m1}$ is given by $UA_{mw}(T_m - T_1)$ where UA_{mw} is the effective thermal conductance between the metal and the node 1. The metal also exchanges thermal energy with the innermost partition wall node. The rate of heat exchange $\dot{Q}_{m1p}$ is given by $UA_{mp}(T_m - T_{1p})$ where UA_{mp} is the effective thermal conductance between the metal and partition node 1.

12. Each wall node exchanges energy with the adjacent wall nodes. For example, the rate of heat exchange between nodes 2 and 3 $\dot{Q}_{23}$ is given by $UA_w(T_2 - T_3)$ where UA_w is the effective therma conductance bewteen the wall nodes. Each partition wall node exchanges energy with the adjacent partition wall nodes. For example, the rate of heat exchange between partition nodes 3 and 4 $\dot{Q}_{3p4p}$ is given by $UA_p(T_{3p} - T_{4p})$ where UA_p is the effective thermal conductance between the partition wall nodes.

13. The outermost wall node exchanges thermal energy with the ambient air. The rate of heat exchange $\dot{Q}_{5amb}$ is given by $UA_{amb}(T_5 - T_{amb})$ where UA_{amb} is the effective thermal conductance between wall node 5 and the ambient air. The outermost partition wall node exchanges thermal energy with the outdoor room air. This rate of heat exchange $\dot{Q}_{5po}$ is given by $UA_{po}(T_{5p} - T_o)$ where UA_{po} is the effective thermal conductance between partition wall node 5 and the outdoor room air.

Governing Equations

Energy Balance for Indoor Room Air:

$$\frac{d}{dt}(mc_{pa}T_a) = (\dot{Q}_R - \dot{Q}_{Rfan})\,f + \dot{Q}_{Rfan} - UA_{a/c}\,(T_a - T_o) - UA_{ma}\,(T_a - T_m) - UA_{ha}\,(T_a - T_h) + \dot{Q}_{evap} - UA_{moist}\,\rho_g\,h_{fg}\,(\omega_a - \omega_o) - \dot{Q}_T \qquad (3.8)$$

Energy Balance for Humidifier:

$$\frac{d}{dt}(mc_{ph}T_h) = UA_{ha}\,(T_a - T_h) + UA_{mh}\,(T_m - T_h) - \dot{Q}_{evap} \qquad (3.9)$$

Table 3.2 Summary of Indoor Room Simulation Model (continued)

Energy Balance for Metal:

$$\frac{d}{dt}(mc_{pm}T_m) = UA_{mh}(T_h - T_m) + UA_{ma}(T_a - T_m) + (\dot{Q}_R - \dot{Q}_{Rfan})(1-f) + UA_{mw}(T_1 - T_m) + UA_{mp}(T_{1p} - T_m) \quad (3.10)$$

Energy Balance for Wall Nodes:

$$\frac{d}{dt}(mc_{pw}T_1) = UA_w(T_2 - T_1) + UA_{mw}(T_m - T_1) \quad (3.11)$$

$$\frac{d}{dt}(mc_{pw}T_2) = UA_w(T_1 + T_3 - 2T_2) \quad (3.12)$$

$$\frac{d}{dt}(mc_{pw}T_3) = UA_w(T_2 + T_4 - 2T_3) \quad (3.13)$$

$$\frac{d}{dt}(mc_{pw}T_4) = UA_w(T_3 + T_5 - 2T_4) \quad (3.14)$$

$$\frac{d}{dt}(mc_{pw}T_5) = UA_w(T_4 - T_5) + UA_{amb}(T_{amb} - T_5) \quad (3.15)$$

Energy Balance for Partition Wall Nodes:

$$\frac{d}{dt}(mc_{pp}T_{1p}) = UA_p(T_{2p} - T_{1p}) + UA_{mp}(T_m - T_{1p}) \quad (3.16)$$

$$\frac{d}{dt}(mc_{pp}T_{2p}) = UA_p(T_{1p} + T_{3p} - 2T_{2p}) \quad (3.17)$$

$$\frac{d}{dt}(mc_{pp}T_{3p}) = UA_p(T_{2p} + T_{4p} - 2T_{3p}) \quad (3.18)$$

$$\frac{d}{dt}(mc_{pp}T_{4p}) = UA_p(T_{3p} + T_{5p} - 2T_{4p}) \quad (3.19)$$

$$\frac{d}{dt}(mc_{pp}T_{5p}) = UA_p(T_{4p} - T_{5p}) + UA_{po}(T_o - T_{5p}) \quad (3.20)$$

Table 3.2 Summary of Indoor Room Simulation Model (continued)

Description of Operation

For validation we use the model to predict temperatures within the facility. In this mode, the operation of the model follows the flow chart below.

Model Flow Chart

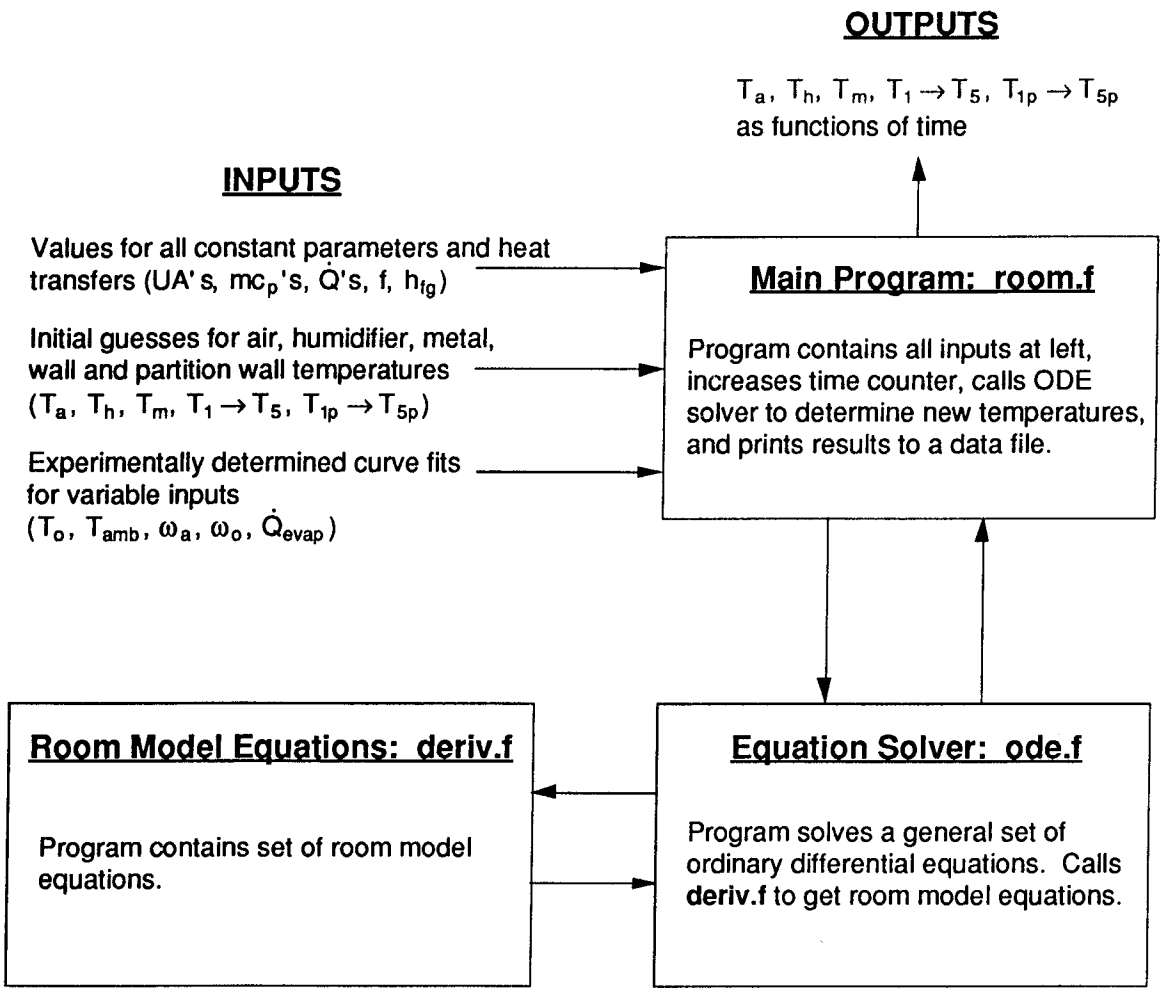

Table 3.2 Summary of Indoor Room Simulation Model (continued)

The program room.f acts as the driver for the indoor room model. All initial guesses, values for constant parameters, and curve fits for variable inputs are found here. This program initializes the time to equal zero and then increases the time by a given time step. At each time increment, the program calls the general equation solver ode.f to solve the differential equations based on the solution found at the previous time step. The solver calls the program deriv.f to obtain the equations for the model. At each time step, room.f writes the time and predicted temperatures to an output file. These temperatures can then be compared with measured facility temperatures to validate the model.

Table 3.3 Values, Uncertainties and Importance of Model Parameters

PARAMETER	VALUE	UNCERTAINTY	IMPORTANCE
f	0.675	±0.040	low
h_{fg}	1105 Btu/lb_m	±10 Btu/lb_m	----
mc_{pa}	10.8 Btu/°F	±0.2 Btu/°F	----
mc_{ph}	220 Btu/°F	+30/–70 Btu/°F	high
mc_{pm}	220 Btu/°F	+30/–70 Btu/°F	medium
mc_{pp}	9.23 Btu/°F	±0.09 Btu/°F	----
mc_{pw}	43.6 Btu/°F	±0.4 Btu/°F	----
$UA_{a/c}$	12.5 Btu/hr–°F	±1.0 Btu/hr–°F	high
UA_{amb}	41.4 Btu/hr–°F	±1.0 Btu/hr–°F	----
UA_{ha}	8.0 Btu/hr–°F	±2.0 Btu/hr–°F	high
UA_{ma}	3000 Btu/hr–°F	±500 Btu/hr–°F	low
UA_{mh}	0.190 Btu/hr–°F	±0.020 Btu/hr–°F	low
$UA_{moist}\rho_g$	14.5 lb_m air/hr	±1.2 lb_m air/hr	very low
UA_{mp}	9.61 Btu/hr–°F	±0.10 Btu/hr–°F	----
UA_{mw}	45.3 Btu/hr–°F	±0.4 Btu/hr–°F	----
UA_p	4.81 Btu/hr–°F	±0.05 Btu/hr–°F	----
UA_{po}	8.61 Btu/hr–°F	±0.09 Btu/hr–°F	----
UA_w	23.9 Btu/hr–°F	±0.2 Btu/hr–°F	----

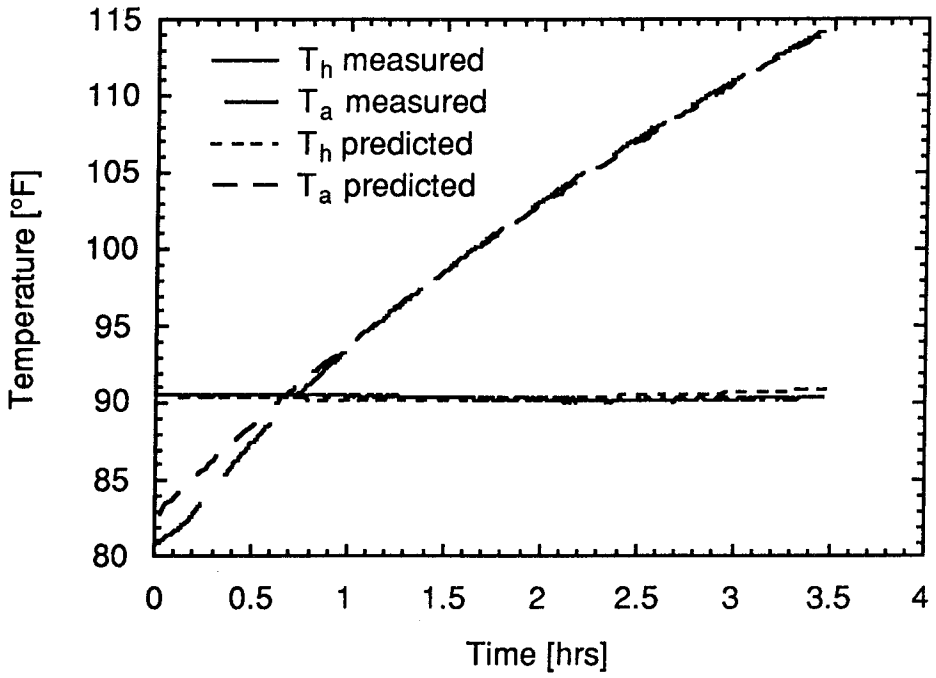

Figure 3.9 Model Comparison for Furnace Test

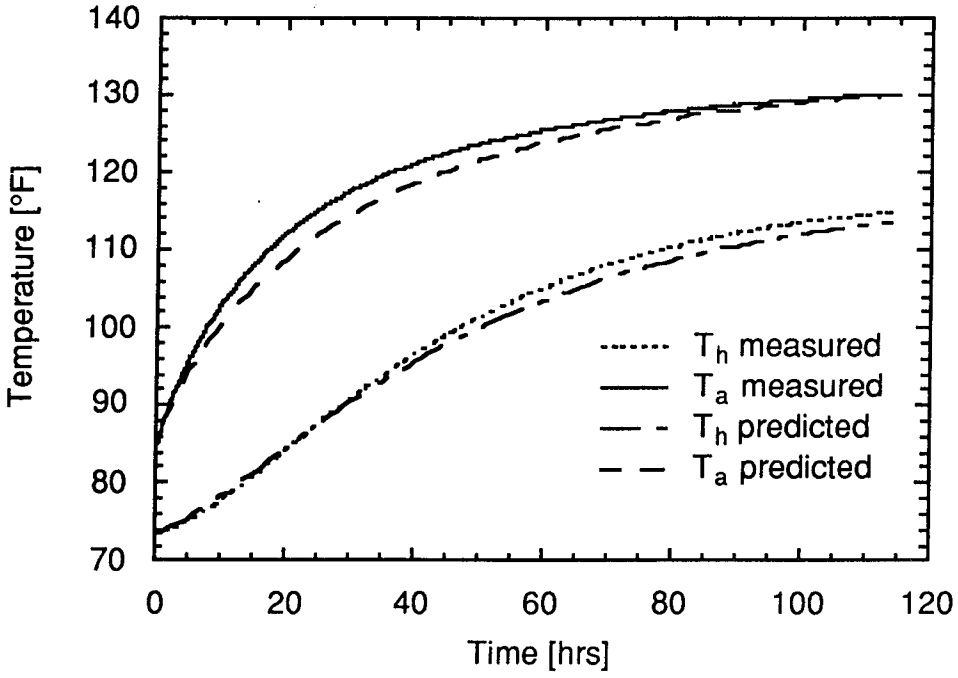

Figure 3.10 Model Comparison for Heat Loss Test with Air Conditioner Fans Running

3.1.2 Outdoor Room

While the energy balance on the indoor room is crucial when determining the capacity of the air conditioner being tested, the energy transfer from the outdoor chamber is not as important. However, for some versions of the indoor room model, it might be necessary to use an equation representing an energy balance on the outdoor room. For this reason, and to further characterize the performance of the test facility, we performed two steady-state heat loss tests in the outdoor chamber. The sensible heat loss from the outdoor room is given by

$$\dot{Q}_o = UA_o (T_o - \overline{T}) + UA_{a/c\text{-}off} (T_o - T_a) , \qquad (3.21)$$

where $\dot{Q}_o$ is the heat loss from the outdoor room, UA_o is the effective thermal conductance of the outdoor room walls, T_o is the outdoor room air temperature, and $\overline{T}$ is the area-weighted temperature of the air spaces surrounding the outdoor room. By substituting in the known parameters and measured values, we find UA_o to be 97.2 Btu/hr–°F. Thus, the heat loss through the outdoor room walls is more than twelve times greater than that through the indoor room walls. This is expected since the indoor room walls contain significantly more insulation than those in the outdoor room. In addition, the lower thermal mass in the outdoor chamber enables it to reach steady state in approximately 16 hr, which is substantially faster than the indoor room. This quicker response is utilized when determining the test matrix for air conditioner performance tests, which is discussed in Section 3.2.1.

3.2 Air Conditioner Performance Tests

After completing the facility characterization tests, the next step is to test the performance of the air conditioners themselves. We can validate our facility and measurements by comparing the measured performance of each unit at a variety of conditions with data supplied by the manufacturers. While an unfavorable comparison doesn't necessarily indicate that our facility is functioning improperly, good agreement between the data sets increases our confidence in the accuracy of the facility and measurements. This comparison also provides information that helps optimize the test facility and our testing methods. As we have previously mentioned, other purposes for testing are to validate the air conditioner simulation model and to observe and quantify trends in the performance of the test unit as temperatures, humidities,

and fan speeds are varied. All air conditioner performance data has been collected with air-side instrumentation only, as is described in Section 2.3.

3.2.1 Determination of Test Matrix

One of the most difficult aspects of performance testing is deciding what tests to run, which we also refer to as determining the test matrix. In an ideal situation, we would desire to test each air conditioner at an extensive number of different conditions. However, it is necessary to put a limit on the number of tests performed because of time constraints. Thus, there is a delicate balance between taking enough data points and not using an unreasonable amount of time to do so. Another consideration is that we need to test at a wide variety of conditions so that we can determine the sensitivity of the test unit performance to various factors. In addition, we may want to test our air conditioners at some of the standard rating conditions used by industry, which provides a common baseline for the comparison of results. A final consideration is the response time of the indoor and outdoor chambers of the facility. We obviously want to minimize the amount of time necessary to reach a steady-state condition, and should choose the order of our tests such that this is achieved.

Figure 3.11 shows the test matrix we used for the performance testing of the 1-ton Amana unit. We anticipate using this matrix as a standard for all air conditioners tested within our facility. There are a total of 43 tests we run for each air conditioner with the air-side instrumentation only. Experience has shown that we can complete approximately three tests in one day, which indicates that the full matrix would require roughly 13 days. We feel this is a reasonable time frame in which to complete the tests, especially if we operate the facility on a continuous basis. The black dots on the matrix indicate test points which are also rating conditions that are frequently used by industry. Since we have chosen several of our points to coincide with the rating conditions, we have a common baseline with which to compare our data to those obtained by the manufacturers.

The test matrix enables us to observe how air conditioner performance is affected by the four variables we are able to control in our facility: (a) indoor room temperature, (b) outdoor room temperature, (c) indoor room relative humidity, and (d) air conditioner fan speed. All other variables, such as the amount of superheat in the evaporator, the refrigerant mass flow rate, and the pressure drop within each component, are determined by these four control variables. We chose the

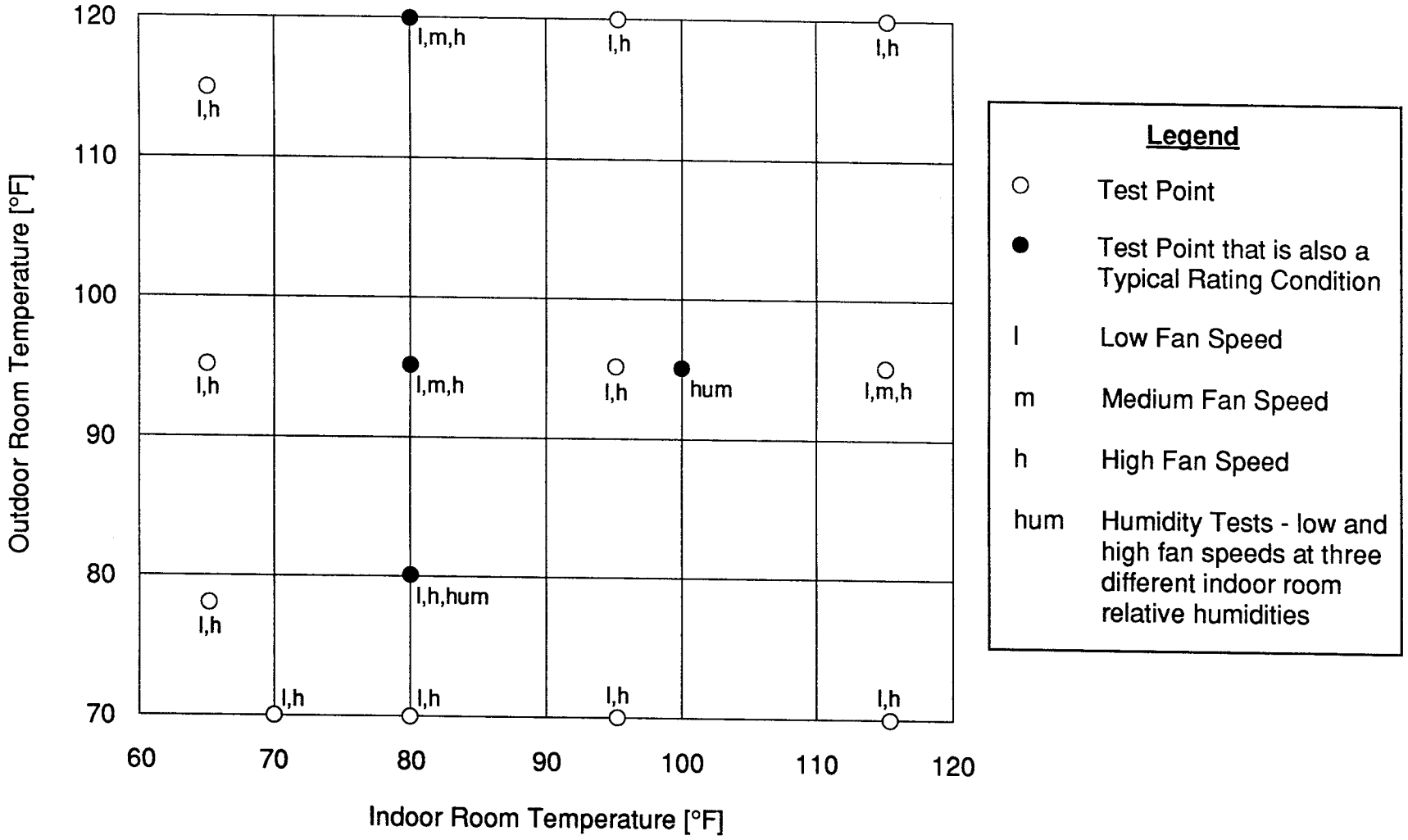

Figure 3.11 Standard Test Matrix

temperatures for our matrix such that the test unit would operate over most of the range of its compressor map. As Figure 3.11 indicates, we vary the indoor room temperature from 65 to 115 °F and from 70 to 120 °F in the outdoor chamber. We operate each unit at 14 different dry (humidifier off) conditions for the low and high fan speed tests, and at three dry conditions for the medium fan speed tests. We felt that a full set of dry tests with the fan set to medium would not be as useful as a larger variety of points at the high and low speeds. We also perform a total of 12 tests with the humidifier operating, which includes three different indoor room relative humidities, two fan speeds, and two sets of indoor and outdoor room temperatures. Thus, we believe the test matrix is sufficiently complete to observe most of the significant trends related to air conditioner performance.

The test matrix consists of not only the test points themselves, but also the order in which the different conditions are achieved. As we have previously mentioned, the indoor room requires a much longer time to reach steady state when the temperature is changed than the outdoor room does. Thus, we wish to operate the tests such that the indoor chamber temperature changes as infrequently as possible. For the 1-ton Amana, we started the test matrix at the bottom-left corner of the grid (70 °F indoor, 70 °F outdoor) with the test unit fans on high speed, and then increased the outdoor room temperature while keeping the indoor chamber at 65 °F. Then the indoor room temperature was changed to 80 °F and the outdoor room was varied from 120 to 70 °F. This pattern was repeated for the 95 and 115 °F indoor room temperatures, with all tests being run with the air conditioner fans on high. Then the six high-fan-speed humidity tests were run, with the indoor room relative humidities ranging from 30 to 68%. After all the high speed tests were completed, the matrix was repeated for the low fan speed tests, with the medium fan tests being performed last. In hindsight, we believe that performing all fan speed tests while at a certain set of indoor and outdoor room temperatures might be somewhat quicker than the order presented above. Future sets of performance tests may incorporate this modification into the testing sequence. Nevertheless, the test matrix is adequate to determine the performance of the air conditioner and was completed roughly on schedule.

3.2.2 Test Results

3.2.2.1 Transient Response

The response time of the facility with an operating air conditioner is important to quantify in order to know when a steady-state condition is achieved. When we adjust

the facility from one test condition to another, usually the temperatures, relative humidities and heat inputs all change, thus requiring a waiting period before the next steady-state data set can be taken. Figure 3.12 shows typical responses for the indoor and outdoor room air temperatures. For this test, the indoor room temperature moved from 80 to 115 °F while the outdoor room temperature increased from 80 to 120 °F. As the graph shows, the indoor chamber air required approximately 3 hr to stabilize at the new condition, while the outdoor chamber needed roughly 5 hr. The temperature changes observed in this particular test are larger than those found in a standard test matrix, and thus so are the response times. Nearly all tests we have performed indicate stable temperatures within 5 hr. These response times are a great improvement over the times found in Figures 3.4 and 3.5, thus indicating a significant change in the forcing function used. This response verifies the importance of utilizing microprocessor control for the temperatures in the indoor and outdoor chambers.

The temperature response time also depends on whether the rooms are being heated or cooled. In the indoor chamber, the furnace can supply over 10 kW of heat to the air, while the test unit normally removes about 3.5 kW. The furnace clearly has more capacity to heat the air than the air conditioner does to cool it. Thus, the indoor room typically responds faster when being heated. In the outdoor room the situation is reversed. The fan/coil unit can remove almost 16 kW of thermal energy, while the test unit adds only a fraction of that energy to the air. Therefore, the outdoor chamber responds more quickly to cooling than to heating.

Understanding the humidity response in each room is equally important to the testing process. Figure 3.13 shows a typical response to a change in the indoor room relative humidity controller setpoint. The humidity in the indoor room actually decreases for the first 40 min while the humidifier heats up and starts to release steam into the air. After that, the relative humidity changes in a matter of minutes and reaches a reasonably steady level of 51% in an additional 50 min. This rapid moisture response is partially due to the fact that there is no storage of moisture within the indoor room. Thus, all latent heat leaving the humidifier remains in the air until removed by the air conditioner. Another reason for the rapid response is that the humidifier can supply much more latent heat than the test unit can remove. For the same reason, however, the relative humidity response is much slower when the humidity in the indoor room is decreasing. The mismatch in capacities between the fan/coil and the air conditioner causes the outdoor room to respond slowly to increases in relative humidity, but more quickly to decreases in moisture content.

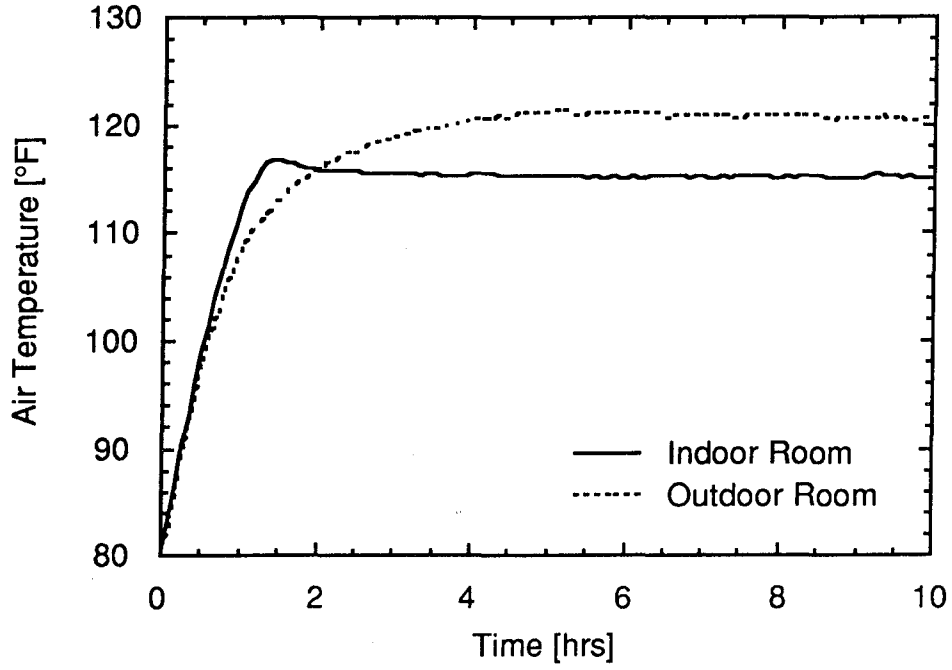

Figure 3.12 Typical Temperature Response for Indoor and Outdoor Chambers

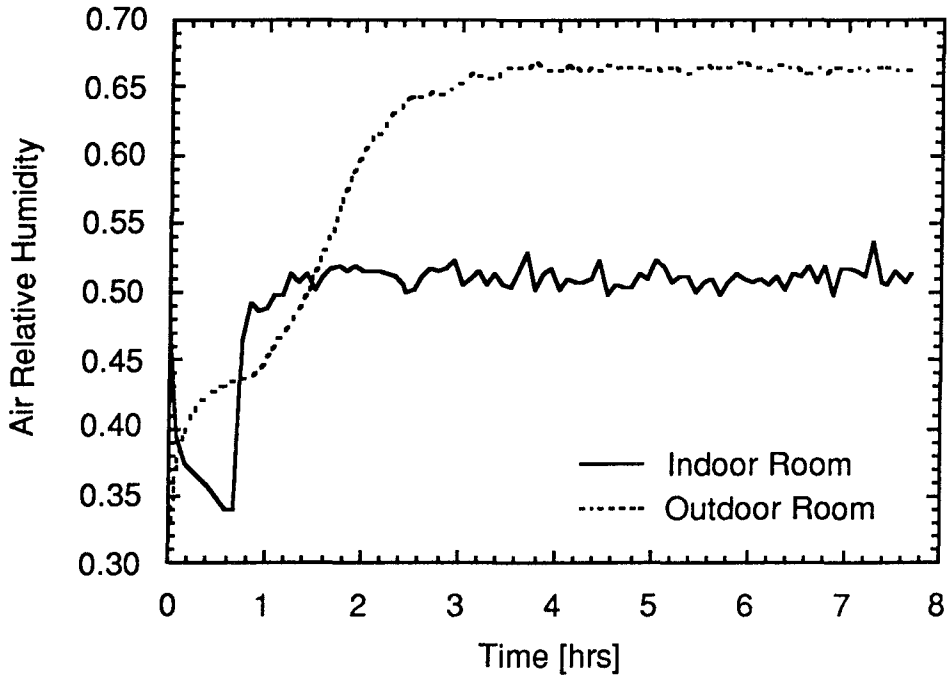

Figure 3.13 Typical Relative Humidity Response for Indoor and Outdoor Chambers

While it is important to understand the temperature and humidity responses of the facility, it is also necessary to know how the power added to the indoor room changes over time. Since the furnace and humidifier controllers adjust the power supplied to that chamber in order to maintain a constant set of conditions, steady temperature and relative humidity readings do not necessarily mean that the power is also constant. For this reason, we performed several tests to monitor the change in indoor room power over time. Figure 3.14 shows the power response for two different tests as they approach the same condition (80 °F indoor, 95 °F outdoor temperatures) from different directions. The test represented by the top curve started at an indoor room temperature of 65 °F. When the indoor room temperature setpoint was changed to 80 °F, the controller supplied more power to reach the new target temperature. As the indoor chamber temperature approached 80 °F, the controller lowered the power level until it reached a relatively steady value (±1%). This fluctuation in power is caused by the normal operation of the controllers. The bottom curve test started at an indoor room temperature of 100 °F. When the setpoint was changed to 80 °F, the power to the indoor room dropped and then slowly increased to reach the same steady level as the first test.

As Figure 3.14 indicates, the average power for each of the tests was within 1% of the steady-state level after 5 hr of operation. Other tests have indicated that generally the response is not quite as quick as we see in these cases. A more universal bound on the power response specifies that the power is within 2.5% of the steady-state value after 5 hr and within 1.5% after 7 hr. If the indoor room temperature has been changed since the last condition, we specify a 7-hr waiting period before taking steady-state data at a new condition . If it is important to take data at a faster rate, the indoor room simulation model can be used to correct for the error in the power supplied to that chamber. In either case, it is necessary to wait until the temperatures and relative humidities in both rooms are stable before analyzing the performance of the test unit.

3.2.2.2 Performance Trends

Because our facility is capable of maintaining a wide range of conditions in each test chamber, we can easily see how the performance of the test unit varies with a number of different factors. One standard method of rating the performance of an air conditioner is to use the energy efficiency ratio, EER, which is defined by

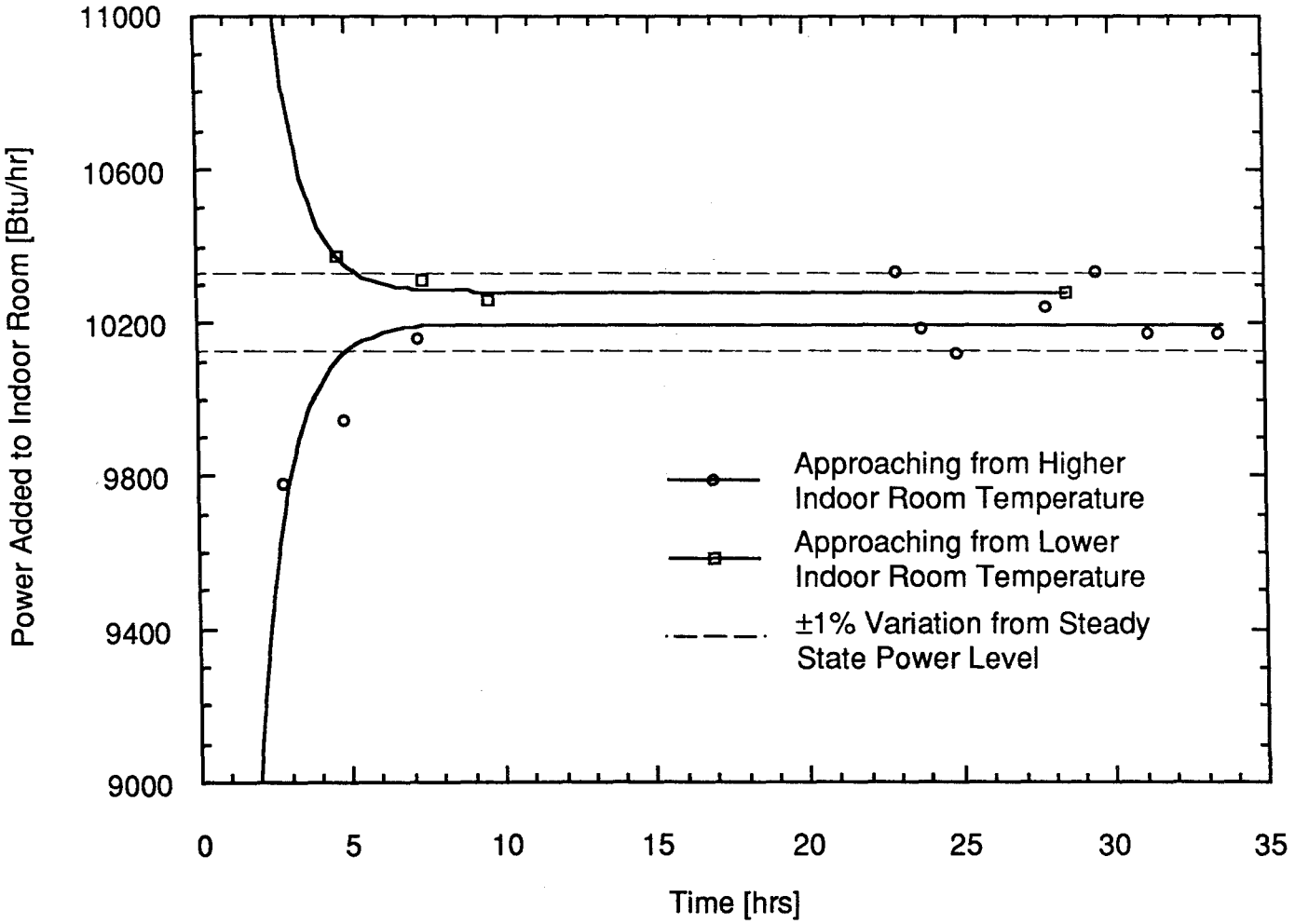

Figure 3.14 Transient Power Addition Response for Two Tests Approaching Same Condition

$$EER = \frac{\text{air conditioner capacity [Btu / hr]}}{\text{power used by air conditioner [W]}} \quad . \tag{3.22}$$

The capacity of the test unit is the amount of energy it removes from the indoor room through the evaporator. The power used by the unit includes the power supplied to both the compressor and the evaporator/condenser fan motor. Figure 3.15 shows the how both the capacity and EER vary with indoor room air temperature for a fixed outdoor room air temperature. This graph indicates that both the capacity and EER increase with indoor temperature. However, because the power used by the air conditioner also increases with temperature, the EER is not as sensitive to the indoor room temperature as the capacity is. Thus, the capacity increases more than 45% over the indoor room temperature range of 65 to 115 °F, while the EER increases only 31%.

The performance of the test unit behaves differently when the outdoor room air temperature is varied, as shown in Figure 3.16. We see that the EER and capacity decrease as the outdoor temperature increases. However, because the compressor power increases at higher temperatures, the EER is even more sensitive to outdoor room temperature changes than the capacity. When the outdoor room temperature is dropped from 120 to 70 °F, the capacity increases 19% while the EER increases more than 83%. A complete discussion of the causes behind these trends is beyond the scope of this paper. However, some of the important factors include changes in compressor efficiencies and irreversibilities within heat exchangers when conditions are varied over wide ranges.

Another interesting trend to observe is to monitor air conditioner performance as a function of fan speed, which also determines the air volumetric flow rate through both the evaporator and condenser. The unit we used for these tests has low, medium and high fan speed settings, and both fans are connected to the same shaft. Thus, increasing the fan speed raises the flow rate through both heat exchangers. We ran low, medium and high fan speed tests at four different dry conditions, and the EER's for all these tests are shown in Figure 3.17. In all four cases, the EER increased with fan speed. This seems to indicate that the heat transfer through the evaporator (and possibly the condenser) is air-side limited in this range of air flow rates. It also supports the idea that increasing the air flow rate even more would only improve the efficiency of the unit. However, performance of the compressor also changes with fan speed because the conditions within the refrigerant loop are

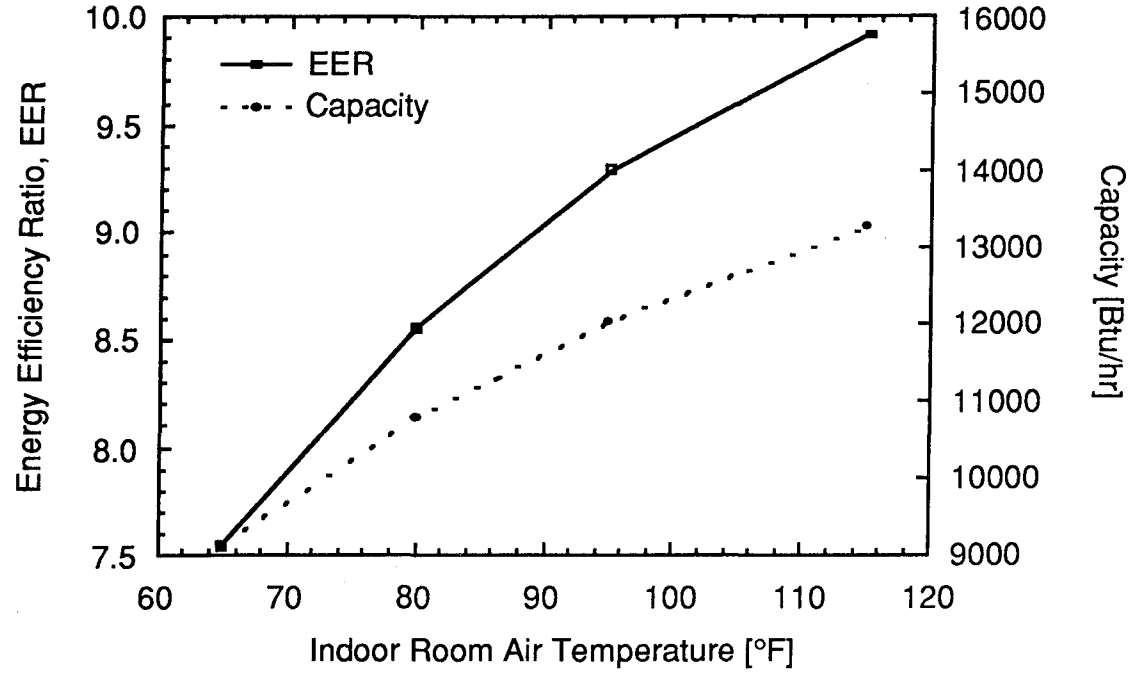

Figure 3.15 EER and Capacity vs. Indoor Room Air Temperature for High Fan Dry Tests with 95 °F Outdoor Room

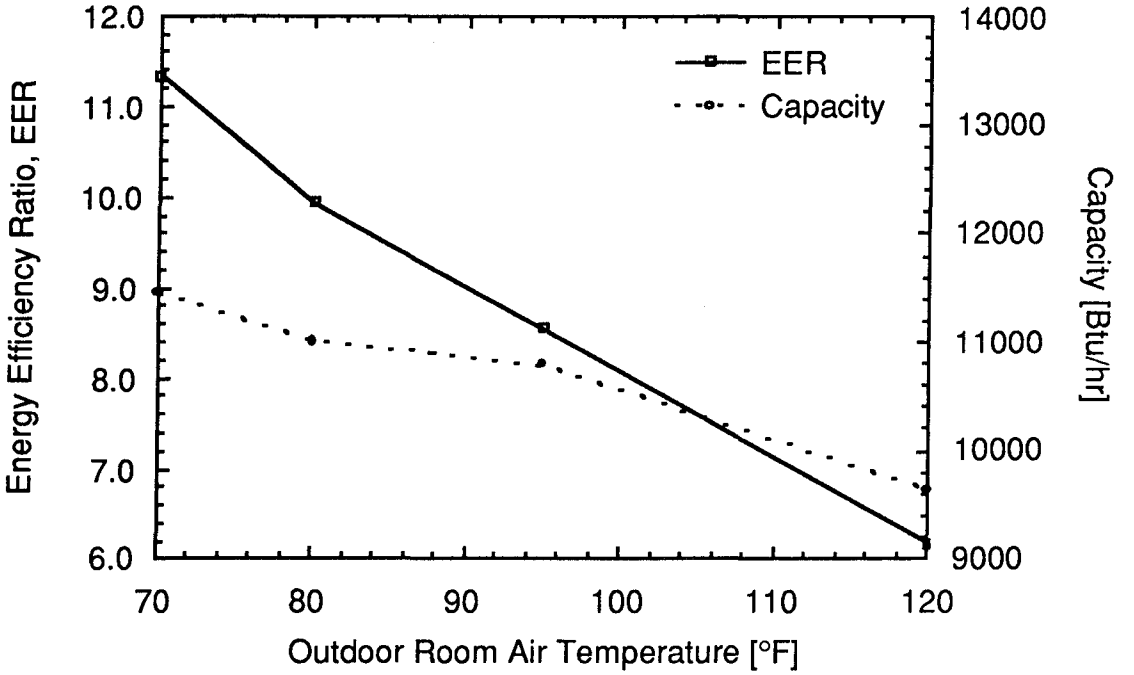

Figure 3.16 EER and Capacity vs. Outdoor Room Air Temperature for High Fan Dry Tests with 80 °F Indoor Room

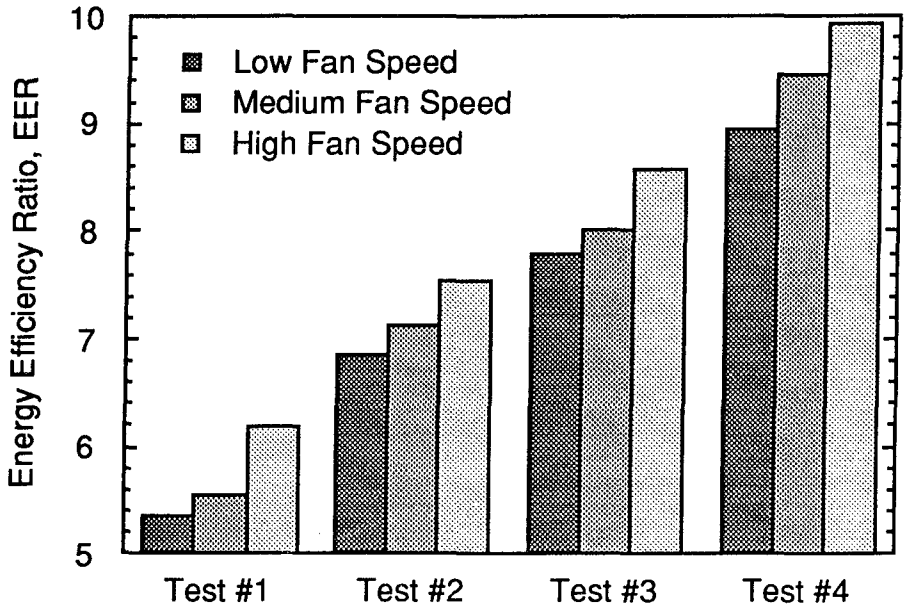

Figure 3.17 EER vs. Air Conditioner Fan Speed for Four Test Points

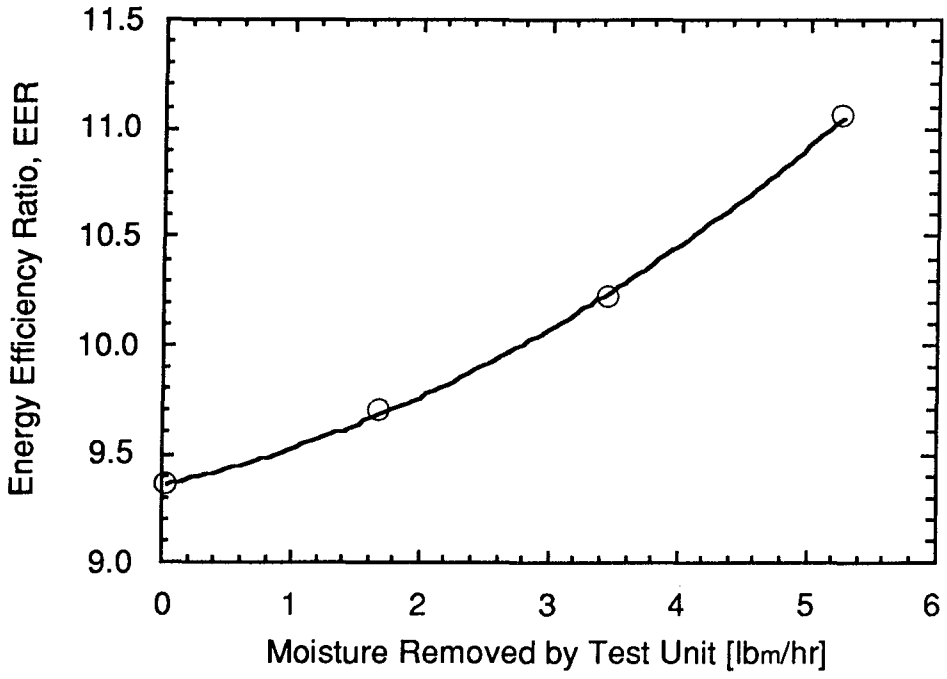

Figure 3.18 EER vs. Moisture Removal Rate for Low Fan Tests at 80 °F Indoor and Outdoor Temperatures

changed. Thus, while there are some gains to be realized, the overall efficiency of the unit depends on several factors.

Another factor that comes into play is the transient effects within the air conditioner itself. If the cooling load desired by the air conditioner operator is less than the steady-state capacity, the test unit will cycle on and off in order to maintain the desired indoor room temperature. However, every time a unit is started up there are substantial losses in efficiency. Thus, operating the air conditioner at a high fan speed may actually be less efficient than using a lower air flow rate if the desired heat load is relatively small. Although one of the future uses of our facility will be to quantify performance during cycling, we currently do not possess any such data and are not able to discuss trends related to that issue. Running a test unit in a cycling mode also increases the level of noise discomfort experienced by the operator. Thus, while the high fan speed setting provides for the most efficient performance of the test unit in a continuous mode of operation, this is certainly not true for all situations.

We also measured the performance of the air conditioner at a variety of indoor room relative humidities. As the humidity in the indoor room increases, the test unit removes greater amounts of moisture from the indoor room. Figure 3.18 shows how the EER varies with moisture removal rate for a fixed set of indoor and outdoor room temperatures. The graph indicates that the EER increases almost quadratically with moisture removal rate. In fact, the compressor uses less power and the capacity is greater at the higher humidities than at dry cases. Thus, this seems to indicate that the air conditioner operates more efficiently at higher relative humidities.

3.2.2.3 Validation of Facility

One of the most important purposes of gathering performance data is to validate the accuracy of our test facility. Comparing our results with those obtained in other facilities can help us identify areas where our facility works well and others where improvements might be necessary. However, it is important to remember that a disagreement between our data and other results does not necessarily discredit the validity of our facility. One comparison we made is between the measured compressor power and the power use predicted by the compressor map, which is provided by the manufacturer. This comparison, shown in Figure 3.19, indicates that our measured values agree with the compressor map within ±5% for all of our dry high fan speed tests. The agreement is similar for all of our other compressor data as well.

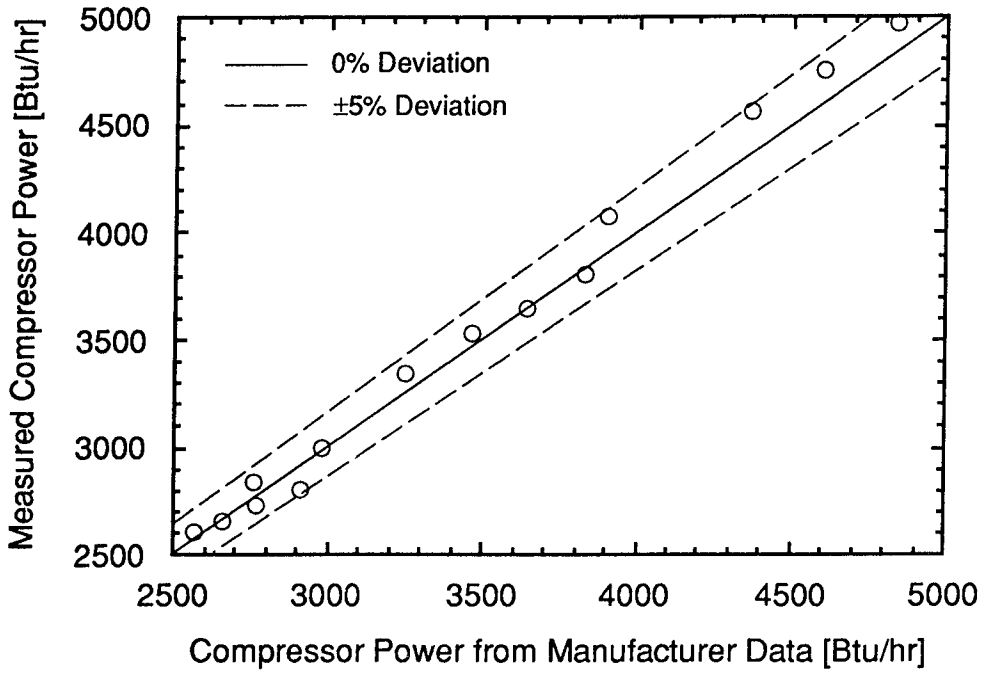

Figure 3.19 Comparison of Measured Power with Manufacturer Data for High Fan Dry Tests

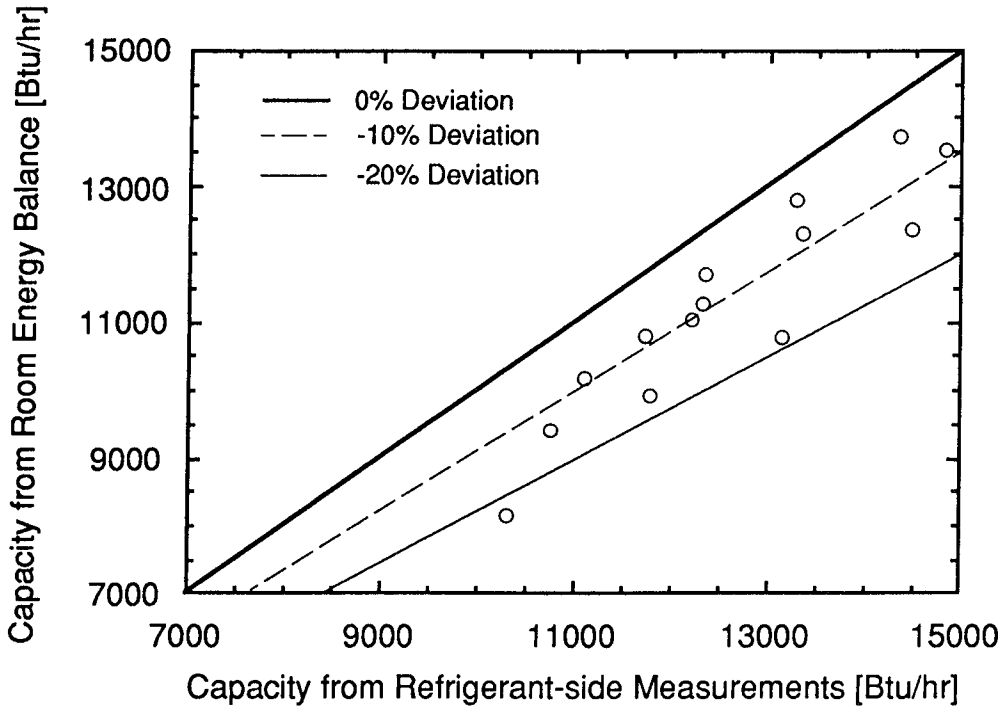

Figure 3.20 Comparison of Capacities from Indoor Room Energy Balance and Refrigerant-side Measurements for High Fan Dry Tests

We feel that ±5% is acceptable for three main reasons. First of all, the compressor map data we possess was not obtained from our particular compressor. It is common for the performance of compressors to vary several percent between different units of the same model type. Secondly, several of the data points we took lie outside of the range of the compressor map. This means that we are assuming that the equations for the compressor map data are still valid when extrapolated to different conditions. This assumption probably contains some error in it and may add to the discrepancies we see in our comparison. Thirdly, the accuracy of our measurement of the compressor power is ±1%. Thus, the agreement we see between our measurement and the compressor map is acceptable and adds validity to our facility.

We are also very interested in how the capacity of the test unit measured by the indoor room energy balance compares with the capacity determined from air- and refrigerant-side measurements. The overall uncertainty in the room energy balance capacity is ±2% based on (a) the observation that the power level fluctuates ±1.5% due to the control algorithm of the microprocessor controller and (b) the accuracy of our power measurement being ±0.5%. Figure 3.20 shows that the evaporator capacity measured from our refrigerant-side data is substantially higher than our power measurement. One of the primary causes of this discrepancy is the fact that the compressor map we use was not generated with our compressor. As we have stated before, it is common for different compressors of the same model and type to have significant differences in performance. Since we do not currently possess a measurement of the refrigerant mass flow rate, we rely on the compressor map to provide this information. This mass flow rate is necessary in order to determine the refrigerant-side capacity.

The other significant cause of the difference in capacities is due to errors in our temperature measurements of the refrigerant loop. Since we are using thermocouples attached to the refrigerant-tube surfaces instead of immersion thermocouples to monitor the refrigerant temperatures, some inaccuracies are introduced. When we are attempting to measure refrigerant temperatures that are higher than the surrounding air temperature, our thermocouples read somewhat lower than the actual refrigerant temperature. Similarly, our measurements of cold refrigerant areas read slightly higher than the actual temperature. The exact magnitude of this error will be quantified when immersion thermocouples are added to the refrigerant loop. Since we expect our surface measurements to read low on the condenser side and high on the evaporator side, the refrigerant-side capacity we determine is higher than the actual

evaporator capacity. Thus, using immersion thermocouples for our refrigerant temperature measurements should reduce the discrepancy between the refrigerant-side and room energy balance capacities.

Figure 3.21 shows how the capacity calculated from air-side measurements compares with the energy balance capacity. We can see that the agreement is much better for this case than for the refrigerant-side capacity. The average error between the capacities is 6%, with none being greater than 10%. However, there is a systematic underprediction of the air-side capacity. While we don't know what causes the systematic bias, there are a few factors that add to the uncertainty of the air-side capacity calculation. First of all, the volumetric flow rate of the air through the evaporator is supplied by the manufacturer and has not been verified in our facility. This flow rate is multiplied by the enthalpy difference between the air inlet and outlet to determine the air-side capacity. Secondly, determining the representative temperature of an air stream can be tricky because of velocity gradients and inadequate mixing at the evaporator inlet and outlet. For both the refrigerant- and air-side comparisons, we are continuing to investigate the systematic discrepancies for other possible effects. Overall, the results from these validation tests show that our test facility is capable of accurately determining air conditioner performance.

3.2.3 Comparison with Room Air Conditioner Simulation Model

A FORTRAN program has been written to simulate the operation of the air conditioners tested in our facility. This model uses the measured data collected within our facility to predict the performance of the test unit. We have compared the measured performance of the test unit to the predicted performance of the model in order to validate the model. Once its accuracy is verified, we are able to use the program to predict the performance of test units with alternative geometry heat exchangers, different compressors and other components, and alternative refrigerants. Running simulations of these configurations is greatly preferred to actual testing with various configurations because it is much cheaper, easier and faster. For these reasons, an accurate model is extremely valuable when designing future air conditioners. Presenting the model or the results from comparisons with facility data is beyond the scope of this document. A complete description of the simulation model and its validation are given by Mullen (1994).

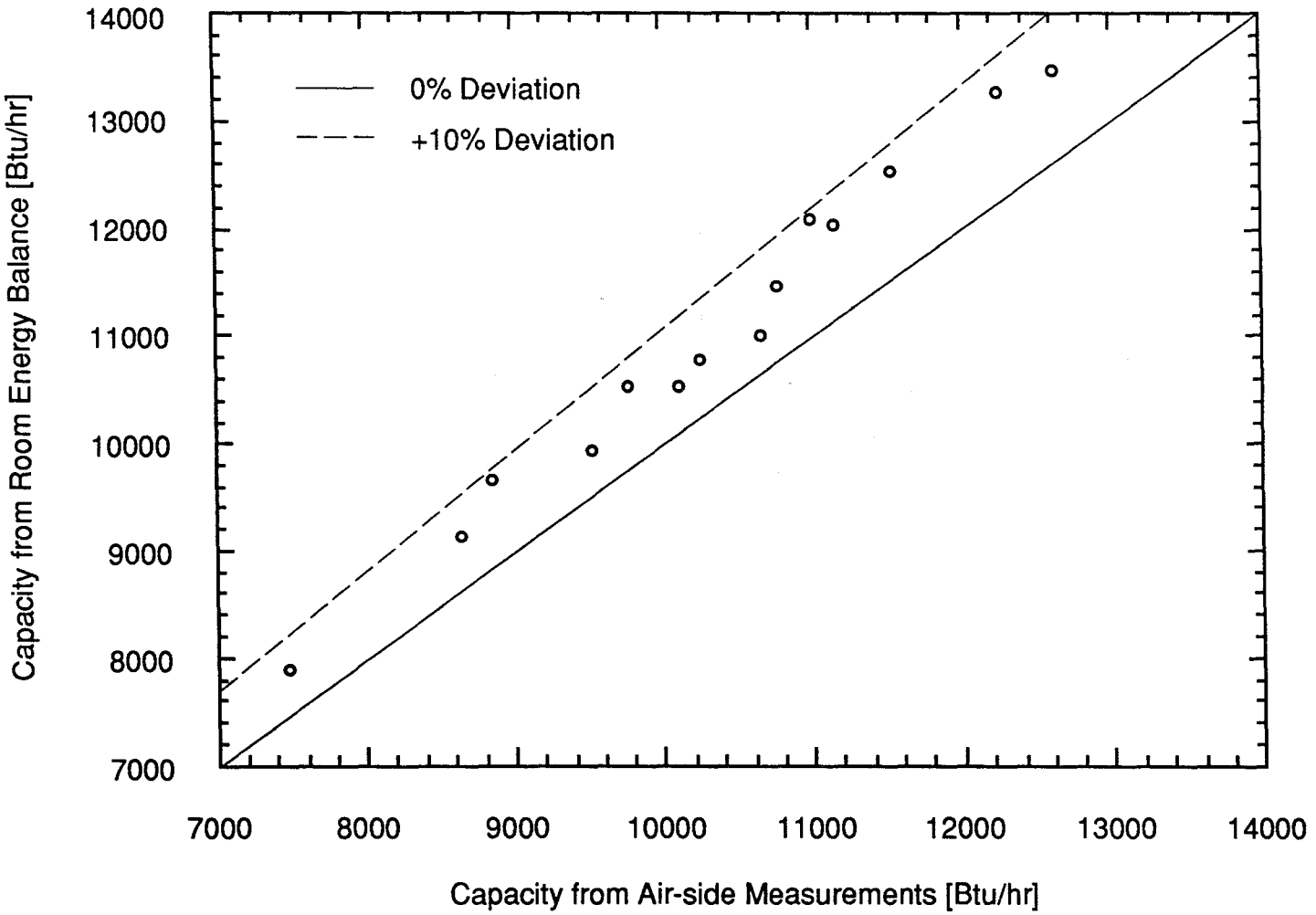

Figure 3.21 Comparison of Capacities from Indoor Room Energy Balance and Air-side Measurements for High Fan Dry Tests

4. SUMMARY AND CONCLUSIONS

The work described within this document is a portion of a larger-scale project, the goals of which are to (a) design, test and validate a room air conditioner test facility, (b) develop and modify a simulation model to predict air conditioner performance at on- and off-design conditions, (c) perform transient and cycling testing to determine performance in these cases, and (d) perform testing with various components and alternative refrigerants. This paper focuses on achieving the first goal in order to establish a foundation for the remainder of the project. The primary conclusions that can be drawn from this work are that (a) the test facility is usable for a wide range of indoor and outdoor room conditions and (b) the facility is functional and has been validated through characterization tests and air conditioner performance tests. Thus, we feel that this work succeeded in accomplishing the desired goals and provides a solid foundation for the project to progress toward future goals.

ASHRAE Standard 16-1983 describes the requirements and capabilities of a test facility used by manufacturers to determine air conditioner performance at a standard rating condition. Because our facility is used for research purposes and will be used to test units over a wide range of operating conditions, many of the requirements for a facility presented by the Standard are not of critical importance to our needs. Thus, we used the Standard as a guide for our design, but also deviated from it when necessary to better achieve our goals.

We designed a test facility capable of testing room air conditioners and split systems with capacities ranging from 0.5 to 2.5 tons of refrigeration. The facility is capable of maintaining a large range of temperatures and relative humidities in both the indoor and outdoor chambers in order to test each unit over the majority of its range of operation. The steady-state capacity of a unit at a given set of conditions is determined by measuring the power being added to the indoor room and subtracting any parasitic losses, such as heat loss through the walls or through the cracks in the test unit itself. Since the facility is sealed to prevent moisture transfer from the indoor room, the amount of latent heat removed by the test unit is easily determined by measuring the power added to the humidifier. The facility also measures the power used by the air conditioner so that we can calculate the EER for each test unit and set of conditions. The performance of the subsystems within the facility has been documented and all devices currently provide satisfactory operation.

The facility contains a large amount of instrumentation for both the air conditioner and the facility itself. Thermocouples are used to measure air- and refrigerant-side

temperatures on the test unit, and to measure the temperature of various components within the facility. Both the indoor and outdoor rooms possess two combined temperature and relative humidity probes to accurately determine the air properties in each chamber. A load cell measures the amount of latent heat added to the indoor room air and two power measurement devices record the amount of electricity used by the air conditioner and the indoor room. A thermistor located within an isothermal junction box is used to provide for an accurate reference temperature for our thermocouple measurements. We currently possess one air-side-instrumented test unit which has been used to performance testing. Future work will investigate the accuracy and the effects on performance of using refrigerant-side measurements for calorimetry.

The facility has undergone a substantial amount of characterization testing in order to (a) quantify heat and moisture losses from the indoor room that are needed for our room energy balance, (b) determine the response time of the facility when various forcing functions are used to implement a change of conditions, and (c) design a test matrix that is the optimal blend of completeness and expediency. An indoor room simulation model has been developed to better understand the interaction of the components within the facility and to predict the response of the facility as a function of time. This prediction capability is important when it is desired to take data for a test unit before the facility has fully reached a steady set of conditions.

We have obtained a full set of performance data for our air-side-instrumented test unit. These data have helped to (a) optimize the test matrix, (b) validate the facility, and (c) observe trends in the performance of the test unit when temperatures, humidities and fan speeds are varied. Our facility is capable of measuring the capacity of a test unit in three ways: from an indoor room energy balance; a refrigerant-side energy balance on the evaporator; and an air-side energy balance on the evaporator. The agreement between these independent measurements has been quantified and helps to indicate possible measurement improvements for future testing. Several performance trends have been observed and documented for this test unit, which provides insights into possible improvements for room air conditioners.

Again, the purpose of the work described herein is to provide a foundation that can be built upon to meet future project goals. That foundation is established because (a) the facility is able to achieve a wide range of conditions in each chamber and (b) the facility has been validated through characterization and performance testing. The remainder of the goals described by the project are currently being investigated and will be addressed in the future.

APPENDIX A. AIR CONDITIONER FAN VOLUME FLOW RATE MEASUREMENTS: TEST SETUP AND RESULTS

A.1 System Description

A schematic of the air volumetric flow rate measurement system is shown in Figure A.1. The exhaust section of the air conditioner fan being tested is connected to a venturi meter with a flexible air duct. An inclined manometer is placed across the venturi to obtain a differential pressure measurement. There are straight PVC pipe sections before and after the venturi to ensure uniform air flow. Because a large amount of air is being forced through a substantially long duct, a significant pressure drop is induced along the length of the duct. To overcome this undesirable effect, a make-up fan is placed downstream of the venturi to overcome the pressure drop. To ensure that the air conditioner sees atmospheric pressure, a frequency controller controls the make-up fan speed such that the pressure increase it introduces to the system is exactly balanced by the pressure drop induced by friction losses in the duct. A second inclined manometer is placed just downstream of the air conditioner fan outlet to verify that the pressure at that location is atmospheric.

A type-T thermocouple is placed in the air flow about three feet downstream of the air conditioner fan. This measurement is used in conjunction with the pressure drop across the venturi to calculate the volumetric flow rate being circulated by the air conditioner fan. The equations used to determine the flow rate are taken from curve fits provided by the venturi manufacturer. Since all of our tests were operated within a somewhat humid environment, we also introduced an air density correction factor for moist air. Because moist air is more dense than dry air, the addition of this correction increases the volumetric flow rates approximately 1.5%.

A.2 Results

Because the PVC entrance and exit lengths for the venturi are quite long, the air flow measurement system does not fit within the test facility chambers, and thus can not test air conditioners in situ. This can present some problems in testing the unit over all operating conditions. The room in which the air flow is tested does not have the temperature or humidity capabilities of our test facility, thus making it much more difficult to determine if the unit is affected by these parameters. While we aren't able to effectively vary the relative humidity of the air entering each air conditioner fan, we can adjust the temperature by using several space heaters, which are mounted in front

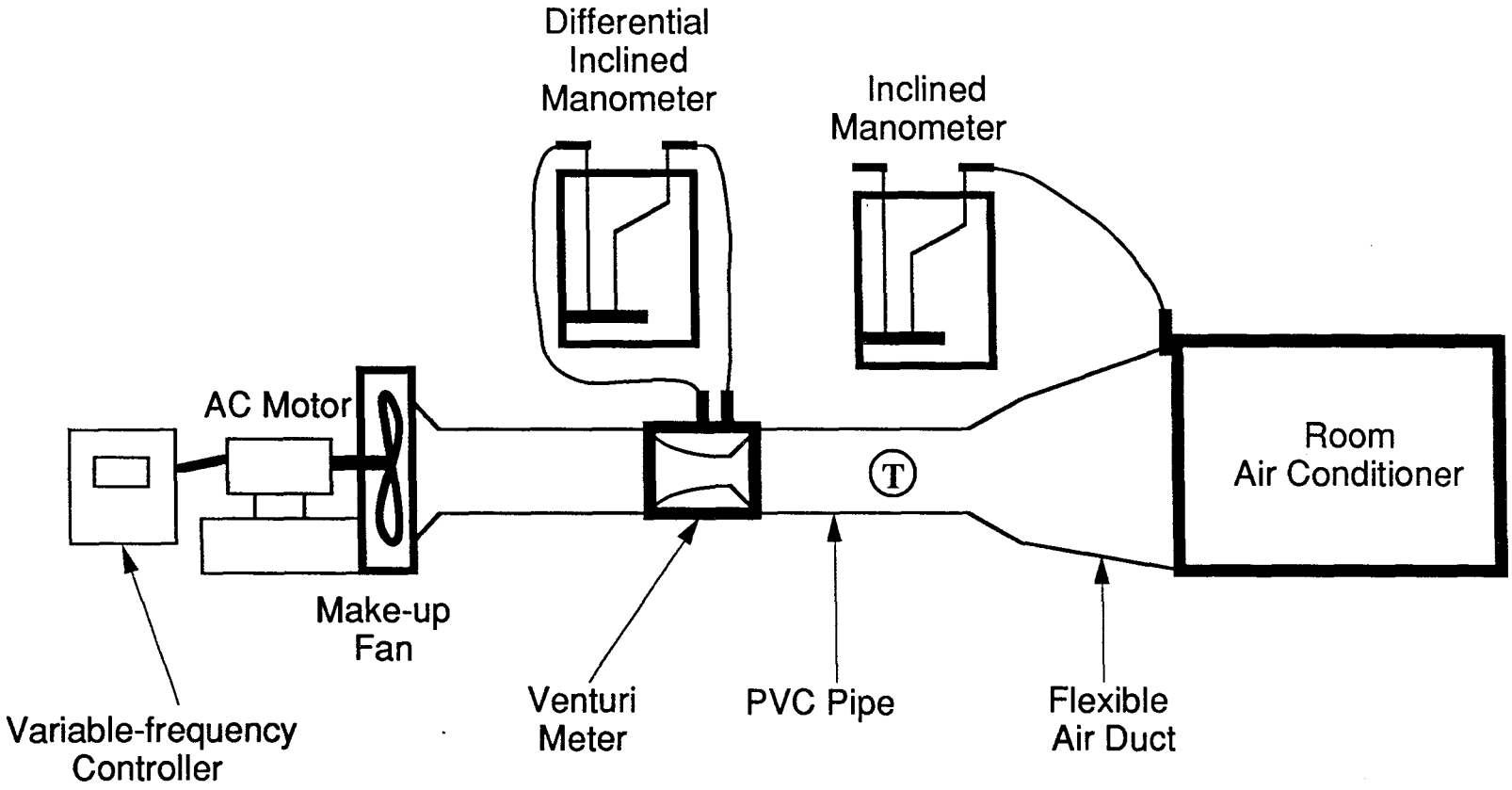

Figure A.1 Air Volumetric Flow Rate Measurement System Schematic

of the fan inlet. Although this doesn't provide the full range of temperatures seen in the test facility, we feel that the range is great enough to determine if the volumetric flow rates are temperature dependent.

We ran the majority of our air flow tests with the air conditioner compressor on. This was done because we don't want to introduce any additional uncertainty to the testing by running some tests with the compressor on and some with it off. In addition, the compressor is always running during air conditioner performance testing within the test facility. However, we do want to quantify the effects (if any) of the compressor on the fan flow rates. For this reason, we took full data sets at each fan speed with the compressor on, and then turned off the compressor and took a few more data points. The data indicates that there is no significant difference in the air flow rates between the compressor on and compressor off cases. The voltage supplied to the test unit increases slightly (up to 5%) when the compressor is off, but this does not have a significant effect on the fan flow rates.

We also looked briefly at the effect of using different size venturi meters for air flow measurement. We possess both four- and six-inch-diameter meters, which were both purchased so that we would have a larger range of capability. The 4-in. meter is intended for flow rates in the 400-800 cfm range while the 6-in. meter is designed for the 800-1400 cfm range. However, the fluctuation in the manometer reading for the 4-in. meter is much higher than that for the 6-in. meter. This fluctuation is possibly due to unstable flow at the venturi inlet. The converging duct from the fan outlet to the inlet of the entrance length has an outlet diameter of six inches. There is no smooth nozzle that then takes this flow from the six-inch size to the four-inch entrance length duct. Although there is a significant length of straight 4-in. PVC duct upstream of the venturi, it may not be long enough to completely damp out all unsteadiness in the flow. Because of this instability, we performed all tests with the 6-in. venturi.

Results from our air flow testing are shown in Figures A.2 through A.4. Figures A.2 and A.3 show the temperature dependence of all the data taken for the 1-ton Amana and 1.5-ton Kenmore units respectively. Also shown are the uncertainty bars, which indicate the accuracy of the volumetric flow rate measurements. As the figures show, nearly all of the data lies inside the uncertainty bars, thus indicating that the volumetric flow rates are not sensitive to temperature variations. For each fan speed, the uncertainty in the air flow rate is ±1.5% for the evaporator and ±2.0% for the condenser. This uncertainty is the same for both the Amana and the Kenmore units that were tested. This error is due to two factors. There is a 1% uncertainty in the accuracy of the venturi itself. The additional error is in reading the inclined

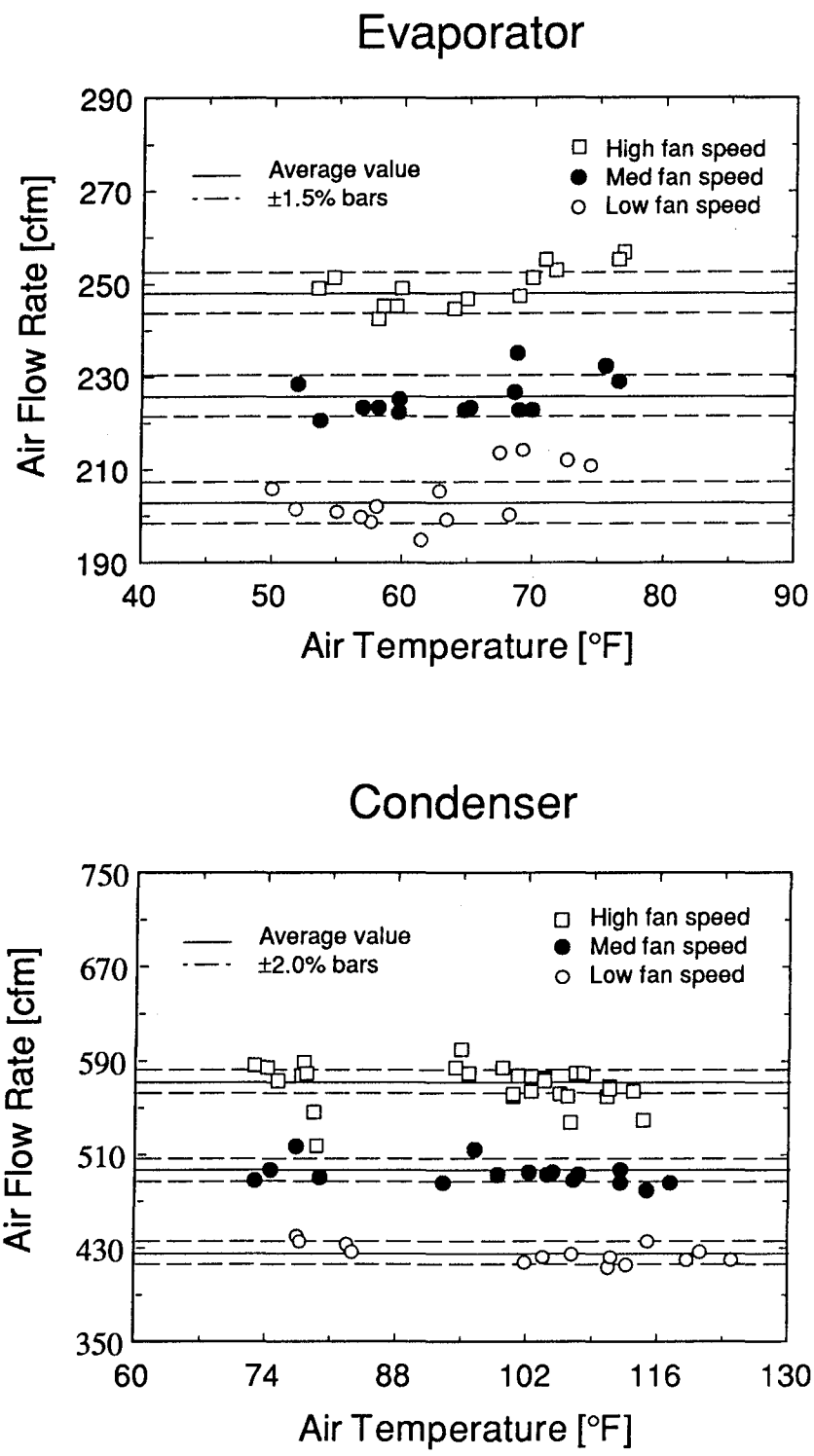

Figure A.2 Air Volumetric Flow Rate Data for 1-ton Amana

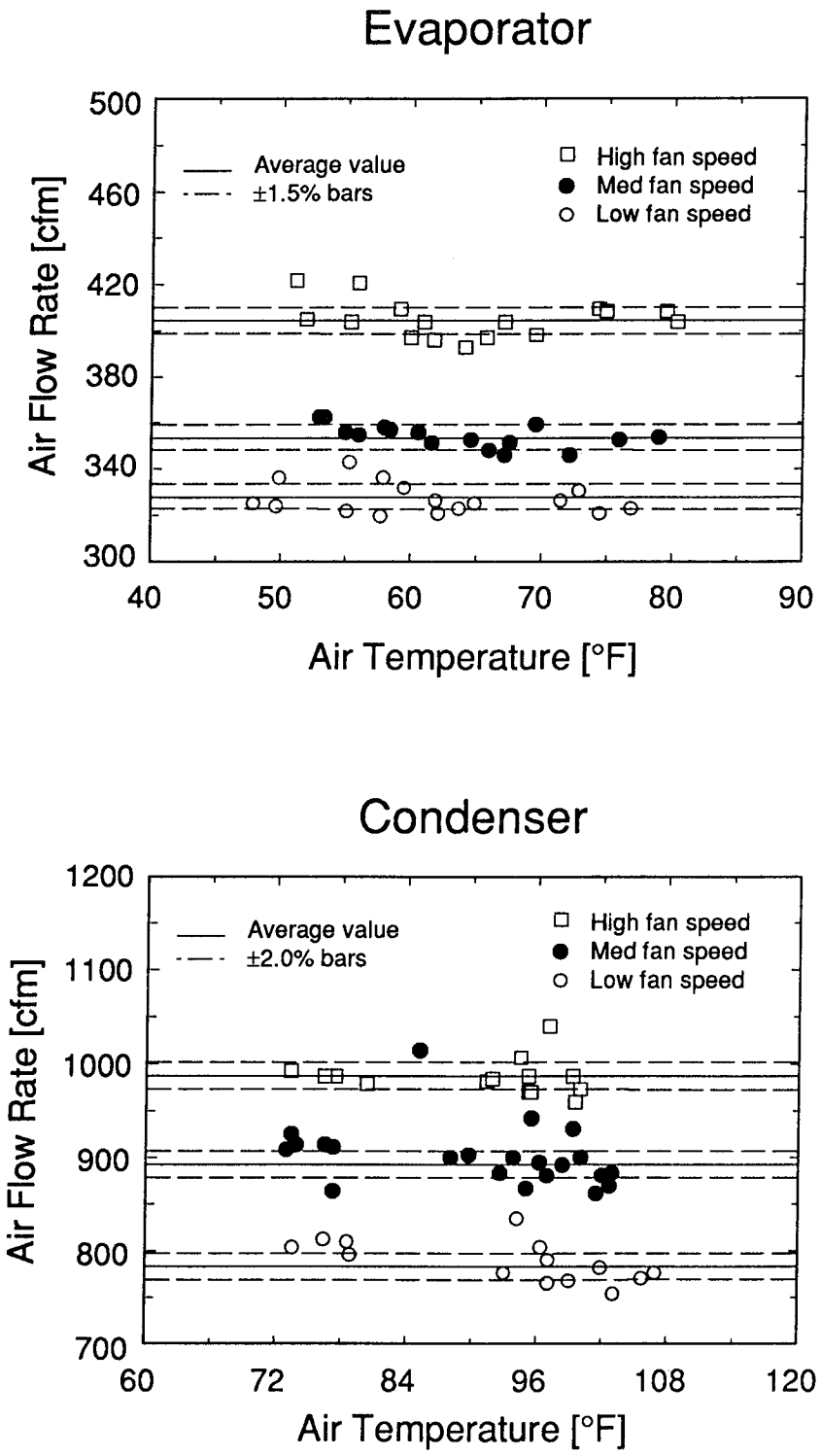

Figure A.3 Air Volumetric Flow Rate Data for 1.5-ton Kenmore

manometer. Because the fluid level within the manometer fluctuates, the accuracy to which this can be read introduces some uncertainty. This error is 1% for the condenser tests, but only 0.5% for the evaporator tests because the portion of the scale used for evaporator tests has much finer gradations than those for the condenser tests. Figure A.4 presents a summary of the data for both test units.

A.3 Conclusions

After comparing our data with values provided by the manufacturers of each test unit, we determined that our air flow measurement method contains a significant systematic bias. However, the data we have obtained is still quite useful to follow trends in a qualitative sense. For example, although the magnitude of the numbers is not fully accurate, we can observe that the air volumetric flow rate is independent of temperature and voltage. Analysis of the data leads us to believe that the error in our measurements is introduced in the contraction section of our test apparatus. The measurement system will undergo further optimization in the future to attempt to reconcile the differences between our experimental data and that provided by the manufacturers.

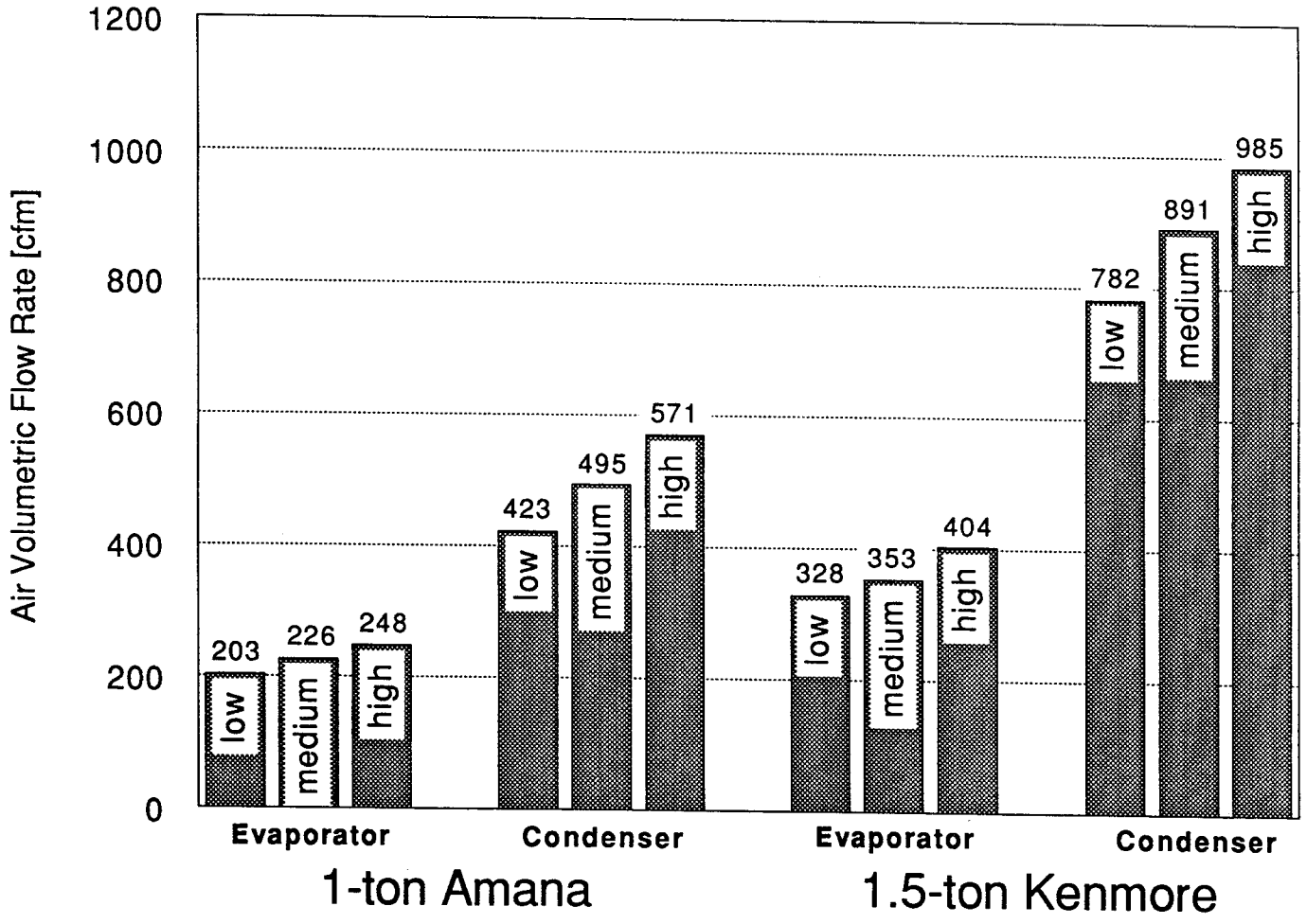

Figure A.4 Air Volumetric Flow Rate Data for 1-ton Amana and 1.5-ton Kenmore

REFERENCES

ASHRAE, 1984: "Method of Testing for Rating Room Air Conditioners and Packaged Terminal Air Conditioners," ANSI/ASHRAE Standard 16-1983, ASHRAE Publications, Atlanta, GA.

Feller, S. D., 1993: "Design of the Outdoor Environmental Chamber of a Room Air Conditioner Test Facility," University of Illinois at Urbana-Champaign, Urbana, IL.

Fleming, J. E., 1993: "Design of the Psychrometric Calorimeter Chamber of a Room Air Conditioner Test Facility," University of Illinois at Urbana-Champaign, Urbana, IL.

Mullen, C. E., 1994: "Modeling of a Room Air Conditioner System," University of Illinois at Urbana-Champaign, Urbana, IL.

Porter, K. J., 1994: "Accuracy of Refrigerant Tube Surface Thermocouples," Technical Memo #12, Air Conditioning and Refrigeration Center, University of Illinois at Urbana-Champaign, Urbana, IL.